UCLouvain

epl

École polytechnique de Louvain

# Environmental Impacts of a Superconducting Quantum Computer Based on a Life Cycle Assessment

Authors: **Arnaud Billat, Dimitri Doeran**
Supervisor: **David Bol**
Readers: **Jean-Pierre Raskin, Martin Lefebvre, Augustin Wattiez**
Academic year 2023–2024
Master [120] in Electro-mechanical and Electrical Engineering

# Acknowledgments

This work would not have been possible without the support and assistance of several individuals, whom we would like to thank.

First of all, we would like to express our gratitude to our supervisor, David Bol, for giving us the opportunity to be among the pioneers in analyzing the environmental impacts of quantum computers-an emerging technology that is sure to receive increasing attention in terms of its ecological footprint. Moreover, we extend our thanks for his time and invaluable advice throughout the year, which has been instrumental in the progression of our work.

Secondly, and equally important, we would like to thank our two assistants (Martin Lefebvre and Augustin Wattiez) who attended every meeting with Mr. Bol and made significant contributions to the development of the work. Their prompt responses outside of meetings also enabled us to address issues and reflections more quickly. In addition to all of this, we thank them for their detailed review of several chapters of this work. We would also like to express our gratitude to Jean-Pierre Raskin for kindly agreeing to serve as the official external reviewer for this work.

Finally, we would like to thank our family and friends for all their support, interest, and even their feedback on this work. We really appreciate their encouragement throughout our studies.

# Abstract

This master thesis investigates the environmental impact of superconducting quantum computers (SQCs), focusing on their global warming potential (GWP) throughout the production and use phases. The study is motivated by the rapid development of quantum computing technology and the need to evaluate its ecological footprint amidst growing concerns about greenhouse gas emissions.

A life cycle assessment (LCA) was conducted to estimate the environmental impacts associated with the production and use of SQCs, using a coarse-grain methodology to analyse key subsystems. The analysis utilised the Ecoinvent database and was managed through the Activity Browser software, with a focus on GWP as the primary impact category, using the EF3.0 method.

The findings reveal that the use phase of SQCs has a significantly higher environmental impact than the production phase, with refrigeration systems, particularly pulse tube cryocooler compressors, being the dominant contributors to $CO_2$ emissions. Over a five-year period, the total carbon footprint is estimated at approximately 50,000 kg $CO_2$-eq for a Belgian energy mix and 150,000 kg $CO_2$-eq for a global energy mix. The cryostat, largely due to its gold components, is identified as the subsystem with the highest impact during the production phase.

The study concludes that while SQCs offer substantial technological advancements, their environmental impacts are considerable, particularly during the use phase. The research highlights the importance of optimising energy consumption and improving the design of refrigeration systems to reduce the ecological footprint of quantum computing. Further research is recommended to refine the LCA by examining specific subsystems in greater detail and exploring other databases for comparative analysis.

# Disclaimer

The development and writing of this masters thesis have benefited from the use of various digital tools and AI technologies, which have been instrumental in enhancing the clarity, precision, and efficiency of the work presented.

The translation service DeepL was extensively used to translate, correct spelling, and reformulate various sections of the text to ensure accuracy and fluency [1].

ChatGPT was utilised throughout this work, primarily to provide advice on the structure and occasionally to rephrase certain sections [2]. Due to this AI's lack of verifiable sources for its generated content, it was not employed for technical writing and discussions.

For creating tables, the LaTeX Tables Generator was used to generate the LaTeX code and manage the layout of the tables [3].

Finally, Consensus AI assisted in gathering and synthesising research, ensuring a comprehensive and precise review of the literature. [4]

# Contents

# Introduction

Quantum computers represent a significant leap in computational power, introducing a new paradigm in processing capabilities. Unlike classical computers, that rely on binary logic, quantum computers harness the principles of quantum mechanics, such as superposition and entanglement, allowing qubits to exist in multiple states simultaneously. This characteristic enables them to tackle complex computational problems with greater efficiency.

Superconducting quantum computers, in particular, utilise superconducting circuits and Josephson junctions to create and manipulate qubits. These computers operate in cryogenic environments to reduce electrical resistance, which facilitates precise qubit control by minimising thermal noise and decoherence. This technological advancement opens up a range of applications in fields such as cryptography, optimisation, material science, and drug discovery. A critical aspect and reason why a lot of effort is put in is that quantum computers can potentially break current cryptographic methods (breaking communication systems, bank systems, etc.). They also enable the development of new, quantum-resistant cryptographic techniques.

Given the significant potential of these technologies in society, it is crucial to estimate the environmental impacts associated with quantum computers, particularly superconducting quantum computers, which are the most developed yet. In 2019, 64% of greenhouse gas (GHG) emissions were attributed to carbon dioxide ($CO_2$) from fossil fuels and industry [5]. Given the role of GHGs in global warming, it is essential to reduce emissions and understand their sources. While quantum technology holds promise for society, it is important to critically examine its development within the context of current global environmental challenges.

This master thesis aims to explore the environmental impacts of superconducting quantum computers, provide insights into their ecological footprint, and advocate for sustainable technological development. By examining the cradle-to-gate environmental impact of these computers, this research takes a first step towards understanding the environmental considerations in the pursuit of quantum technology.

A systematic methodology known as life cycle assessment (LCA) is employed to estimate the environmental impacts of products, processes, or activities throughout their entire life cycle. LCA considers all stages, from raw material extraction to production, use, and disposal, aiming to identify opportunities for environmental improvement and inform decision-making.

Given the complexity and numerous components of superconducting quantum computers, a coarse-grain methodology is adopted. This involves breaking down the system into main subsystems for detailed analysis. This method has influenced some key stages in LCA, such as the scope boundaries.

The choice of database is critical in LCA. This study uses Ecoinvent, one of the most comprehensive and widely used databases for LCA, to offer extensive data on the environmental impacts of various materials and processes. This database ensures that the data used in the assessment is reliable and up-to-date. The software Activity Browser from Brightway is used to manage and analyse this data. Activity Browser provides an interface for accessing Ecoinvent and allows for the categorisation of activities and quantification of environmental impacts for each subsystem.

The impact assessment presents different impact categories, with a focus on global warming potential (GWP), to identify hotspots within the superconducting quantum computers. The goal is to enable future research on the eco-design of quantum computers by pinpointing areas where environmental improvements can be most effective.

Investigations into the environmental impacts of superconducting quantum computers reveal dominant contributions from the use phase and cryostat production, due to the gold present. In the use phase, refrigeration, in particular, is a major source of $CO_2$ emissions. Addressing these findings involves optimising the structure, improving operational efficiency, and reducing energy consumption.

This thesis is structured into four chapters. The first chapter introduces the basics and state of the art of quantum computers. The second chapter outlines the methodology and tools used in the LCA. The third chapter applies the LCA to a superconducting quantum computer and gives the results and interpretation. The final chapter concludes all the work done with a key outline to keep in mind.

# Chapter 1

# Basics and State of the Art of Quantum Computers

In the field of engineering and generally in the realm of new technologies, where innovation is the key to progress, the advent of quantum computers represents a revolution. This master thesis delves into this fascinating universe, exploring the emerging technologies and their implications, applications, and, above all, their environmental impact.

Over the last thirty years, scientists have entertained the idea of combining two influential and revolutionary theories: information theory and quantum mechanics [6]. This new perspective on information, quantum information, stems from a simple concept: to describe quantum systems and mechanisms. Describing or predicting quantum processes is an insurmountable challenge for classical computers, owing to the fundamental laws of physics that dictate the reversibility of time. In classical mechanics, replacing $t$ with its negation $-t$ results in equations that remain fundamentally unchanged. The connection between quantum theory and computing processes was initially established by Paul Benioff in 1980, who outlined a computer based on quantum concepts, particularly the Hamiltonian operator [7]. Richard Feynman, a scientist in the 1990s, proposed a visionary idea: to leverage the computational power inherent in quantum phenomena to surpass the limitations of current computers.

Until the mid-1990s, physicists remained divided on the practical feasibility of implementing quantum computing , partly due to the challenges posed by the interaction of quantum systems with their environment, leading to phenomena such as decoherence and information loss [8]. However, a significant turning point occurred in 1994 when researcher Peter Shor demonstrated the feasibility of factoring large numbers efficiently using a quantum computer, sparking a surge of interest and investment in the field [9]. Subsequent breakthroughs followed rapidly: in 1995, one of the first error correction codes tailored for quantum systems was introduced [10]. In 1998, IBM unveiled the first 2 qubit quantum computer, followed by a 7 qubit quantum computer in 2001, marking a seminal milestone in the field [11]. These early quantum computers, composed of chloroform molecules, boasted brief operational lifespans of mere minutes. In 2007, D-Wave announced the development of a solid-state quantum computer featuring 28 qubits, and simultaneously, the University of Queensland pioneered research into optical quantum circuits [12]. In 2009, D-Wave unveiled a quantum chip containing 128 qubits, signalling significant progress in quantum computing capabilities. Finally, in 2011, D-Wave achieved a historic milestone by commercialising the 'D-Wave One,' with Lockheed Martin and NASA among the pioneering purchasers. In the next sections, some of those concepts and milestones will be explained.

Subsequent years witnessed a proliferation of advancements, culminating in a pivotal moment in 2017 when researchers at Google neared completion of a 49 qubit quantum computer [13]. This milestone heralded the concept of 'quantum supremacy,' denoting the threshold beyond which classical supercomputers would be incapable of simulating the exponential growth of memory and communication bandwidth required to emulate their quantum counterparts. IBM's achievement of operating a 50 qubit quantum computer for 90 microseconds marked a seminal milestone, ushering in the era of noisy intermediate-scale quantum (NISQ) computing [14]. This era, characterised by imperfect qubit control, paves the way for the exploration of quantum advantagewhere practical applications of quantum computations emerge as a tangible reality.

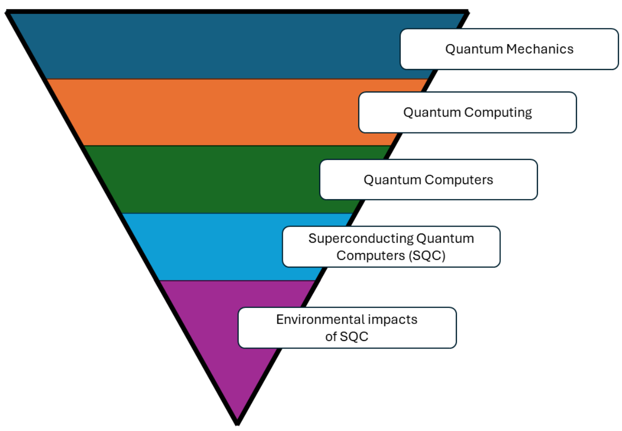


Figure 1.1: Pyramidal abstraction approach

The aim of this chapter is to explain how a superconducting quantum computer works, as well as its challenges and limitations. To do this, it is first necessary to start from a higher level of abstraction, such as the elementary principles of quantum mechanics related to the subject. Then, reducing the abstraction a little further, it's necessary to review quantum computing in order to introduce what a "qubit" is to understand the next part, which introduces how these quantum computers work. Once this stage has been reached, the analysis can be further refined by focussing solely on the operation of superconducting quantum computers. Finally, this leads to important questions about the ecological implications of quantum computers and their impact on the environment. This idea of the chapter is represented in Figure 1.1.

## 1.1 Basic Principles of Quantum Mechanics

Quantum mechanics is a fundamental branch of physics that focusses on the atomic and sub-atomic realms. Unlike rigorous classical physics, quantum mechanics emphasises concepts such as quantisation, uncertainty, and wave-particle duality [15].

In the context of this work, concepts such as the quantum state, quantum superposition, quantum entanglement, and quantum tunnelling are essential quantum mechanical concepts to understand in order to move on to the next level of abstraction.

### 1.1.1 Quantum States and Superposition

In classical physics, the state of a system takes into account all the information concerning it, such as its velocity, position, acceleration, instantaneous direction, and so on. These can all evolve over time, but at any given time, the system has a single and unique state.

However, in quantum mechanics, a quantum state is a mathematical object that fully describes the quantum system at the only difference that this system can be described by several states for a given time. All these states are admissible, and the system can be represented by a linear combination of these states weighted by their probability to occur. This is called the quantum superposition of a quantum system, and this is a crucial step in understanding the behaviour of the quantum bits that will be described later in Section 1.2.1.

To better represent this idea, let $\Psi(x)$ be the quantum state of a quantum system at a given time. Then,

$$\Psi(x) = \alpha\Psi_1(x) + \beta\Psi_2(x)$$

where $\alpha$ and $\beta$ are complex numbers that describe the probability amplitudes of the system being in states $\Psi_1(x)$ and $\Psi_2(x)$, respectively.

### 1.1.2 Quantum Entanglement

Entanglement is a quantum phenomenon where the states of particles become interdependent, such that the state of one particle instantaneously affects the state of the other, regardless of the distance separating them.

The entangled state of two particles, for example, can be represented as:

$$|\psi_{AB}\rangle = \frac{1}{\sqrt{2}}(|0_A\rangle|1_B\rangle + |1_A\rangle|0_B\rangle) \tag{1.1}$$

In this state, if particle A is measured and found to be in state $|0\rangle$, particle B will instantly be found in state $|1\rangle$, and vice versa. This approach applies perfectly to qubits applications [16, 17].

This concept was famously discussed by Albert Einstein, Boris Podolsky, and Nathan Rosen, known as the EPR paradox. They argued that quantum mechanics was incomplete because it allowed for entangled particles to influence each other instantaneously, a phenomenon Einstein referred to as "spooky action at a distance." Despite Einstein's scepticism, entanglement has been experimentally confirmed and is a cornerstone of quantum mechanics [18].

For quantum computing and quantum information processing, this resource enables quantum algorithms to perform complex computations more efficiently than classical algorithms. Key applications include :

- **Quantum Teleportation:** Entanglement allows for the transmission of quantum information between distant particles without physically transferring the particles themselves [19].
- **Quantum Key Distribution:** Protocols like BB84 use entangled particles to ensure secure communication channels, where any eavesdropping attempt would be detectable [20].

- **Quantum Error Correction:** Entanglement is used in error correction codes to protect quantum information from decoherence and other quantum noise [10].

### 1.1.3 Quantum Tunnelling

Quantum tunnelling is a fundamental phenomenon in quantum mechanics where particles can pass through a potential energy barrier, even if their energy is less than the height of the barrier. Particles are described by wave functions, which provide the probabilities of finding particles in particular states or locations. When a particle encounters a potential barrier, its wave function doesn't drop abruptly to zero at the barrier, as one would expect classically. Instead, it decays exponentially inside the barrier but remains non-zero. This allows for a non-zero probability that the particle will tunnel through the barrier and emerge on the other side.

Mathematically, the probability of tunnelling can be derived from the Schrödinger equation, and it decreases exponentially with the thickness and height of the barrier:

$$P \propto e^{-2\kappa d}$$

where $\kappa = \sqrt{\frac{2m(U-E)}{\hbar^2}}$, $m$ is the mass of the particle, $U$ is the barrier height, $E$ is the energy of the particle, $\hbar$ is the reduced Planck constant, and $d$ is the thickness of the barrier.

This phenomenon is fundamental to the operation of qubits in certain types of quantum computers. In these systems, the solution is obtained through qubit tunnelling to find the lowest energy state.

## 1.2 Fundamentals of Quantum Computing

### 1.2.1 Qubits: The Building Blocks of Quantum Computers

A qubit, or quantum bit, is the fundamental unit of quantum information, analogous to the classical bit in classical computing. Unlike a classical bit, which can exist in one of two distinct states (either 0 or 1), a qubit can exist simultaneously in a superposition of both states. This unique property arises from the principles of quantum mechanics, as seen in Section 1.1.

Mathematically, the state of a qubit is represented as $|\psi\rangle = \alpha|0\rangle + \beta|1\rangle$ , where $|0\rangle$ and $|1\rangle$ are the basis states, and $\alpha$ and $\beta$ are complex numbers known as probability amplitudes. The probabilities of the qubit being measured in the $|0\rangle$ or $|1\rangle$ state are given by $|\alpha|^2$ and $|\beta|^2$, respectively, with the condition that $|\alpha|^2 + |\beta|^2 = 1$.

This superposition allows a qubit to perform multiple computations simultaneously, providing a significant advantage in processing power for certain types of problems. Furthermore, qubits can be entangled with one another, creating correlations between their states that are stronger than any classical correlations. This entanglement is a key resource for many quantum algorithms and protocols.

Physically, qubits can be realised using various quantum systems, each leveraging the unique properties of quantum mechanics. The three primary methods of qubit realisation are:

- **Superconducting Circuits:** In these systems, qubits are formed using tiny superconducting loops interrupted by Josephson junctions. These circuits exhibit quantum properties at low temperatures, allowing them to represent and manipulate qubits with microwave pulses. Superconducting qubits are highly controllable and have become a leading platform for quantum computing due to their scalability and integration with existing semiconductor technology.

- **Trapped Ions:** Trapped ion qubits use ions confined and suspended in free space by electromagnetic fields. The internal energy levels of the ions serve as the qubit states. Quantum operations are performed using laser pulses that manipulate the internal states and the motion of the ions. This method is known for its high fidelity and long coherence times, making it a robust platform for quantum computation.

- **Photons:** Photonic qubits use the polarisation states of photons to represent qubit states. Photons are advantageous for quantum communication due to their ability to travel long distances with minimal decoherence. Quantum gates and operations are performed using linear optical elements like beam splitters and phase shifters. Photonic qubits are particularly well-suited for networking quantum computers over large distances.

In addition to these primary methods, other approaches to qubit realisation include quantum dots, nitrogen-vacancy centers in diamonds, and topological qubits. Each of these systems offers advantages and poses specific challenges, contributing to the diverse landscape of quantum computing research.

### 1.2.2 Quantum Algorithms

Just like a classical computer, a quantum computer performs tasks using programs or algorithms. These are mostly written in the programming language created by Microsoft, Q#. Although it is necessary to write an algorithm, it is often represented in schematic form (Figure 1.2) even before encoding, because unlike a variation in electricity, which defines the state of a classical bit, quantum entanglement and superposition are involved here.

One of the most promising applications lies in cryptography, where quantum algorithms such as Shor's algorithm threaten to undermine classical encryption methods [21]. Quantum computers can efficiently factor large numbers, rendering conventional cryptographic techniques vulnerable to attacks. Conversely, quantum cryptography offers unbreakable security through the principles of quantum mechanics, providing secure communication channels [22]. It can be a game changer for a every security system in the world, which is why big companies and states are investing a lot [23]. This algorithm won't be explained in this work considering its complexity, however, a simple but impressive algorithm will be demonstrated below.

#### Deutsch-Jozsa algorithm

This alogrithm is actually not very useful in practice, but it is a very simple and easy way to understand the strength of the quantum approach.

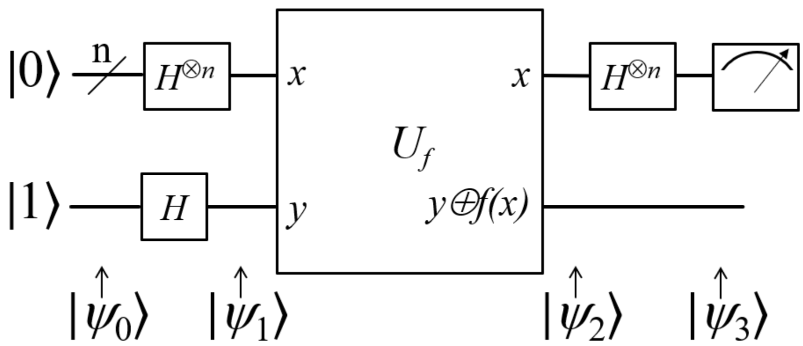


Figure 1.2: Deutsch-Jozsa Algorithm Quantum Circuit

This algorithm can determine whether a function f is balanced (the output returns 0 for exactly half of the inputs and 1 for the other half) or constant (the same output, 0 or 1, for all inputs). The only operation that can be executed is sending an input and reading the output.

$$f : \{0,1\}^n \to \{0,1\}$$

Considering at first that there is only one argument to the function, this reduces to $f : \{0,1\} \to \{0,1\}$ which is actually the Deutsch algorithm from which the Deutch-Jozsa extends [24]. The corresponding system is :

$$\begin{cases} \text{if} f(0) = f(1) & \text{then f is constant} \\ \text{if} f(0) \neq f(1) & \text{then f is balanced} \end{cases}$$

With classical computation, $f(0)$ and $f(1)$ should be computed to test the equation above. However, with the quantum approach, this can be done with only one computation. This will be demonstrated step by step just below.

1. **Initialize the qubits:** Start with two qubits in the state $|0\rangle \otimes |1\rangle$ or $|01\rangle$.

$$|\psi_0\rangle = |0\rangle \otimes |1\rangle = |01\rangle$$

2. **Apply Hadamard gates:** Apply the Hadamard gate $H$ to each qubit (see more on quantum gates on Annex A). The Hadamard gate transforms the basis states as follows:

$$H|0\rangle = \frac{|0\rangle + |1\rangle}{\sqrt{2}}, \quad H|1\rangle = \frac{|0\rangle - |1\rangle}{\sqrt{2}}$$

Thus, after applying Hadamard gates to both qubits, the state becomes:

$$|\psi_1\rangle = H|0\rangle \otimes H|1\rangle = \left(\frac{|0\rangle + |1\rangle}{\sqrt{2}}\right) \otimes \left(\frac{|0\rangle - |1\rangle}{\sqrt{2}}\right)$$

$$|\psi_1\rangle = \frac{1}{2}\left(|0\rangle + |1\rangle\right) \otimes \left(|0\rangle - |1\rangle\right)$$

3. **Apply the oracle:** The oracle $U_f$ is a quantum gate that implements the function $f$ such that:

$$U_f|x\rangle|y\rangle = |x\rangle|y \oplus f(x)\rangle$$

Applying $U_f$ to $|\psi_1\rangle$ gives:

$$|\psi_2\rangle = U_f\left(\frac{1}{2}\left(|0\rangle + |1\rangle\right) \otimes \left(|0\rangle - |1\rangle\right)\right)$$

$$= \frac{1}{2}\left(|0\rangle \otimes |0 \oplus f(0)\rangle - |0\rangle \otimes |1 \oplus f(0)\rangle + |1\rangle \otimes |0 \oplus f(1)\rangle - |1\rangle \otimes |1 \oplus f(1)\rangle\right)$$

$$= \frac{1}{2} (|0\rangle \otimes |f(0)\rangle - |0\rangle \otimes |\neg f(0)\rangle + |1\rangle \otimes |f(1)\rangle - |1\rangle \otimes |\neg f(1)\rangle)$$

4. **Apply Hadamard gate to the first qubit:** Apply the Hadamard gate to the first qubit of $|\psi_2\rangle$:

$$|\psi_3\rangle = H \otimes I \left( \frac{1}{2} (|0\rangle \otimes |f(0)\rangle - |0\rangle \otimes |\neg f(0)\rangle + |1\rangle \otimes |f(1)\rangle - |1\rangle \otimes |\neg f(1)\rangle) \right)$$

$$= \frac{1}{2} \left( \frac{|0\rangle + |1\rangle}{\sqrt{2}} \otimes |f(0)\rangle - \frac{|0\rangle + |1\rangle}{\sqrt{2}} \otimes |\neg f(0)\rangle + \frac{|0\rangle - |1\rangle}{\sqrt{2}} \otimes |f(1)\rangle - \frac{|0\rangle - |1\rangle}{\sqrt{2}} \otimes |\neg f(1)\rangle \right)$$

$$= \frac{1}{2\sqrt{2}} ((|0\rangle + |1\rangle)(|f(0)\rangle - |\neg f(0)\rangle) + (|0\rangle - |1\rangle)(|f(1)\rangle - |\neg f(1)\rangle))$$

5. **Measure the first qubit:** Finally, measure the first qubit. If the result is 0, then the function $f$ is constant. If the result is 1, then the function $f$ is balanced. Here is the two cases than can occur :

**Case 1: $f$ is constant**
If $f$ is constant, $f(0) = f(1)$. Let's assume $f(0) = f(1) = c$. Therefore:

$$|\psi_3\rangle = \frac{1}{2\sqrt{2}} ((|0\rangle + |1\rangle)(|c\rangle - |\neg c\rangle) + (|0\rangle - |1\rangle)(|c\rangle - |\neg c\rangle))$$

Since $|c\rangle - |\neg c\rangle$ will be zero for constant functions:

$$|\psi_3\rangle = \frac{1}{2\sqrt{2}} ((|0\rangle + |1\rangle)0 + (|0\rangle - |1\rangle)0) = 0$$

Thus, when we measure the first qubit, we get 0 with probability 1, indicating that $f$ is constant.

**Case 2: $f$ is balanced**
If $f$ is balanced, $f(0) \neq f(1)$. Assume $f(0) = 0$ and $f(1) = 1$. Therefore:

$$|\psi_3\rangle = \frac{1}{2\sqrt{2}} ((|0\rangle + |1\rangle)(|0\rangle - |1\rangle) + (|0\rangle - |1\rangle)(|1\rangle - |0\rangle))$$

$$= \frac{1}{2\sqrt{2}} ((|0\rangle + |1\rangle)(|0\rangle - |1\rangle) + (|0\rangle - |1\rangle)(-|0\rangle + |1\rangle))$$

$$= \frac{1}{2\sqrt{2}} (|0\rangle|0\rangle - |0\rangle|1\rangle + |1\rangle|0\rangle - |1\rangle|1\rangle - |0\rangle|0\rangle + |0\rangle|1\rangle - |1\rangle|0\rangle + |1\rangle|1\rangle)$$

$$= \frac{1}{2\sqrt{2}} (0 + 0 + 0 + 0 - 0 + 0 - 0 + 0) = 0$$

Thus, when measuring the first qubit, we get 1 with probability 1, indicating that $f$ is balanced.

As explained earlier, the Deutsch algorithm can be extended to the Deutsch-Jozsa algorithm, which generalises the problem to functions with $n$ input bits. This extension demonstrates a significant advantage of the quantum approach: the time complexity remains constant, $O(1)$, regardless of the number of input bits. In contrast, the time complexity for the corresponding classical algorithm increases exponentially, highlighting the efficiency and power of quantum computation. However, this will not be demonstrated here again because the development is very similar to that of the Deutsch algorithm [25].

### 1.2.3 Error Correction in Quantum Computing

Now that quantum algorithms have been introduced with an example, it's important to note that, for the moment, they remain highly theoretical. In fact, the cryostat does not fully isolate the qubits from the outside world, which can induce decoherence or thermal noise. But it's also possible that material imperfections occur or even quantum noise, which is inherent in the quantum nature of things. That's why it's so important to be as precise as possible in order to limit these external disturbances as much as possible.

In particular, these disturbances can cause these different types of errors:

- **Dephasing Errors :** Loss of coherence in the quantum superposition.
- **Amplitude Errors :** Unintentional changes in the probabilities associated with quantum states.
- **Quantum Gate Errors :** Inaccuracies in the application of quantum operations.
- **Measurement Errors :** Inaccuracies when reading the state of qubits.

In order to correct and prevent these errors, certain techniques are available and listed here below [26] :

- **Stabiliser codes :** Stabilizer codes use a group of operations that can detect and correct errors in quantum states. They measure specific properties (syndromes) of the qubits to identify errors and apply corrections accordingly.
- **CSS (Calderbank-Shor-Steane) codes :** CSS codes combine two classical error-correcting codes to fix both bit-flip and phase-flip errors. They simplify error correction by handling different types of errors separately, making them efficient and effective.
- **Logical operators :** Logical operators manipulate encoded quantum information without leaving the protected code space. They perform operations on the encoded data, ensuring the integrity and correctness of the computation.
- **Quantum LDPC (low-density parity check) codes :** Quantum LDPC codes use sparse matrices to detect and correct errors. They are efficient in terms of resources and can be combined with other codes to enhance error correction performance.
- **Bosonic codes :** Bosonic codes encode quantum information into states of light or other continuous variables. They protect against errors by leveraging the unique properties of these states, often improving the robustness of quantum information.

Even if quantum error correction (QEC) techniques are essential in ensuring fault-tolerant quantum computing, they have some fundamental limitations.

One major limitation is their high resource requirements, as they often require many more physical qubits than would be necessary to encode one logical qubit. This increased demand presents scalability problems for real-world quantum computers. Additionally, the decoding algorithms associated with QEC are often computationally intensive and thus may not be practical in terms of efficiency and applicability.

Another significant limitation is that these techniques depend on keeping error rates below critical values. Beyond those points, increasing rates of physical qubit errors make any potential solution less effective; thus, attaining robust fault tolerance becomes very difficult.

Furthermore, several QEC techniques involve complicated experimental implementations, which tend to be hard to realise in real life due to the need for accurate control mechanisms or sophisticated equipment.

## 1.3 Quantum Computers

Now that all the concepts seen in the previous chapters have been explained, it's now possible to understand how a quantum computer works. However, as already explained, there are different types of quantum computers. All of those have their own pair of advantages and disadvantages. In this report, three types of quantum computers will be explained, since those are the most common at the moment. The quantum computers that will be presented are the trapped ions, the photonics and the superconducting ones. A summary table can be found in Table 1.1.

### 1.3.1 Trapped Ions

Trapped ions quantum computers employ single ions as qubits while utilising electromagnetic fields to trap and manipulate them [27]. The process begins with trapping ions such as calcium, beryllium, or ytterbium using electromagnetic fields generated by ion traps. Two main types of ion traps are usually used: the Paul trap, which combines static electric with oscillating radio frequency (RF) fields, and the Penning trap, which combines static electric with magnetic fields.

Once the ions are contained within these spaces, they should be cooled using laser cooling techniques until they reach very low temperatures close to absolute zero. It is crucial to decrease the thermal motion of ions in order for them to stay in fixed positions, which are also stable and accurately defined. The initial quantum state of the ions is prepared using laser pulses through a process called optical pumping, where usually this process leads the ions into their ground states, thereby denoting it as $|0\rangle$.

Quantum gates and operations utilise laser beams that are controlled with precision to generate and transmit specific frequencies. In the case of single-qubit gates, the lasers tuned to particular transition frequencies cause Rabi oscillations. The ions move between the $|0\rangle$ and $|1\rangle$ states. When the duration and intensity of these laser pulses are adjusted, it is possible to set the ions into any desired superposition state. Multi-qubit gates, like the controlled-NOT (CNOT) gate, depend on the collective motion of the ions. Find some of those gates in Appendix A.

Entanglement is essential for quantum computation and is achieved through these shared motional states. When certain laser pulses are applied simultaneously to several ions, their collective vibrational modes allow their quantum states to become entangled. This entanglement forms one of the pillars for quantum algorithms and computations during the execution of quantum computing processes.

The measurement of quantum states in trapped ions quantum computers is performed using state-dependent fluorescence. A laser beam at a specific frequency causes ions in the state $|1\rangle$ to fluoresce, emitting light, while ions in the state $|0\rangle$ remain dark. Photodetectors then measure the presence or absence of fluorescence, allowing for the determination of the quantum state of each ion.

Trapped ions quantum computers are renowned for their high precision and long coherence times, making them a robust platform for quantum computation. However, they face challenges in terms of scalability and the complexity of controlling multiple ions simultaneously. Despite these challenges, the well-understood physics and high-fidelity operations of trapped ions make them a prominent candidate in the ongoing development of quantum computing technologies.

### 1.3.2 Photonic

Photonic quantum computers employ photons to be treated as qubits, which comprise basic particles of light; they modify their quantum states through various optical components [28]. The principal idea behind this approach deals with storing quantum information in the attributes of photons, for instance, polarisation, phase, or path.

Generally, photons are produced from sources such as spontaneous parametric down-conversion (SPDC) or quantum dots. SPDC is a nonlinear optical phenomenon where two entangled ions emerge from laser rays travelling through a nonlinear crystal. On the contrary, single photons can be emitted upon request by quantum dots. Consequently, it remains imperative that single photons are generated in an efficient way, ensuring photonic quantum computing operates reliably.

After they are made, photons can be changed around with the help of a mixture of things such as non-linear procedures and linear optical equipment. A few examples of linear optical devices are beam splitters, wave-plates, and phase shifters, respectively. Whereas beam splitters are used for changing multiple paths of light, creating superpositions, wave plates serve to modify polarisation states. Phase shifters change the phase of photon wave functions by allowing them to create different quantum gates.

Photo-controlled quantum computing is faced with the challenge of building two-qubit gates because photons interact weakly. To create effective interactions, one often employs nonlinear optical processes or intermediaries, for instance atoms or quantum dots. For instance, one can achieve a controlled-Z (CZ) gate by using a combination of linear optics and measurements or by taking advantage of Kerrs effect in nonlinear materials. Find in Annex A the description of the CZ Gate.

Using methods such as statistical photon counting (SPDC), or postselection in linear optics, pairs of photons that are entangled can be produced right away. These types of photons play a role in quantum algorithms and are also used for quantum teleportation.

The measurement in photonic quantum computers is performed using detectors that can detect a single photon. Such detectors identify the quantum state of these photons by observing their polarisation, path or other enclosed features. Successful detection therefore depends on photon detection accuracy so that one can accurately decode quantum information.

There are various benefits to photonic quantum computing, such as operating at room temperature and the natural scale of photon-based systems. Long distances can be travelled by photons with minimal loss, making them perfect for quantum communication and networking purposes. Furthermore, optical operations can be carried out at very high speeds, which enables fast quantum calculation.

However, photonic quantum computers have shortcomings such as generating and guaranteeing the detection of single photons, as well as doubting the performance of the two-qubit gates. Nevertheless, lots of research is going on in this area to find solutions to all these issues affecting photonic quantum computing which seem to be just beginning to grow with opportunities.

### 1.3.3 Superconducting

Superconducting quantum computers (SQC) tap into the workings of superconductivity to generate and manipulate qubits with superconducting circuits [29]. These circuits cool down to temperatures closely approaching absolute zero, at which point they show vital behaviours for a quantum computer based on quantum mechanics.

SQC rests on superconducting circuits built from materials having zero electrical resistance when taken below a critical temperature. Josephson junctions are nonlinear components used in these circuits that precisely control the quantum states involved. A Josephson junction is composed of two superconductors separated by an insulator that is extremely thin, enabling the passage through it of the Cooper pairs electrons that are highly coldly linked together pair-wise.

Often, superconducting circuits called transmons or flux qubits are used to represent qubits in SQC. A transmon qubit is a nonlinear oscillator whose energy levels form the basis for its quantum information storage. The various levels of this oscillator represent the different states of a qubit. On the other hand, the different states of flux qubits correspond to different magnetic flux values that can go through a particular superconducting loop.

Microwave pulses, which act as quantum gates that are necessary for carrying out quantum computations, are used in these quantum computers. They have specific frequencies, which cause them to induce transitions between superconducting qubits quantum states. Accurate single-qubit gates manipulate an individual qubits state with precise microwave pulses while multi-qubit gates like the CNOT gate use resonant coupling or ancilla qubits (extra bits being used to implement irreversible logical operations) mediated by interactions among qubits.

Entanglement, is accomplished through these interactions among qubits. By applying microwave pulses with care and altering coupling parameters, qubits can become entangled, thereby allowing for intricate quantum operations and the execution of algorithms. In superconducting circuits, entanglement is essential for carrying out algorithms and protocols that necessitate correlated qubit states.

Superconducting quantum computers perform measurement techniques like dispersive readout. Coupling the qubit to the readout resonator measures its frequency shifts depending upon the state of the qubit. Through probing the resonators response with microwave pulses, it can reveal information about the qubits state based on the shift in the resonator itself.

The quickness of gate dealings and their high allegiance are the things that people often notice about superconducting quantum computers. This is due to the well-known way superconductive circuits work, as well as the methods used in making them. However, they face challenges such as hot and heavy dilution fridges, which are supposed to keep the low temperatures required for superconductivity; moreover, it is hard to control mistakes and noise levels. These problems raise calls for further studies of error correction techniques and fault tolerance mechanisms.

In comparison with other types of quantum computers, though, superconducting quantum computers stand out as very developed kinds of error-rate correction system integration gadgets. Various major world companies, in addition to universities, take part in this development process by significantly contributing towards improving their own designs of superconductor-based processors. Their possibility of fitting into current semiconductor designs while executing fast quantum computations makes them a guiding structure for all ongoing work on quantum computer architectures.

| **Aspect** | **Trapped Ions** | **Photonic** | **Superconducting** |
|---|---|---|---|
| **Working Principle** | Ions trapped using electromagnetic fields, manipulated with lasers. | Photons used as qubits, manipulated with optical components. | Superconducting circuits cooled to near absolute zero, manipulated with microwave pulses. |
| **Advantages** | - High Fidelity<br>- Long Coherence Times<br>- Well-Understood Physics | - Room Temperature Operation<br>- Scalability<br>- Integration with Communication<br>- Fast Operations | - Mature Technology<br>- Fast Gate Operations<br>- Integration with Existing Technology |
| **Disadvantages** | - Scalability Challenges<br>- Slower Gate Operations<br>- Complex Control Requirements | - Photon Generation Challenges<br>- Photon Detection Issues<br>- Difficult Photon Interaction | - Requires Complex Cooling<br>- Error Rates and Noise<br>- Scalability Challenges |

Table 1.1: Comparison of Trapped Ions, Photonic, and Superconducting Quantum Computers

## 1.4 Superconducting Quantum Computers

Now that all the basic concepts have been presented, this work will focus exclusively on superconducting quantum computers. This choice is based on the fact that these computers are currently the most advanced due to their scalability and the extensive knowledge already acquired in quantum physics about superconductivity.

In superconducting quantum computers, the primary objective is to minimise interactions between the quantum circuits and their external environment. Achieving this requires several key measures: cooling the superconducting circuits to temperatures near absolute zero, shielding the system from electromagnetic interference, and ensuring isolation from external temperature fluctuations. Despite these efforts, quantum error correction remains necessary to address any residual errors and maintain computational accuracy.

### 1.4.1 Cooling Systems

The SQC's challenge is to keep the temperature as low as possible and avoid any fluctuations. This is why the whole process is monitored by a control unit (CU).

To begin with, the cryostat needs to be plunged into a vacuum using a turbo pump, which reduces the pressure to around millibar, thus minimising interaction between the particles.

Next comes the pre-cooling phase, which introduces a bath of cryogenic liquid into the cryostat. This liquid cools the system by means of heat exchangers and valves that control the flow of liquid to regulate and stabilise temperature [30]. Once the cooling is done, the gas is usually recovered from a vent so it can be cleaned, compressed, and reused again. These liquids used are liquid nitrogen and liquid helium, with boiling temperatures of 77K and 4.2K respectively. It is possible to operate with helium only, but it is preferable to cool down first with liquid nitrogen and then with liquid helium. This allows better temperature control and avoids drastic thermal shocks.

Once the temperature has reached around 4K, it's time to switch to the dilution refrigerator which will bring the temperature down to around 20 mK [31]. This process benefits, again, from the use of helium but from two different isotopes: the common $^4$He but also $^3$He. As it can be seen in Figure 1.4, below 870 mK, the mixture of $^3$He/$^4$He is separated into a $^3$He rich phase (green) and a $^3$He poor phase (yellow).

The $^4$He bath, as seen before, surrounded by the nitrogen bath, surrounds the entire dilution refrigerator system. Part of the $^4$He bath is injected into a cavity known as the 1K bath, as the pressure in this cavity is reduced, allowing the $^4$He to reach a temperature of around 1K. This cavity is used to cool and condense the

$^3$He used for the system to work.

The operating principle uses the fact that when $^3$He passes from the concentrated phase to the dilute phase, it absorbs heat, the reaction is endothermic. This takes place in the mixing chamber (see Figure 1.3) into which the $^4$He was injected before.

The $^3$He present in the dilute phase is then evaporated in the still using a heater, due to its lower boiling point compared to $^4$He. It is then pumped and purified before being condensed to cycle through the circuit again. Gradually, the temperature decreases to mK levels (a nice YouTube video from the University College London explains nicely this principle [32]).

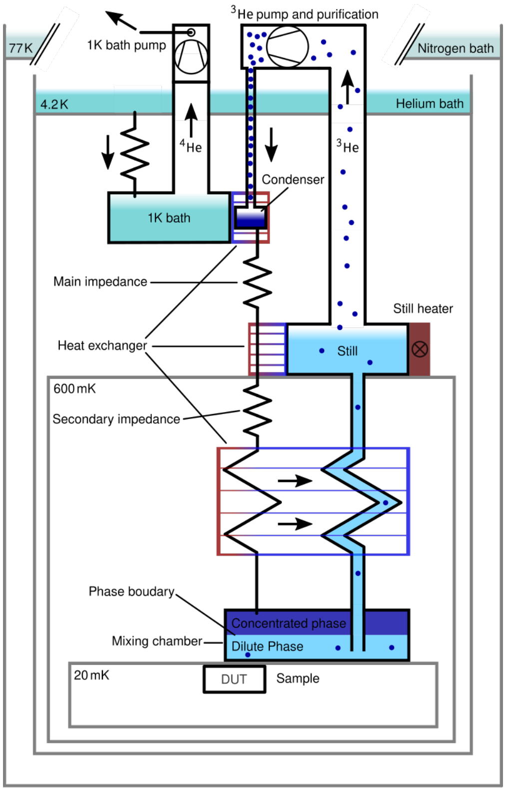


Figure 1.3: Helium Dilution Refrigirator [33]

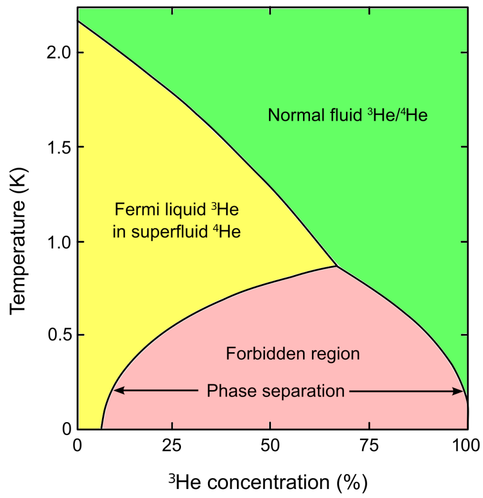


Figure 1.4: Helium Phase Diagram [33]

### 1.4.2 Shields from External Fluctuations

Since the environment is now cryogenic, it is important to protect the RF signals passing through the cryostat. In that effect, wires are made of niobium alloy, most of the time niobium-titanium alloy. They are used because NbTi becomes superconducting at relatively high temperatures (9-10K) and can resist high magnetic fields (15T) [34].

Moreover, the quantum bits that are at the lowest temperature level are additionally protected by a cryoperm shielding or mu-metal shield in order to prevent magnetic noises.

Finally, Faraday cages and/or copper and aluminum shields can be added to prevent high frequency electromagnetic interference around the quibit housing.

## 1.5 Challenges and Limitations

Developing and using SQC comes with a variety of challenges and limitations that affect how practical and advanced this technology can become. These issues generally fall into three main categories: technical challenges, scalability problems, and environmental impacts. All of them are crucial for shaping the future of this technology.

### 1.5.1 Technical Challenges

The difficulties that are faced by superconducting quantum computers mainly deal with maintaining the coherence of qubits while also trying to keep their error rates as low as possible. Superconducting qubits are prone to decoherence, which refers to the loss of quantum information owing to an interaction with surrounding elements. It is therefore a rising task to ensure that such qubits retain their quantum state long enough for meaningful computations. There is also the added factor of external disturbances and variations that can destroy the fragile quantum states, necessitating very controlled environments and accurate manipulation.

One of the other really key technical problems is error rates in superconducting qubits. These qubits are vulnerable to operational errors, which could affect the reliability of quantum computations. To correct for these errors, advanced quantum error correction protocols are required. Adding extra qubits as a form of redundancy, however, means that such implementations become more complex and entail higher resource demands on the system. Finding effective error correction methods that are both scalable and practical is still a major focus for researchers.

Another technical challenge includes facing the complexity of qubit control and readout. Superconducting qubits require precise microwave control signals to perform operations, so managing these signals becomes increasingly complex with the increasing number of qubits. Additionally, there is a demand for maintaining the accuracy of qubit measurements over a large number of qubits, which results in huge engineering challenges. Therefore, it necessitates developments in control electronics and measurement methods to solve such issues.

### 1.5.2 Scalability Issues

The creation of larger scale quantum computers using superconductors has some major problems. When there are more qubits in a quantum computer, they become more difficult to keep from interacting with the environment. This means that as one component is added to the system, the problems associated with managing their quantum states also increase, which makes it more difficult to avoid decohering them all.

As already explained the implementation of efficient error correction requires additional qubits that consequently increase the demand for resources exponentially. As a result, increasing the size of the system will not only require adding more qubits, but also intricate error-correcting systems that magnify the difficulty of constructing bigger quantum computers.

Thermal management and creation capability also have problems. With more qubits, superconducting systems operate at very low temperatures while thermal loads rise. Scaling is highly dependent on efficient cooling methods and reliable fabrication techniques because any small changes or flaws in the production can influence both performance and stability.

### 1.5.3 Environmental impact

The environmental footprint of quantum computing encompasses several aspects, including energy consumption, resource utilisation, and waste generation. This master thesis challenges that information and will try to provide some news.

### Energy Consumption

As already explained SQC requires significant amounts of energy to operate due to the need for cryogenic cooling systems to maintain the qubits at ultra-low temperatures. The operation of dilution refrigerators and other cooling infrastructure contributes to the overall energy consumption of quantum computing facilities. According to a study by Martin et al., the energy required for cooling quantum computers is substantially higher than that needed for computation itself [35]. This is a stark contrast to classical computing systems, where the majority of energy is consumed by computation rather than cooling. To minimise energy usage, it's essential to design quantum systems that reduce cooling demands and enhance thermal management efficiency.

### Resource Utilization & Waste Generation

The manufacturing and operation of quantum computing hardware require various resources, including rare earth metals, semiconductors, and specialised equipment. For example, superconducting qubits are fabricated using materials such as niobium and aluminium, which have specific requirements for purification and processing. The production of these materials and the manufacturing processes involved contribute to resource consumption and environmental impact. Additionally, the construction and maintenance of quantum computing facilities entail resource-intensive activities, such as infrastructure development and cooling system installation.

The lifecycle of quantum computing technologies also involves waste generation, including electronic waste (e-waste) from the disposal of outdated or malfunctioning hardware, as well as waste from manufacturing processes and facility operations. The disposal of electronic components and hazardous materials poses environmental challenges, requiring proper recycling and disposal practices to mitigate negative impacts on ecosystems and human health.

Unfortunately, there is very little, if any, discussion of these subjects in the literature, which makes it difficult to carry out this work. This work will therefore be an additional building block for future projects.

## 1.6 Current Developments

In Europe, the TU Delft in the Netherlands stands out as a notable hub for quantum computing research and development. Their efforts have contributed to the advancement of quantum computing technologies and the realisation of operational quantum computers [36]. TU Delft's quantum computing initiatives encompass a wide range of research areas, including quantum hardware development, quantum algorithms, and quantum error correction. The QuTech research center, a collaboration between TU Delft and the Netherlands organization for Applied Scientific Research (TNO), plays a role in quantum technology research and fosters collaborations with industry partners. TU Delft's pioneering work in quantum computing has established it as a leading institution in the global quantum computing landscape, attracting top researchers and students from around the world. In our pursuit of quantum computing research, we initially considered basing our design on the work conducted at TU Delft. However, due to confidentiality constraints, a collaborative partnership could not be established.

Although not directly involved in quantum computer research, our institution (UCLouvain) possesses a cryostat identical to the BlueFors LD400 utilised by TU Delft. The same cryostat is used in the Gerhing Lab to work on supraconductor. The Gehring Lab focusses on understanding the physics of mesoscopic and nanoscale functional devices [37]. It investigates functionalities like the spin-to-charge conversion in topological materials or the thermoelectric heat-to-charge conversion in single-molecule devices using cryogenic magnetotransport experiments and scanning probe microscopy.

As you will see in the following sections, this work is based on these two references to describe the SQC used.

# Chapter 2

# Life Cycle Assessment Methodology

There are several tools and approaches available for assessing the environmental footprint of an SQC, but the Life Cycle Assessment approach is chosen for its ability to comprehensively estimate environmental impacts throughout the entire life cycle of a product or process. This approach gathers information from raw material acquisition to end-of-life, including all input and output environmental flows at each phase (see fig. 2.1). This chapter describes LCA principles. They will be applied later in Chapter 3.

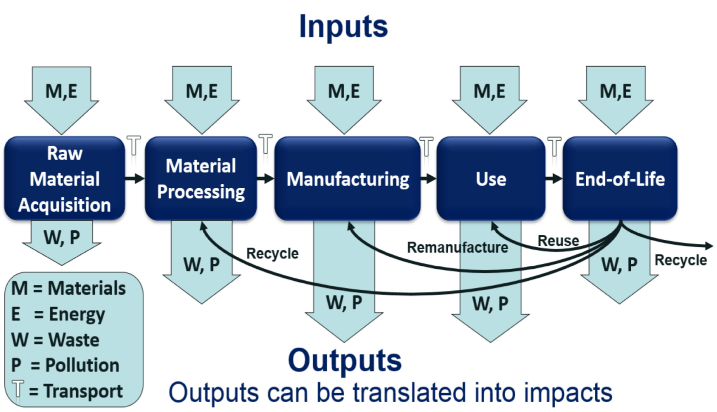


Figure 2.1: Life cycle phases of a generic product system [38]

## 2.1 Life Cycle Assessment Theory

The historical development of LCA can be divided into two main periods: 1970-1990 and 1990-2000 [39, 40].

During the 1970s to 1990s, LCA emerged in response to growing public concerns about environmental issues such as energy efficiency, pollution control, and waste management. Early studies, albeit unpublished, focused on analysing resource usage, emissions, and waste generated by products, notably highlighted in a study by the Midwest Research Institute (MRI) for Coca-Cola in 1969. Despite initial interest, there was a lack of international collaboration and standardisation, leading to varied approaches and inconsistent results. LCA was often used by companies to support marketing claims, but discrepancies in findings hindered its widespread acceptance.

In contrast, the period from 1990 to 2000 marked a shift towards standardisation and collaboration. This decade saw increased scientific activity, coordination efforts, and the establishment of guidelines and standards by organisations such as the Society of Environmental Toxicology and Chemistry (SETAC) and the International Organisation for Standardisation (ISO). These efforts aimed to harmonise methodologies and terminologies, resulting in the publication of ISO standards 14040 and 14044 (ISO 14040 focusses on the overall framework, while ISO 14044 delves into the detailed procedures and practices for conducting an LCA), which provided a framework for conducting LCAs. Additionally, LCA began to influence policy-making, particularly in areas such as packaging legislation. Despite these advancements, ongoing research and debate continued to refine LCA methodologies and explore new concepts such as consequential LCA and allocation methods.

In summary, the 1990s represented a period of standardisation and convergence in LCA practices, laying the groundwork for its integration into policy and further scientific development. However, challenges and ongoing refinement persist in the field, reflecting the complexity of assessing environmental impacts across product life cycles.

In recent years, there has been a notable increase in the number of LCA-related scientific papers in the literature. This trend is driven by the growing recognition of climate change and the urgent need to address environmental sustainability. As technological innovations continue to emerge, it becomes crucial to not only develop these new technologies but also to comprehensively understand their environmental impacts. LCA provides a framework for estimating these impacts, from the acquisition of raw materials to the end-of-life of products. By performing a hotspot analysis, it identifies the elements of a product's life cycle that contribute most to its environmental impact. By comparing an existing technology with a new one, we can assess which is more environmentally beneficial. The HS analysis helps visualise the distribution of impacts between the two technologies, highlighting the factors that contribute to the improvement. However, compromises often need to be made because one technology could outperform another regarding environmental performance in certain impact categories while performing less well in others. This awareness is essential for making informed decisions that align with our sustainability goals and mitigate the negative environmental effects of technological advancements on our planet.

The following sections will delve into the application of the LCA approach, which primarily consists of four steps: defining the goal and scope, conducting an inventory analysis, performing the impact assessment, and concluding with the interpretations and discussion. This methodology is represented in the following chart (Figure 2.2).

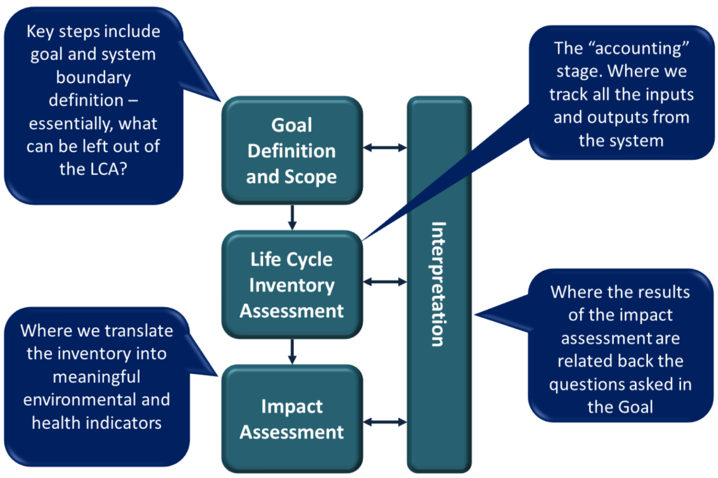


Figure 2.2: LCA framework [38]

### 2.1.1 Goal and Scope

In LCA, the initial stage of goal and scope definition serves as the cornerstone of the entire study. This step establishes the purpose, context, and boundaries of the assessment, ensuring clarity, consistency, and relevance throughout the process [38, 41].

### Goal Definition

This first step identifies the fundamental reasons for conducting the study, the specific questions it aims to address, and the intended audience. The goal not only sets the direction for the assessment but also reflects the environmental objectives, policies, and values of the organisation spearheading the study. For instance, a goal might be to evaluate the environmental impacts of pavement construction to inform strategic planning and public policy decisions.

### Scope Definition

Complementing the goal definition, the scope of the LCA outlines the boundaries and key aspects of the analysis. It encompasses :

- Functional Unit: A quantified measure of the function provided by a product, system, or service. It serves as the reference point for all input and output data in the LCA, ensuring that comparisons between different products or systems are based on the same functional outcome. The selection of the functional unit is critical, as it directly influences the scope, data collection, and interpretation of the LCA results.
- Product System Scoping: Deciding which activities and processes are to be included in the life cycle of the product under study.
- Assessment Parameters Selection: Identifying the environmental impacts to be evaluated and shaping the focus of the analysis.
- Geographical and Temporal Boundaries: Specifying the geographic and temporal scope of the study, along with relevant technological contexts.
- Perspective Selection: Determining whether the study will adopt a consequential or attributional perspective, influencing the assessment approach.
- Critical Review Consideration: Recognizing the need for critical review, especially for comparative studies intended for public disclosure.

By defining the scope, the LCA ensures consistency and relevance in data collection, modelling, and assessment methods. This meticulous approach enhances the validity of the study's conclusions, providing a solid foundation for informed decision-making, strategic planning, and environmental stewardship.

### 2.1.2 Inventory Analysis

The inventory analysis aims at quantifying the input and output environmental flows associated with the product system under study. It involves identifying and assessing all materials, through a bill of materials (BoM), if available, and energy flows throughout the life cycle stages, encompassing resource extraction, production, use, and end-of-life phases.

During the inventory analysis, environmental flows such as material inputs, energy consumption, and waste are identified and quantified. This entails establishing a detailed life-cycle model of the system being evaluated, detailing the functional unit. For instance, in the case of an asphalt or concrete mixing plant, inputs may include energy sources like electricity and fuel, raw materials such as aggregates and cementitious materials, as well as outputs like emissions and waste.

Data collection for the inventory analysis is varied, drawing from diverse sources including public databases, commercial data, and on-site measurements. Given the complexity of most product systems, reliance on generic data for certain processes is common, often sourced from databases housing unit processes or cradle-to-gate information. Techniques such as environmentally extended input-output analysis may complement the data collection process, providing additional insights and validation.

The outcome of the inventory analysis is the life cycle inventory (LCI), comprising a detailed list of quantified physical flows associated with the product system's provision of the desired service or function, aligned with the defined functional unit. These data serve as the foundation for subsequent phases of the LCA, enabling the evaluation of environmental impacts and informing decision-making processes towards sustainable product development and management.

### 2.1.3 Impact Assessment

Life Cycle Impact Assessment (LCIA) is the phase where data from the LCI is used to evaluate potential environmental impacts. During this step, emissions and resource uses from the LCI are categorised into specific environmental impact categories. The LCIA methods vary, but they typically follow midpoint or endpoint approaches. Midpoint methods assess impacts at an intermediate stage (e.g., global warming potential), while endpoint methods aggregate these into broader damage categories (e.g., human health).

The choice of LCIA method and impact categories depends on the goal and scope of the study. The process of LCIA includes several steps, as shown in 2.3.

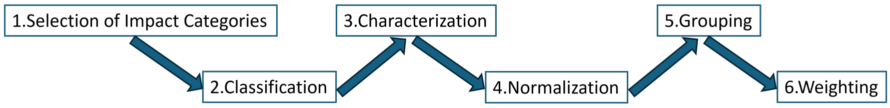


Figure 2.3: The six step of the life cycle impact assessment

Those six steps of the LCIA are :

1. Selection of Impact Categories: Impact categories are selected based on their relevance to the Goal and Scope. Common impact categories include: Climate change, Ozone depletion, Acidification, Eutrophication, Human toxicity.

2. Classification: This step involves assigning emissions and resource use from the LCI to the selected impact categories. Each flow from the LCI is associated with the impact categories it affects. The level of aggregation depends on the type of method used [42]:

   (a) Midpoint impact categories focus on specific environmental problems, such as climate change, ozone depletion, or acidification. These indicators are located along the cause-effect chain closer to the environmental interventions, providing more detailed information on the specific types of damage.

   (b) Endpoint impact categories reflect the broader environmental impacts at a higher level of aggregation, such as impacts on human health, ecosystem quality, and resource depletion. These indicators represent the end of the cause-effect chain, offering a more comprehensive view of the potential overall damage.

   Interpreting the LCIA results is often easier with endpoint methods due to their broader perspective, but the results are less specific as they aggregate impacts into larger-scale outcomes. Figure 2.4 shows a representation of this difference.

3. Characterisation: This step quantifies the contributions of inventory flows to their respective impact scores (IS). The IS reflects the magnitude of the potential environmental impact within a specific impact category. They are computed using characterisation factors, which indicate the relative contribution of each emission and resource use in the LCI to the corresponding impact category. This step converts and aggregates LCI results within each category to estimate the potential environmental impacts. For instance,

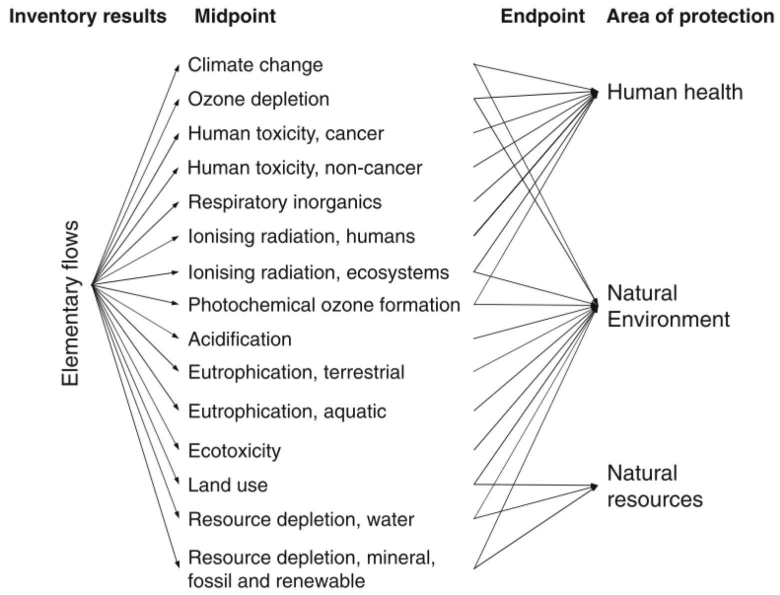


Figure 2.4: Illustration of midpoint and endpoint categories [43]

greenhouse gas emissions are converted into $CO_2$ equivalents, with each category having its own reference unit.

4. Normalisation (optional) : The characterised results are compared to a reference value, such as the total impacts in a region or globally. This comparison helps understand the magnitude of impacts relative to a larger context. The reference value depends on the method used in the LCIA. It converts result into percentages of the reference value per impact category.

5. Grouping (optional) : It involves sorting and possibly aggregating impact categories into sets. For example, all human health impacts might be grouped together. It is the difference between midpoint and endpoint impact categories.

6. Weighting (optional) : The different impact categories are assigned weights according to their relative importance. This helps in comparing different impact categories on a common scale. The weighting process introduces value judgements and subjectivity to get a single score. The score could be used to compare products under the same scope and assumptions.

### Different methods

Below is a comparison of some of the most widely used impact methods, along with their descriptions and common usage. The choice of method is made in the next chapter.

| Methodology | Description | Common Usage |
|---|---|---|
| **EF 3.0** [44] | The Environmental Footprint (EF) method is designed to evaluate the environmental impacts of products, services, and organizations. It includes 16 impact categories and is aligned with the European Commission's recommendations. | Commonly used in Europe for regulatory and compliance purposes, particularly in product environmental footprinting. |
| **ReCiPe 2016** [45] | ReCiPe 2016 provides a comprehensive evaluation of environmental impacts through midpoint and endpoint indicators (18 indicators and 3 indicators), including human health, ecosystems, and resource scarcity. The method is applicable fror three perspectives : (i) Indivudalist, (ii) Hierachist, and (iii) Egalitarian. | Widely used in both academic research and industry due to its detailed and versatile nature. It is a representative method for a global scale instead of the European scale, as it was for ReCiPe 2008. |
| **CML-IA** [46] | The CML-IA method focusses on midpoint indicators and provides a framework for assessing impacts like climate change, ozone depletion, and acidification. The normalisation is provided, but there is no weighting | Popular in European academic and industry applications for its straightforward approach to impact assessment. |
| **ILCD** [47] | The International Reference Life Cycle Data System (ILCD) guidelines offer a comprehensive framework for LCA, emphasising consistency and reliability in impact assessment. Created in 2005. | Used globally, especially for detailed and harmonised environmental reporting. |

Table 2.1: Comparison of Different Impact Assessment Methodologies - Part 1

| Methodology | Description | Geographical Common Usage |
|---|---|---|
| **EDIP 2003** [48] | The Environmental Design of Industrial Products (EDIP) 2003 method focusses on life cycle impact assessment with a strong emphasis on product design and improvement, including categories like global warming, acidification, and eutrophication. It has 19 impact categories. | Commonly used in Europe (it is a Danish method), particularly in the context of product design and development. |
| **Impact 2002+** [49] | Impact 2002+ integrates midpoint and endpoint approaches in a consistent framework, covering human health, ecosystem quality, climate change, and resource depletion. Created by EPFL - Lausanne, it links via 14 midpoint categories to four damage categories. | Widely used in Europe and Asia for both academic research and industrial applications. |
| **Impact World+** [50] | Impact World+ is an update of Impact 2002+ and offers a global perspective on life cycle impact assessment, including regionalised impact categories. | Increasingly adopted globally due to its comprehensive and regionalised approach. |
| **BEES** [51] | The Building for Environmental and Economic Sustainability (BEES) method developed by the National Institute of Standards and Technology (NIST) includes both environmental and economic performance measures for building products. It includes classification, characterisation and normalization. | Primarily used in North America for evaluating the sustainability of building products. |
| **TRACI** [52] | The Tool for the Reduction and Assessment of Chemical and other environmental Impacts (TRACI) developed by the U.S. EPA includes impact categories such as global warming, acidification, and eutrophication. It is a midpoint orientated LCIA that does not aggregate between environmental impact categories. | Primarily used in North America for environmental assessments and regulatory reporting. |

Table 2.2: Comparison of Different Impact Assessment Methodologies - Part 2

### 2.1.4 Interpretation & Discussion

This step involves the analysis and evaluation of the methodological inputs and outputs at each stage of the process. If necessary, adjustments can be made to the study's goals and scope. The results from the life cycle impact assessment need to be critically examined and compared with current state-of-the-art practices for the' sake of consistency. By identifying key contributors highlighted in the LCIA results, practitioners can refine the inventory analysis, thereby enhancing the precision of the results. The iterative nature of LCA allows for continuous improvement and refinement of the assessment process. In this masters thesis, the results are first presented, followed by an interpretation that links these results with the input flows, ensuring a coherent and thorough understanding of the study's findings.

## 2.2 LCA tools

This section presents the different LCA tools used in this study. Firstly the software used for LCA, in this section on overview of software used, the one chosen and why this one, would be explain. Then, a second choice particular to this study was the coarse-grain methodology applied during the implementation of the software.

### 2.2.1 Overview of LCA Software

This section provides an introduction to several prominent LCA software tools. A brief comparison is made to highlight their features, which will justify the selection made in the following Section 3.2.5.

#### LCA for Experts

LCA for Experts is one of the leading LCA software tools, widely used in both academia and industry. Developed by Sphera, LCA for Experts provides a robust platform for modelling, analysing, and optimising product sustainability [53]. It offers to work with its own databases, including industry-specific data, and supports a wide range of impact assessment methods, but also with other databases. The software's intuitive interface and powerful features make it suitable for complex LCA projects, allowing users to perform detailed scenario analyses and identify key areas for environmental improvement. It was the first software considered for this study, due to the experience and advice from the professor and assistants.

### SimaPro & OpenLCA

SimaPro, developed by PRé Sustainability, is another LCA software tool used for environmental assessment [54]. It is designed to handle large datasets and complex product systems. SimaPro offers a variety of impact assessment methods and provides access to several comprehensive databases, such as Ecoinvent and Agri-footprint. Its versatility and extensive documentation support users in conducting rigorous LCA studies and generating reliable results.

OpenLCA, an open-source LCA software developed by GreenDelta, is known for its flexibility and transparency [55]. It supports various databases and impact assessment methods, and its open-source nature allows for customisation and integration with other tools. OpenLCA is suitable for both academic research and practical applications, providing users with the ability to develop detailed life cycle models and perform in-depth analyses. Its user community and support forums facilitate knowledge sharing and collaboration among LCA practitioners.

While both SimaPro and OpenLCA present strong capabilities, the lack of experience with these tools within UCLouvain's lab led this master thesis to focus on a software tool with more established use and familiarity.

### Activity Browser (AB)

Activity Browser, developed by the Ecoinvent Association, is a user-friendly LCA software tool designed to streamline the LCA process [56]. AB serves as a graphical user interface (GUI) for Brightway, an open-source LCA framework. It integrates with the ecoinvent database, allowing users to access high-quality data for their assessments. AB's intuitive interface and visualisation capabilities make it easy to model life cycle systems and interpret results. The software supports various impact assessment methods and provides tools for sensitivity and uncertainty analyses (Monte Carlo simulation, scenario analysis, etc.), similar to other LCA tools. However, its integration with the Brightway framework and open-source nature make it particularly attractive for users seeking transparency and customisation in their analyses. This feature also enables a good exchange between users. AB is a valuable tool for both beginners and experienced LCA practitioners, offering a comprehensive suite of analytical capabilities that are on par with or exceed those provided by other LCA software.

### 2.2.2 Coarse Grain Analysis

Conducting a LCA for complex systems, such as superconducting quantum computers, poses significant challenges due to the extensive variety of the components involved. To address this challenge, a coarse-grain methodology is adopted, allowing for a manageable analysis in terms of time and resources.

The superconducting quantum computers consist of numerous highly specialised components, ranging from superconducting qubits and cryogenic systems to control electronics and cooling infrastructure. The complexity and diversity of these components necessitate a streamlined approach to accurately capture the overall environmental footprint without going into excessive detail. The time spent delving deeper into the inventory analysis must be carefully managed, as it directly competes with the overall time available for this study. It will be developed in Section 2.2.2.

A coarse-grain methodology simplifies the system into larger, manageable subsystems. Each of them is essential for the quantum computer to operate, enabling a more straightforward analysis of its environmental impacts. Then a methodology diagram was implemented to ensure that the granularity remained the same throughout the whole system. This granularity could easily be modified based on this diagram, which would facilitate future work based on this one.

#### Implementation of Coarse-Grain Methodology

The first step in implementing the coarse-grain methodology was to identify the key subsystems of the superconducting quantum computer. Once those had been established, the diagram was made in order to always follow the same decomposition.

Figure 2.5 illustrates this methodology. The starting point is the orange frame "Input component", with each of blue boxes containing a question and the withe boxes containing the resulting actions. The Ecoquery website was used for this task since it regroups every activity from the Ecoinvent database 3.9 cut-off [57].

As described in Figure 2.5, sometimes an LCA was already made on the evaluated subsystem (or a close one), so it was possible to directly retrieve the carbon footprint.

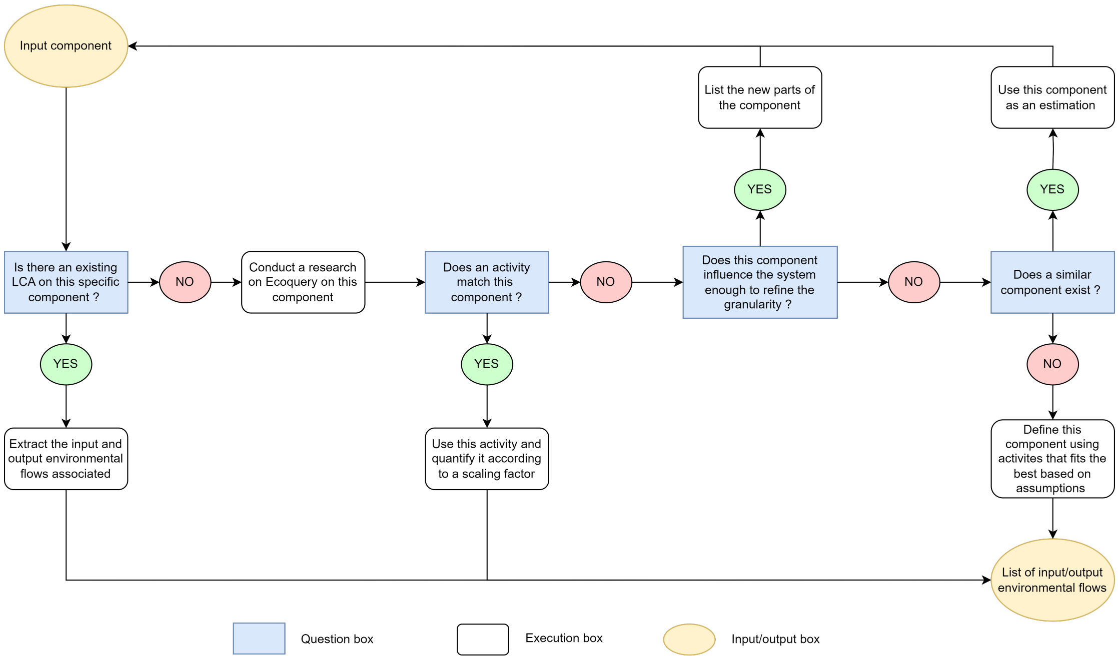


Figure 2.5: The methodology of granularity

### Limitation of Coarse-Grain Methodology

This approach has limitations :

- **Data granularity**: May overlook specific impacts of individual components due to the aggregation of data into larger blocks.
- **Uncertainty introduced by approximations**: It relies on approximations and analogies where direct data is lacking, potentially affecting the precision of the results as it has been explained.
- **Component interaction**: Simplified blocks may not fully capture the complex interactions and dependencies between different components, affecting the overall impact assessment.

# Chapter 3

# Life Cycle Assessment of a Superconducting Quantum Computer

This chapter applies the LCA methodology to a superconducting quantum computer system. The bill of material is established based on visual teardowns of hardware components. Section 3.1 introduces the goal of the study. Section 3.2 addresses the scope of the LCA, including the functional unit, boundaries, and other relevant details. Section 3.3 performs the inventory analysis for the entire system following the described methodology explained in Section 2.1.2. After completing the LCI, the LCIA results are analysed from a single indicator perspective, focussing on GWP.

## 3.1 Goal of the Study

As explained in Section 2.1.1, this section determines the goal and objectives of the study. The goal of this LCA is to estimate the GWP impacts associated with the production and use of a superconducting quantum computer using data derived from the teardown of hardware components. This LCA is conducted in the context of a Master's thesis at UCLouvain to provide insight into the environmental footprint of such cutting-edge computing technology. The LCA results could assist companies and researchers currently developing and using SQCs. These results are used to identify and discuss the environmental hotspots of this technology.

## 3.2 Scope of the Study

### 3.2.1 Functional Unit

This LCA examines the environmental impact of producing a superconducting quantum computer (SQC), assuming implementation in Belgium (Europe). However, as discussed in Section 1.6, there is currently no SQC implementation in Belgium. Therefore, this study focusses on the available information from the Ghering Lab and the SQC at TU Delft, including not only production but also the transport and use phases. The functional unit of the LCA is defined as : **Production, transport, and use - for five years in Belgium - of a superconducting quantum computer**.

The definition of the functional unit is based on the answers to the following questions :

| | |
|---|---|
| Which function is performed by the product system ? | The product system provides an operational QC to compute different algorithms. |
| What is the needed amount of the required product system to fill the function ? | One superconducting QC. |
| What is the duration of the function? | 5 years, with 253 business days, assuming 8 working hours per day. |

Table 3.1: Questions asked to define the functional unit

### 3.2.2 System Boundaries

Life-cycle phases are analysed from cradle to gate. Figure 3.1 illustrates the phases of the life cycle and highlights the production, the distribution, and the use, that are included in the scope.

As shown in Figure 3.1, the production phase includes the raw material extraction phase and the manufacturing phase. The manufacturing phase is followed by assembly and transport phases. Indeed, the sub-assemblies of the product can be manufactured elsewhere and transported to the assembly site. It is important to consider it because otherwise the result omits some emissions. The distribution phase is the transport from the country where the product is manufactured to the country where the product is consumed, in this case Belgium. The phase "assembly on site" is the phase during which the user assembles the subsystems and connects

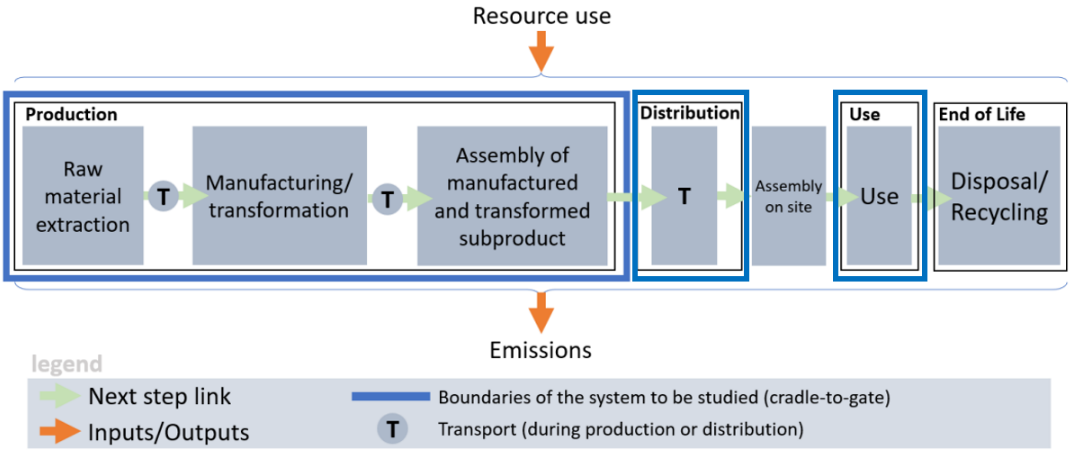


Figure 3.1: System boundaries of the LCA of the QC [58]

them together to create the operational SQC. Finally, the use corresponding to the functional unit is described.

### 3.2.3 Selection of the Database

The Ecoinvent 3.9 database is selected for this study due to its comprehensive and detailed inventory data, which covers a wide range of industrial processes and products. Ecoinvent is an exhaustive and widely used database, despite some modelling errors, which still makes it a suitable source for this work, as explained in Section 2.1.3. Moreover, the database includes datasets with environmental flows, enabling a multicriteria evaluation and thus also allowing for a thorough analysis of the GWP.

### 3.2.4 Selection of LCIA Method

The EF3.0 method evolved from the product environmental footprint (PEF) and organisation environmental footprint (OEF) guides published by the European Commission. The initial PEF and OEF guides were released in 2013 as part of a broader effort to create a harmonised framework for environmental assessment [59]. EF3.0 builds on these previous versions (EF2.0), incorporating feedback from stakeholders, advancements in scientific understanding, and updates to life cycle impact assessment methods. This version aims to improve the robustness and applicability of environmental footprinting, making it a vital tool for policymakers and industry leaders in the EU. A new version EF3.1, is enabled, but EF3.0 has been in use longer and has undergone extensive validation and testing. Its stability and well-documented methodologies make it a reliable choice for environmental footprint assessments [60, 61].

### Impact Categories in EF3.0

EF3.0 includes a set of impact categories that cover a wide range of environmental issues. These categories are designed to capture the most significant environmental impacts associated with the life cycle of products. Each impact is a biosphere flow to take into account, with a factor to put it in the unit of the impact. The main impact categories in EF3.0 are:

- **Climate Change**: Measures the impact of greenhouse gases (GHGs) on global warming, expressed as kg $CO_2$ equivalents.
- **Ozone Depletion**: Assesses the potential for substances to deplete the ozone layer, expressed as kg CFC-11 equivalents.
- **Human Toxicity, Cancer Effects**: Evaluates the potential for chemicals to cause cancer in humans, expressed as comparative toxic units (CTU).
- **Human Toxicity, Non-Cancer Effects**: Evaluates the potential for chemicals to cause non-cancer health effects in humans, expressed as CTU.
- **Particulate Matter**: Assesses the health impacts of particulate matter emissions, expressed as disease incidence.
- **Ionising Radiation, Human Health**: Measures the impact of ionising radiation on human health, expressed as kBq U235 equivalents.
- **Photochemical Ozone Formation**: Evaluates the contribution to ground-level ozone formation, expressed as kg NMVOC (non-methane volatile organic compounds) equivalents.
- **Acidification**: Measures the potential for acidifying substances to cause damage to terrestrial and aquatic ecosystems, expressed as mol $H+$ equivalents.
- **Eutrophication, Terrestrial**: Assesses the potential for nutrients to cause over-fertilisation of terrestrial ecosystems, expressed as mol N equivalents.

- **Eutrophication, Aquatic (Freshwater and Marine)**: Measures the potential for nutrients to cause over-fertilization of freshwater and marine ecosystems, expressed as kg P equivalents and kg N equivalents, respectively.
- **Ecotoxicity, Freshwater**: Evaluates the potential for toxic substances to harm freshwater ecosystems, expressed as CTU.
- **Land Use**: Assesses the impacts of land occupation and transformation, expressed as points based on a biodiversity damage potential model.
- **Water Use**: Measures the potential impact of water consumption on water scarcity, expressed as cubic meters ($m^3$) equivalents.
- **Resource Use, Minerals and Metals**: Evaluates the impact of mineral and metal resource depletion, expressed as kg Sb (antimony) equivalents.
- **Resource Use, Fossils**: Measures the impact of fossil resource depletion, expressed as $MJ$.

**Importance of EF3.0 in Environmental Assessment**

EF3.0 offers several advantages for environmental assessment:

- **Standardisation**: Provides a harmonised approach for assessing environmental impacts, facilitating comparison across studies and products. This standardisation is crucial for achieving consistency in environmental reporting across the EU [59].
- **Comprehensiveness**: Covers a wide range of impact categories, ensuring a holistic evaluation of environmental performance. This broad scope allows stakeholders to understand the full spectrum of environmental impacts associated with a product or service [62].
- **Transparency**: Encourages clear documentation and reporting, enhancing credibility and stakeholder trust. Transparency in methodology and results is essential for building confidence among consumers, policymakers, and industry partners [63].
- **Policy Relevance**: Aligns with EU environmental policies and goals, supporting regulatory compliance and sustainability initiatives. EF3.0's alignment with policy frameworks ensures that assessments are relevant and useful for decision-making processes [61].

**GWP Focus**

This study focusses on the climate change impact category, specifically the Global Warming Potential over a 100-year time horizon (GWP100), expressed in kg $CO_2$ equivalents. The "100" refers to the period over which the potential warming effects of greenhouse gases are measured. This focus is chosen for several key reasons.

Firstly, the goal of the characterisation is to determine the greenhouse impact of the superconducting quantum computer, making other indicators less relevant for this study. Given that GWP is a well-established metric, it allows for a consistent and reliable assessment of climate-related impacts. The methodologies for calculating GWP are relatively uniform across different impact assessment methods because climate change mechanisms are well-understood. This consistency provides a solid foundation for evaluating and comparing results across various studies.

Secondly, the EF 3.0 method, which is employed in this study, uses GWP100 as its standard measure for climate impact [64]. Although GWP20 (a 20-year time horizon) could be used, it is not considered here because EF3.0 is based on the GWP100 metric. The 100-year horizon is commonly used in LCA studies because it balances short-term and long-term climate impacts, providing a view of potential global warming effects.

An additional argument in favour of GWP-centred studies is that, a priori, global warming is the only environmental issue with the potential to trigger a mass extinction event. This makes GWP a critical focus for understanding the broader implications of technological developments on planetary health.

Lastly, the selected coarse-grain methodology necessitates the inclusion of external evaluations of the impact in kg $CO_2$-eq, as the methodologies for obtaining these impacts are well-established and widely accepted. The focus on GWP ensures that the results are both relevant and aligned with global standards in environmental impact assessment. While the LCA will provide a comprehensive analysis, the results for all impact categories will be shown, but they will not be interpreted in detail.

### 3.2.5 Software Selection

As already explained for this study, Activity Browser was chosen as the primary LCA tool due to several reasons.

AB's integration has a lot of advantages, as presented in Section 2.2.1. The most important factor was the possibility of carrying out sensitivity analyses, as the aim of this study is to highlight the key elements of the SQC in terms of environmental footprint. The support of various impact assessment methods also ensures that the study can adhere to international standards and best practices in LCA.

Finally, the AB software is really well suited to cooperation between multiple users. Indeed, as this study was realised by two students, it was important to have an easy exchange of information. In AB, the created databases could be exported and imported easily in Excel files, which was also clearly a point for the choice of the software since it eased the collaboration on the work.

### 3.2.6 Limitations

The main limitations of this LCA include:

- Lack of primary data on the components of the QC is due to the availability of specific primary data acquired from the teardown of hardware equipment. It was decided to limit the QC to a coarse-grain analysis for reasons of convenience.
- Time constraints prevented a more detailed analysis, due to a one year work timeline.
- Datasets available in the LCA databases impact the quality of the LCI model.

## 3.3 Inventory Analysis

Once the scope is clearly defined, it is necessary to establish a life-cycle model. Typically, inventories are constructed by collecting detailed data on all components, processes, and activities associated with the product's life cycle. This data is then used to model the environmental impacts of each phase of the life cycle, from raw material extraction to manufacturing, use, and disposal. However, in this case, constructing a detailed inventory is not feasible due to the size of the quantum computer, time constraints, and lack of specific information about the components. As a result, a coarse-grain methodology is applied to address these challenges. This approach involves breaking down the system into its main subsystems and conducting a higher-level analysis based on the available data.

The coarse-grain methodology (cfr. Section 2.2.2) is then applied to the five main subsystems identified as blocks of the quantum computer. These five blocks are represented in Figure 3.2.

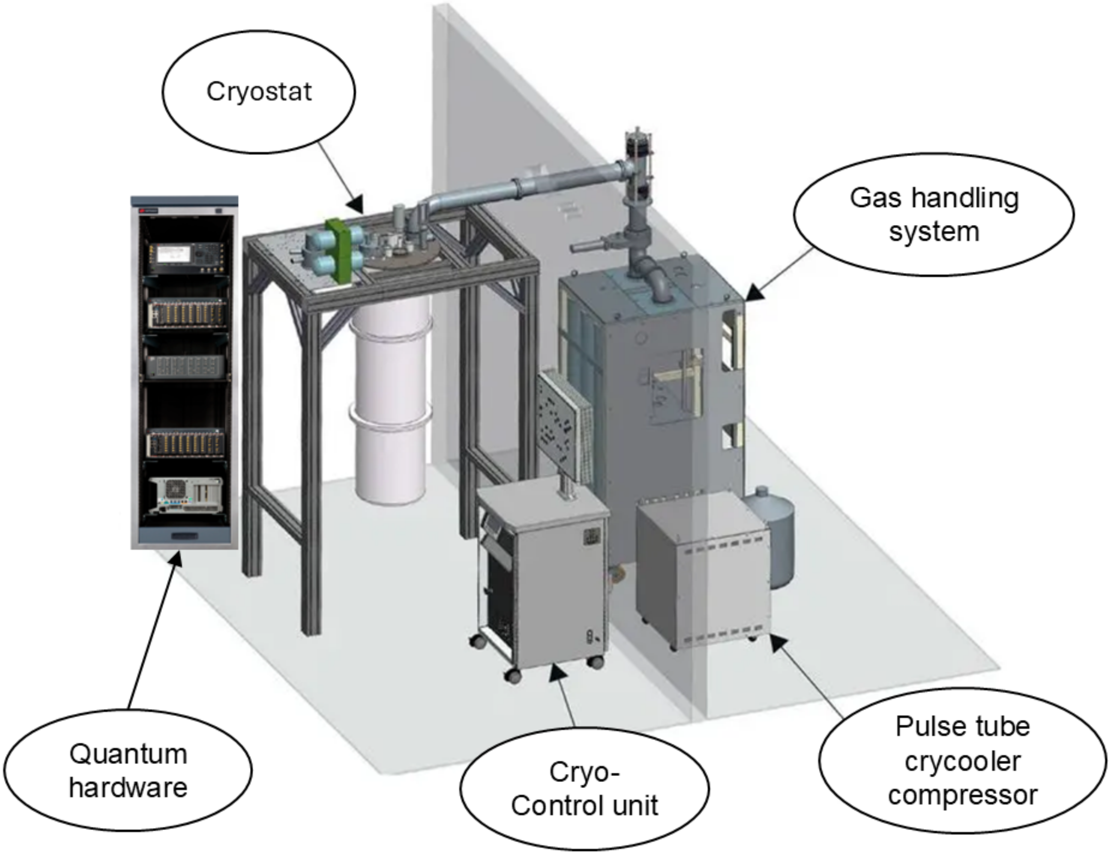


Figure 3.2: Identification of the five subsystems constituting a typical QC [65]

Once these five subsystems are identified, they can still be subdivided to facilitate LCA integration. Indeed, it will not be possible to find an activity from the Ecoinvent database matching each subsystem. To ensure consistency in the level of detail, a standardised methodology is applied across all subsystems, as defined in Figure 2.5. Inevitably, certain assumptions must be made, as not all activities in the database precisely match the exact output product. The specific assumptions made for each subsystem are detailed in Appendix B.

### 3.3.1 Cryostat

The cryostat is the subsystem that is cooled down to 50 mK with temperatures descending from top to bottom. It is at the very bottom of the cryostat, the coldest part, that the quantum operations are processed with the proper materials and components.

This cryostat can be divided into five subcategories : the structural components, the shields, the dilution refrigerator parts, the wiring, and the microwave devices. Those subdivisions are explained as follows :

- **Structural components**: This includes the holding structure that is supporting the cryostat and its shields, as well as the flanges and supports that constitute the internal structure of the cryostat itself, as represented in Figure 3.5.
- **Shields**: These shields literally act as barriers, protecting against external perturbations. There are five of them : The vacuum shield, the 50K shield, the 4K shield, the still shield, and the mixing chamber shield. These shields are nested within each other to ensure maximum protection, as it can be seen in Figure 3.6.
- **Wiring**: There are two types of wires : DC and RF wires. The RF wires are responsible for sending signals to the qubits (usually passing through KF63 ports), and the DC wires are mainly in charge of monitoring the temperature along the cryostat (usually passing through KF40 ports). The ports, which are actually just the different types of gates through the flanges, are represented in Figure 3.3.
- **Dilution refrigerator components**: Those are the components responsible for the dilution refrigeration process once the precooling is done. It is composed of a still, heat exchangers and a mixing chamber represented in Figure 3.4.
- **Microwave Devices**: Since the environment inside the cryostat is extreme in terms of temperature, some devices are used to maintain a good signal along the path of the RF signal. Those devices are amplifiers, attenuators, and filters.

In the use phase, whose impact mostly depends on power/energy consumption, a key assumption was made regarding the cryostat. It was considered an insulated container, which inherently does not consume energy aside from some DC devices within it. Since these devices require a small amount of power to operate (a few watts) and due to the lack of specific information about them, they are considered negligible. Therefore, the assumption of no significant energy consumption for the cryostat is a reasonable approximation.

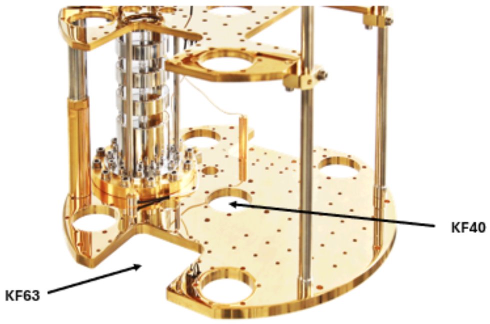


Figure 3.3: KF ports in the LD Cryostat [66]

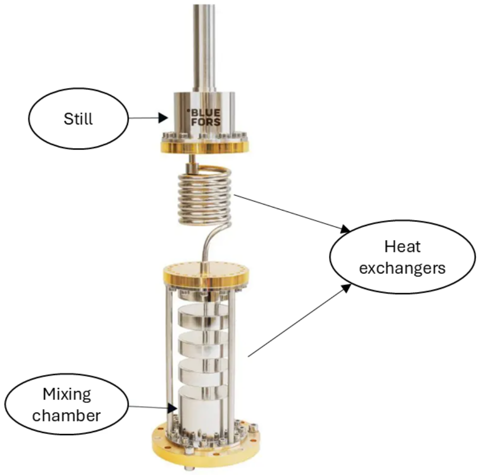


Figure 3.4: Dilution refrigerator components [67]

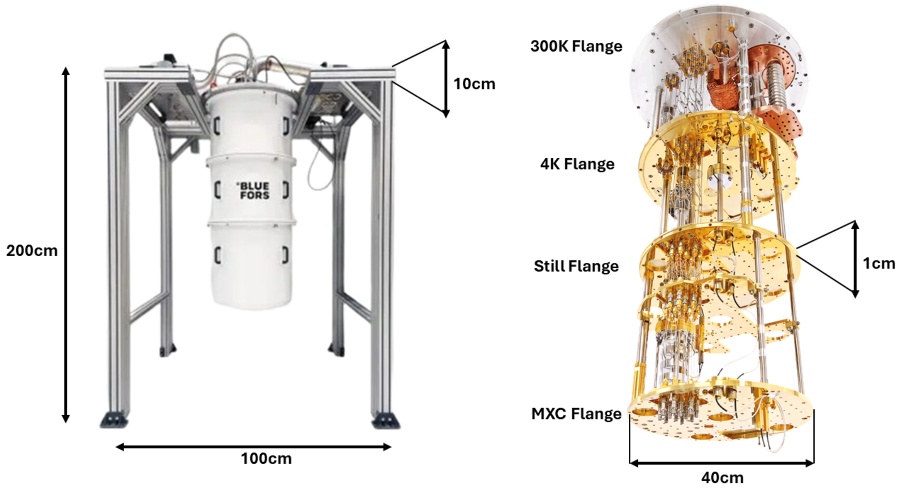


Figure 3.5: Structure components of the Cryostat [66]

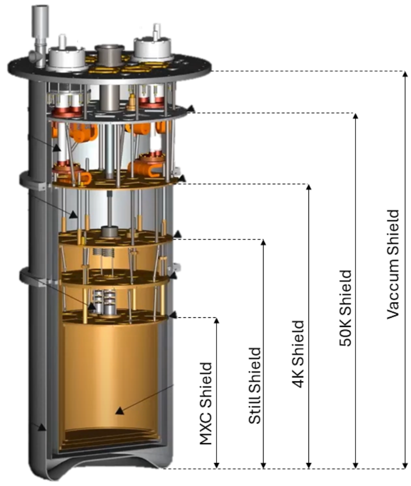


Figure 3.6: Shields of the Cryostat [68]

### 3.3.2 Gas Handling System

The gas handling system (GHS) is essential for maintaining the operational environment required for the dilution refrigerator, which is responsible for cooling the quantum processor to near-absolute-zero temperatures. The gas handling system ensures the proper circulation and management of the gas mixture necessary for the refrigeration process.

The GHS is represented on both sides in Figures 3.7 and 3.8 [69]. This subsystem can be split into main components that need to run into the coarse-grain methodology. The other components included in this subsystem are discarded since they do not have a significant impact based on the chosen granularity. Here is a brief description of the main components:

- **Structure**: The structure provides the physical framework that houses and supports the various components of the gas handling system.
- **Mixture Tank**: This tank stores the helium gas mixture used in the dilution refrigerator. It is designed to maintain the appropriate pressure and purity levels of the gas mixture for the refrigeration process.
- **Mixture Circulation Turbo Pump**: The turbo pump is used to circulate the helium mixture through the system.
- **Mixture Circulation Scroll Pump**: Similar to the turbo pump, the scroll pump aids in the circulation of the helium mixture. It operates on a different

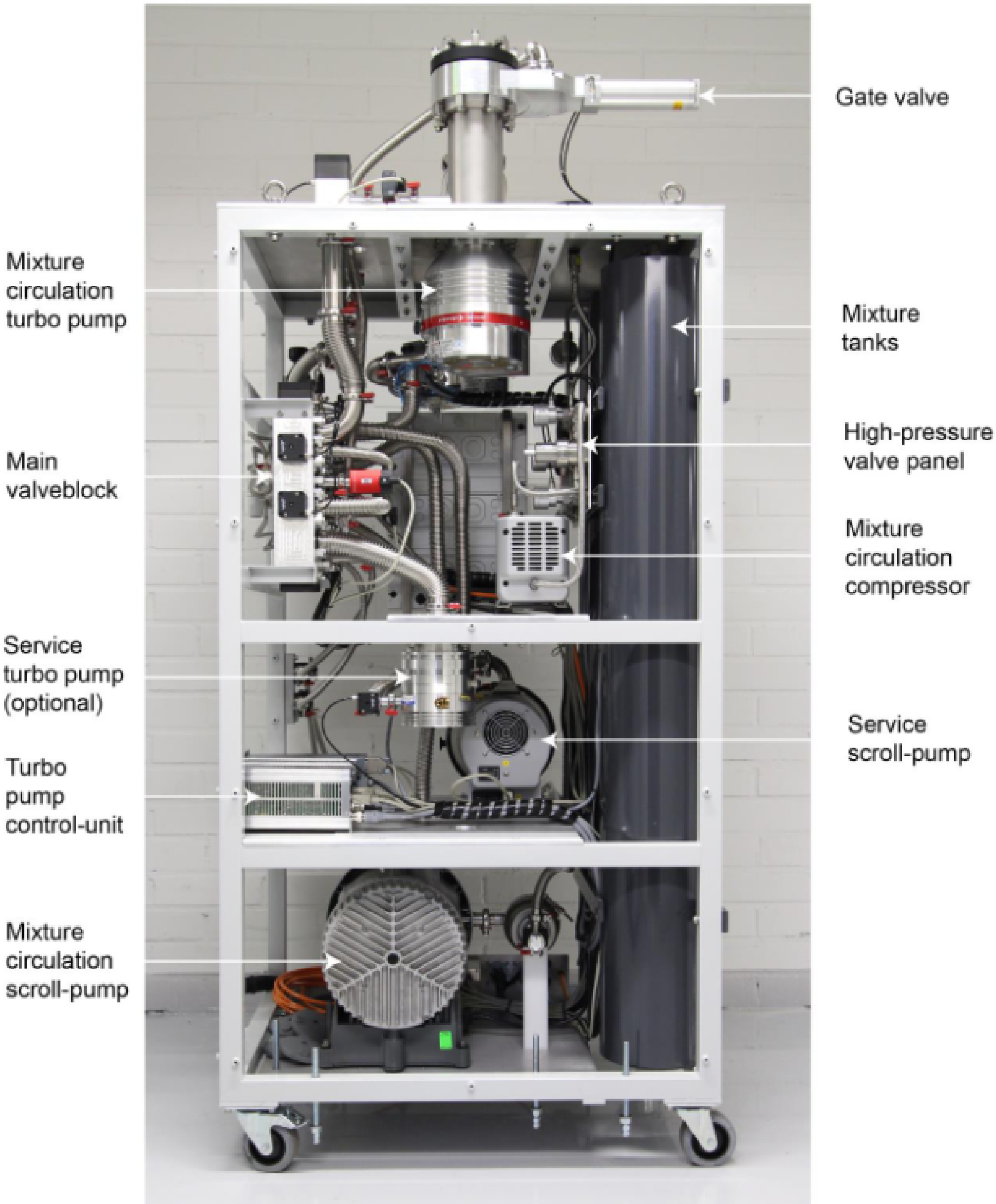


Figure 3.7: Gas handling system (GHS) main component[69]

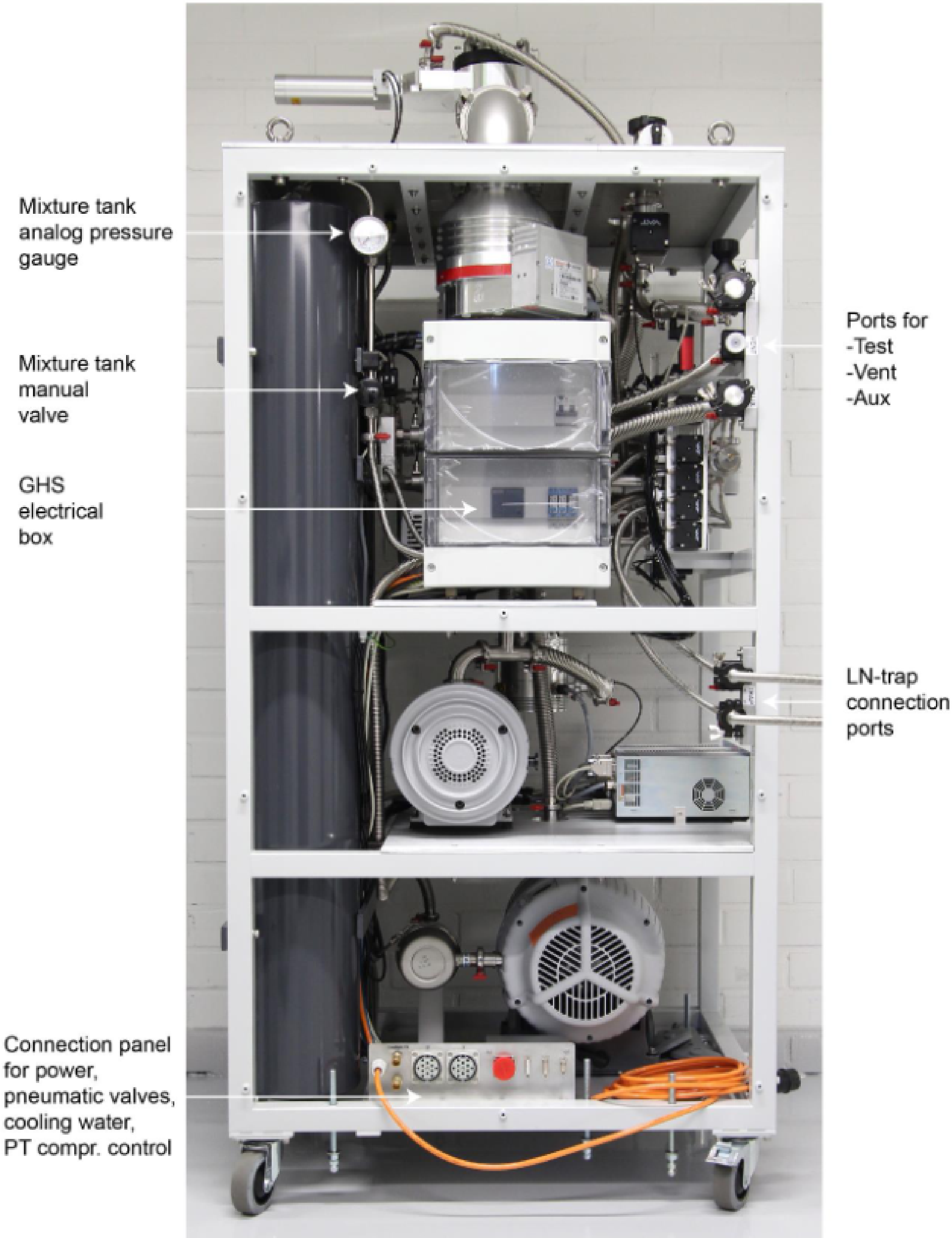


Figure 3.8: GHS main component (other side view) [69]

mechanical principle and is used in conjunction with the turbo pump to maintain a steady flow of gas.

- **Mixture Circulation Compressor**: The compressor increases the pressure of the helium mixture, facilitating its movement through the refrigeration system.
- **Service Scroll-Pump**: This pump is used for maintenance and service operations within the gas handling system.
- **Wires**: The wires are used for electrical connections, controls within the gas handling system, and simply to transfer the gas for the dilution refrigerator.
- **Pure Helium Mixture**: Helium (-3 and -4) is used due to its unique properties at low temperatures, allowing for efficient cooling. The helium mixture in the system needs to be pure and correctly pressurised to ensure optimal performance of the quantum computer.

In the use phase, the GHS is not passive like the Cryostat. According to information found in the User Manual from 2022, it is known that the models GHS400 and GHS200 require specific electrical properties, namely 230VAC and 16A [70]. Consequently, the GHS has a power of 3.68 kW. This indicates that the GHS is an active component, consuming a significant amount of power during operation.

### 3.3.3 Pulse Tube Cryocooler Compressor

The pulse tube cryocooler compressor (PT) is an essential component in quantum computers, providing the necessary cooling to achieve and maintain the ultra-low temperatures required for qubit operations. The system consists of three main components: the compressor, the cold head, and the wiring.

- **Compressor**: The compressor is crucial for compressing helium gas, which serves as the working fluid in the cryocooler. It typically consists of a motor, pistons or scrolls, and various control systems to regulate the flow and pressure of the helium gas. Figure 3.10 shows a Cryomech CP970, which closely resembles the CPA1110 model used in our modelling.
- **Cold Head**: The cold head is the component where the actual cooling occurs, see Figure 3.9. It operates based on the principles of thermodynamics and fluid mechanics, utilising compressed helium gas to remove heat from the quantum processor. The cold head includes heat exchangers, pulse tubes, and regenerators to facilitate the heat transfer process. It is designed to minimise

thermal losses and achieve temperatures close to absolute zero (10mK in this case).

- **Wiring**: The wiring in the pulse tube cryocooler system connects the compressor to the cold head and other auxiliary components. It includes electrical cables for power and control signals, as well as helium gas lines for the circulation of the working fluid. The wiring must be carefully insulated and shielded to prevent heat leaks and ensure the efficient operation of the cryocooler.

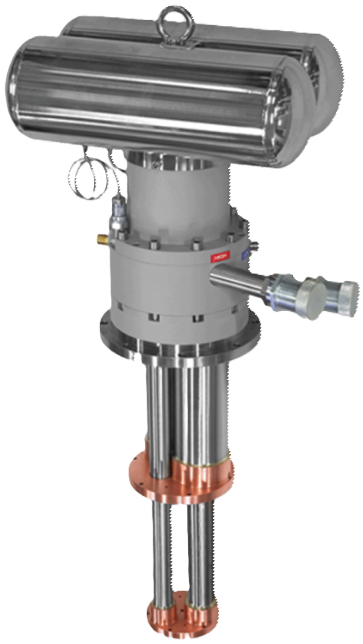

Figure 3.9: Cold Head of the PT415 [71]


Figure 3.10: Cryomech CP970 Helium Compressor [72]

For the use phase, according to information available on Bluefors' website, the compressor has a power of 9.1 kW [71]. No other assumptions were made regarding the use phase.

### 3.3.4 Control Unit

The control unit is responsible for managing and orchestrating the operations of the various subsystems (such as pulse tube, GHS, etc). The control unit ensures that the dilution refrigerator functions correctly by providing a control panel for every pump used. The main components of the control unit, see Figures 3.13 and 3.12, are described below:

- **Structure**: The physical structure of the control unit houses all the components and provides necessary protection and support.
- **Air Filters**: Air filters are integrated into the flow of the control unit to maintain a clean internal environment, preventing dust and other particles from contaminating the pneumatic system. These filters help ensure the longevity and reliability of the control unit.
- **USB-Hub**: The USB hub facilitates connectivity and communication between the control unit and peripheral devices. It allows for the integration of various input and output devices, ensuring seamless data transfer and control operations.
- **Flow Meter Control Unit**: This component monitors and controls the flow of gases within the system, ensuring precise regulation of the operational parameters.
- **5V Supplies**: The 5V power supplies provide the necessary low-voltage power to various components within the control unit, including sensors, controllers, and communication devices.
- **24V Supplies**: Similar to the 5V supplies, the 24V power supplies deliver the higher voltage required by certain components of the control unit.
- **Main Circuit Breaker**: The main circuit breaker protects the control unit from electrical faults by interrupting the flow of electricity in the event of an overload or short circuit.
- **Main Board**: The main board, or motherboard, is the central printed circuit board (PCB) that interconnects all the components of the control unit.
- **NI DAQ**: The National Instruments Data Acquisition (NI DAQ) system is used for collecting and analysing data from the flow meter.
- **Pneumatic Valve and Pneumatic Wiring**: Pneumatic valves and their associated wiring are used to control the flow of gases within the system.
- **Control Panel and Backside**: The control panel includes various connectors, wiring, and interfaces that connect the control unit to other subsystems of the quantum computer. It ensures that all signals and power lines are correctly routed and managed.

Figure 3.11: Control unit (CU) of the cryostat system [69]

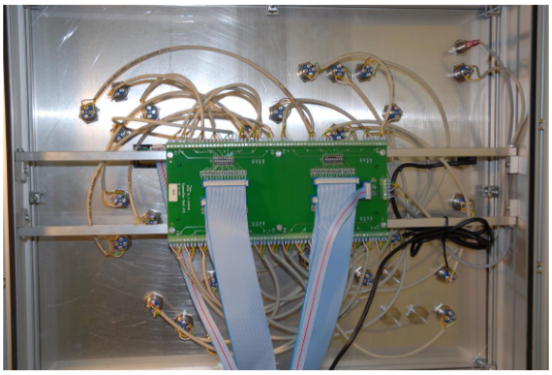

Figure 3.12: Control panel backside with push button distribution circuit board[69]

The extension board and some other components were neglected, as the methodology suggests, and by the fact that this is an addition to the standard control unit.

In terms of power during the use phase, it is important to note that, according to the Bluefors user manual, the power requirements are specified [70]. The control unit operates at 230VAC and 10A, corresponding to a power of 2.3 kW.

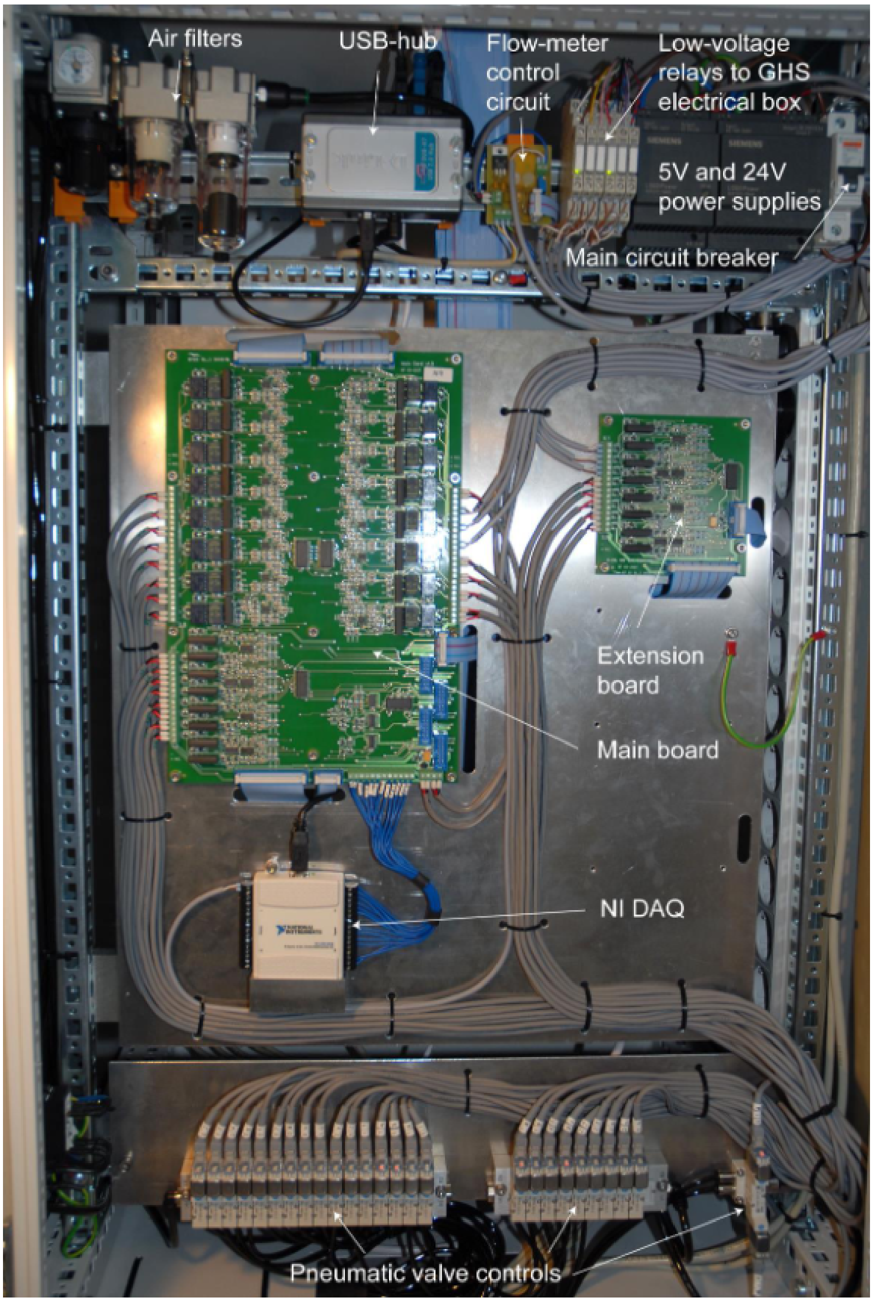


Figure 3.13: Control unit main component [69]

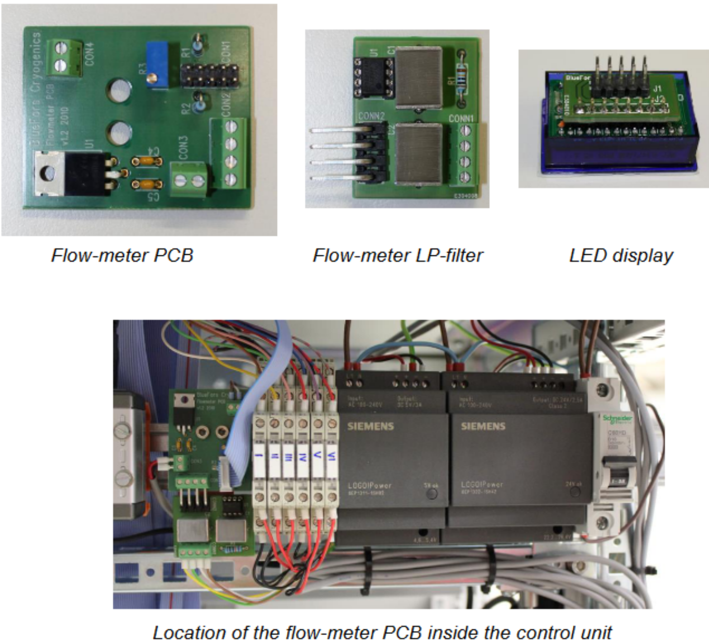


Figure 3.14: Pictures of the flow-meter read-out parts [69]

### 3.3.5 Quantum Hardware

The quantum hardware is the subsystem required in order to generate the microwaves that will be sent through the quantum chip to perform applications and then sent back for measurement. This includes a powerful working station, some microwave equipment, and a quantum chip. This is basically the system that applies the quantum program or algorithm to the qubits. The main components are shown in Fig. 3.15 and described below :

- **Rack Cabinet**: The rack cabinet is the holding structure for all the components of the subsystem.
- **Workstation**: The workstation is basically a computer but slightly different and more powerful than a classical one. It is the center of the operation, where all the commands for microwave generation are taken but also where the output measurement is interpreted.
- **PXIe modules**: The necessary modules are the Dual DDS (Direct Digital Synthesis) responsible for generating periodic signals, the AWG (Arbitrary Waveform Generator) module used to generate electrical signals of any waveform, and the digitiser module for digitising analog signals. All these modules

are integrated into a dedicated chassis.

- **I/Q Modulator/Demodulator**: This is a standard microwave modulator/demodulator used to better interact with the quibits.
- **Vector Signal Generator**: This enables the generation of complex vector signals in radio frequency (RF).

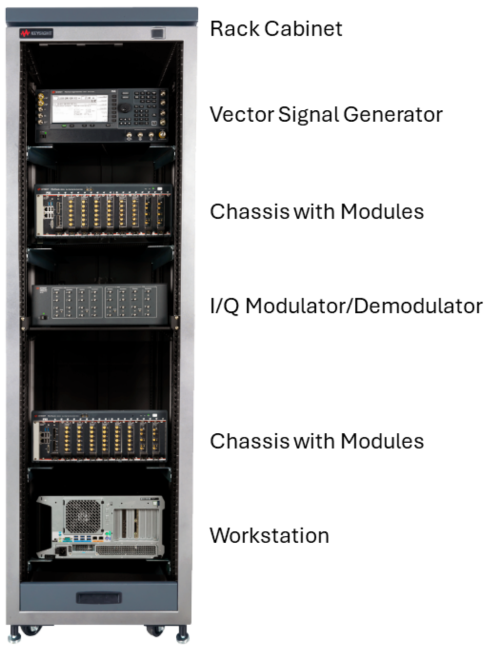


Figure 3.15: Quantum Hardware [73]

Regarding the power of the quantum hardware, this information can be found in the device manuals on the Keysight website [73]. Combining the power of the workstation, the chassis, including the modules, the vector signal generator, and the I/Q modulator/demodulator, the resulting power is 4kW.

## 3.4 Results and Interpretation

This chapter presents the LCIA results and their interpretation. It is important to emphasise that the reported impact categories represent potential impacts, which are approximations of environmental effects that could occur if the emissions follow specific impact pathways and meet certain conditions in the receiving environment. Additionally, the inventory captures only the portion of the total environmental load that corresponds to the chosen functional unit, reflecting a relative approach to the overall result. These results will be discussed and interpreted based on the assumptions made and the information found.

The LCIA results provide an initial estimate of the impacts and are relative to the assumptions made and the information available. Therefore, they do not predict actual impacts, exceedances of thresholds, safety margins, or risks. The impact of GWP will be discussed in detail in the following section, as the overall conclusions are applicable to other impact categories, and GWP is considered the most robust and widely used impact category; see Section 3.2.4. A summary table of all LCIA results for GWP is provided below, with detailed diagrams available in Appendix E.

### 3.4.1 Overall Results

Two scenarios are defined based on the regions where the superconducting quantum computer is produced and used:

- Europe, Belgium (functional unit)
- Global Labor Organization (GLO), around the world

This analysis is based on the following assumptions, derived from online information:

- Manufacturing of most components takes place in GLO datasets.
- Assembly takes place in GLO datasets.
- Transportation is accounted for by the "market" type activities, including global transport, for the production phase and the use phase.
- The use phase takes place in Belgium and in the GLO.

Even though this work is only estimating the GWP impact, it is important to remember that other impacts could have been discussed. Therefore, Table 3.2

presents the values for different impact categories for each scenario, see Appendix E for more details. Since there are several impact categories covered by EF3.0 as explained in Section 3.2.4, for clarity, some of them are not shown.

| Superconducting quantum computer | Senarios | | |
|---|---|---|---|
| Impact categories | GLO | Belgium | Production |
| Acidification, accumulated exceedance (AE) [mol H+ -Eq] | 8.25E+02 | 2.38E+02 | 1.14E+02 |
| Climate change, global warming potential (GWP100) [kg $CO_2$-eq] | 1.50E+05 | 4.89E+04 | 9.59E+03 |
| Ecotoxicity: freshwater, comparative toxic unit for ecosystems [CTUe] | 4.91E+06 | 2.87E+06 | 1.84E+06 |
| Energy resources: non-renewable, abiotic depletion potential (ADP): fossil fuels [MJ] | 1.91E+06 | 1.83E+06 | 1.19E+05 |
| Eutrophication: freshwater, fraction of nutrients reaching freshwater end compartment (P) [kg P-Eq] | 8.26E+01 | 2.60E+01 | 1.76E+01 |
| Eutrophication: marine, fraction of nutrients reaching marine end compartment (N) [kg N-Eq] | 1.51E+02 | 4.23E+01 | 1.59E+01 |
| Eutrophication: terrestrial, accumulated exceedance (AE) [CTUh] | 1.54E+03 | 4.42E+02 | 1.80E+02 |
| Human toxicity: carcinogenic, comparative toxic unit for human [CTUh] | 1.28E-04 | 1.09E-04 | 8.24E-05 |
| Human toxicity: non-carcinogenic, comparative toxic unit for human [CTUh] | 3.13E-03 | 2.23E-03 | 1.21E-03 |
| Ionising radiation: human health, human exposure efficiency relative to u235 [kBq U235-Eq] | 2.04E+04 | 6.99E+04 | 8.66E+02 |
| Land use, soil quality index | 3.79E+05 | 3.64E+05 | 7.17E+04 |
| Material resources: metals/minerals, abiotic depletion potential (ADP): elements (ultimate reserves) [kg Sb-Eq] | 6.12E+00 | 6.21E+00 | 5.36E+00 |
| Ozone depletion, ozone depletion potential (ODP) [kg CFC-11-Eq] | 1.10E-03 | 1.75E-03 | 1.51E-04 |
| Particulate matter formation, impact on human health [disease incidence] | 6.73E-03 | 1.74E-03 | 7.40E-04 |
| Photochemical oxidant formation: human health, tropospheric ozone concentration increase [kg NMVOC-Eq] | 4.56E+02 | 1.35E+02 | 5.18E+01 |
| Water use, user deprivation potential (deprivation-weighted water consumption) [m3] | 4.06E+04 | 2.42E+04 | 5.30E+03 |

Table 3.2: LCIA results for all scenarios and all impact categories of EF3.0

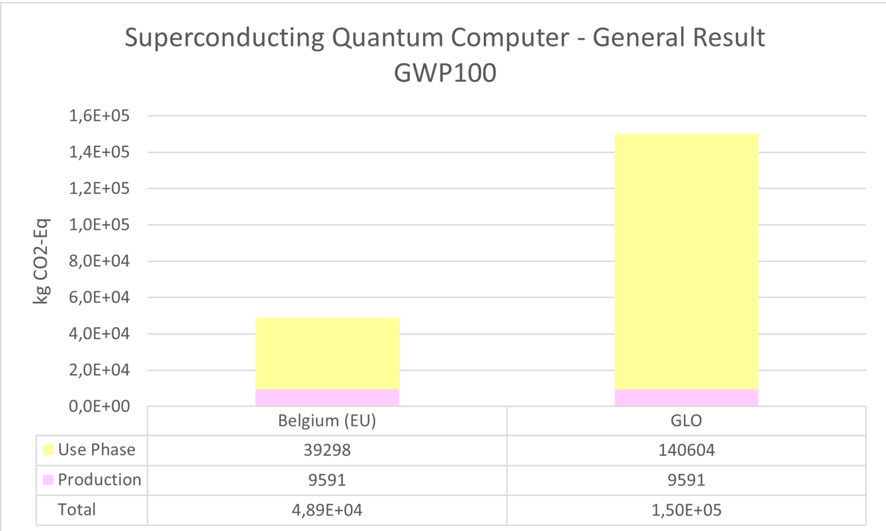


Figure 3.16: LCIA results per life-cycle phases in GWP100 [kg $CO_2$-eq], comparing production, Belgium usage and GLO usage

As shown in Table 3.2 and Figure 3.16, the LCIA results indicate that the use phase has the most significant impact within the study's scope. The production phase is consistent between the EU and GLO scenarios, with the difference arising from the use phase. Since the impact of transport is considered within the phases, it remains the same for the production phase (due to the assumptions) and is included in the use phase. The difference is particularly evident in the GLO scenario, which exhibits the highest impact. This outcome is due to the energy mix used in Activity Browser, specifically the dataset "market group for electricity, low voltage." This dataset represents a collection of markets to form larger, geographically relevant datasets for convenience and ease of use. Although this dataset does not include losses and relevant exchanges (e.g., transport, transport infrastructure), these are included in the other datasets used to define this market group. The "market group for electricity, low voltage" in the global geography considers each market for "electricity, low voltage."

The results in Table 3.2 indicate that in each impact category, the GLO results exceed those of the functional unit. Specifically, for the GWP100, the impact is almost ten times higher than the functional unit, corresponding to a 307% increase in emissions. Additionally, Figure 3.16 illustrates the difference in the residual impact from the production phase between the Belgium and GLO scenarios. For the Belgium case, there is almost a 20% residual impact from the production phase, while for the GLO case, just over 6% remains, still accounted for in the use phase. As expected, the environmental impact varies significantly depending on the geographical scenario, particularly during the use phase. In the functional unit, the "market for electricity, low voltage" refers specifically to Belgium. This dataset includes assumptions regarding the amount of transmission network per kWh transported, with emissions per kWh based on Swiss data. The data on electricity losses is derived from IEA and Swiss sources. Therefore, it can be inferred that Switzerland could potentially have a similar impact when using a SQC.

For a comparative understanding of the impact of this technology, let us examine the difference between the functional unit used here and more familiar technological devices such as a data server, a laptop, and an electric vehicle. Figure 3.17 presents a comparative graph.

- **Data server:** According to a report supported by the Federal Energy Management Program of the U.S. Department of Energy, the energy use of data centres in the United States was substantial [74]. The annual energy consumption of an average server is estimated to be around 4,000 kWh, leading to annual emissions of approximately 2,000 kg $CO_2$-eq (GWP100) assuming an average emission factor of 0.5 kg $CO_2$-eq per kWh. This figure includes both operational energy requirements and the cooling systems needed to maintain optimal server temperatures. Over a typical server lifespan of five years, this results in lifetime emissions of around 10,000 kg $CO_2$-eq.

- **Laptop:** In contrast, a typical laptop's lifetime emissions are estimated to be around 200 to 300 kg $CO_2$-eq (GWP100) [75]. This lower impact is primarily due to the energy efficiency of laptops and their relatively short use phase compared to servers and quantum computers. The majority of these emissions are associated with the manufacturing phase, given that laptops consume significantly less power during use compared to servers. The average power consumption of a laptop is around 50 kWh per year, leading to minimal annual emissions.

- **Electric vehicle:** It is interesting to compare that to SQC. The production impact of the SQC is similar (in terms of order, see Figure 3.18) to the complete life cycle emissions of an electric vehicle. The life-cycle emissions of a mid-sized electric vehicle, including production and use over its lifetime, are estimated to be around 20,000 to 25,000 kg $CO_2$-eq. This includes emissions from battery production, electricity consumption during use, and vehicle manufacturing [76]. The high impact of electric vehicles is mainly due to the energy-intensive processes involved in battery production and the electricity used during the vehicle's operation.

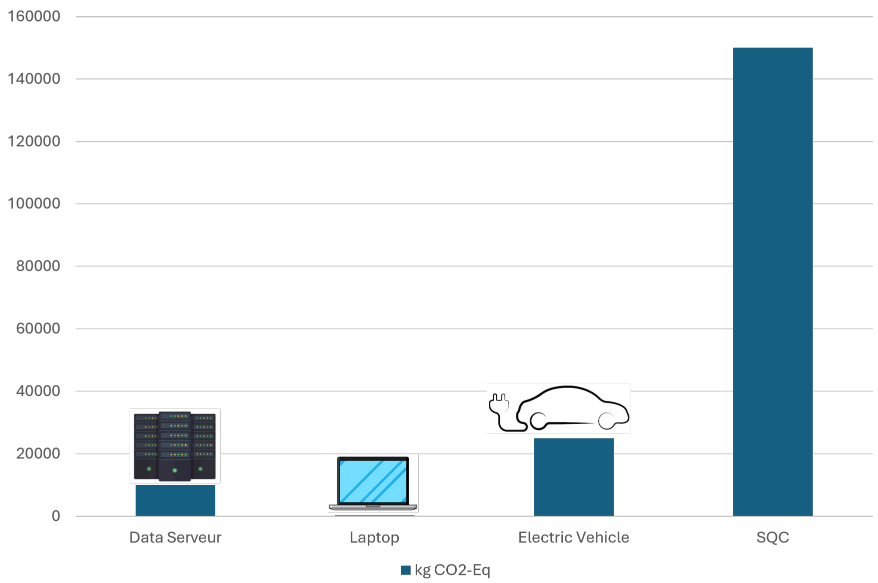


Figure 3.17: Comparative graph of GWP impact across different examples

The superconducting quantum computer, particularly in the GLO scenario, exhibits a higher GWP100 value of approximately 150,000 kg $CO_2$-eq for only five years of use, excluding the end-of-life phase. This difference underscores the intensive energy demands and environmental impact associated with cutting-edge quantum computing technology when compared to conventional computing devices. It is essential to clarify that the computational work performed by a classical computer cannot be directly compared to that of an SQC; the comparison is provided merely as a reference point. The higher impact of SQCs is primarily attributed to their energy-intensive operation and cooling requirements. Additionally, it is also important to note that the examples cited from the literature are based on data before 2017, so it is possible that due to optimisation and recent technologies, the impact is lower now, making the gap between the SQC and other devices even larger.

A focus on the use phase will be provided in Section 3.4.3. Let us now delve deeper into the production phase and key points of results.

### 3.4.2 Production Phase

This section focusses on the production phase. The aim is to provide an overview of the $CO_2$ footprint associated with producing the complete SQC unit. This will be followed by a more detailed analysis of each subsystem and the impact of each sub-subsystem on the GWP category. The second part will examine the different types of activities and their respective contributions to the impacts. Finally, a sensitivity analysis has been performed to identify the hotspots of the production phase.

Before proceeding further with this analysis, Monte Carlo simulations (MCS) can be generated for these three scenarios using Activity Browser. A Monte Carlo run is a statistical technique used to assess uncertainty in a model's outcomes by performing multiple simulations with varying input values based on their probability distributions [77]. Conducting a MCS helps to (i) assess uncertainty by quantifying how these uncertainties propagate through the model and affect the outcomes; (ii) improve decision-making by understanding the range and likelihood of different outcomes, enabling stakeholders to make more informed decisions; and (iii) identify sensitivity, as MCS is essential for sensitivity analysis in Activity Browser. MCS primarily addresses parameter uncertainty, which refers to the variability in input data values due to measurement errors, natural variability, or a lack of precise information. In this case, the number of runs is fixed at 200, with variations in technosphere and biosphere activities. This number is determined by the computational power available and the capabilities of the computers used for the simulations. While 200 runs provide a reasonable starting point to gauge accuracy and convergence, increasing the number of runs would yield more robust and relevant results. To ensure that 200 runs were sufficient, an MCS was conducted for the production phase with 1 000 runs, yielding the same results (see Appendix D, Figure 4.1).

Figure 3.18 shows the result of the Monte Carlo simulations for the production phase. Even when the technosphere and the biosphere activities vary, the final result stays in the range of 10 000 to 14 000 kg $CO_2$-eq. It is important to note and keep in mind that even if the SQC model done could vary in terms of quantities for each activity described, it will stay in this order for the final GWP result.

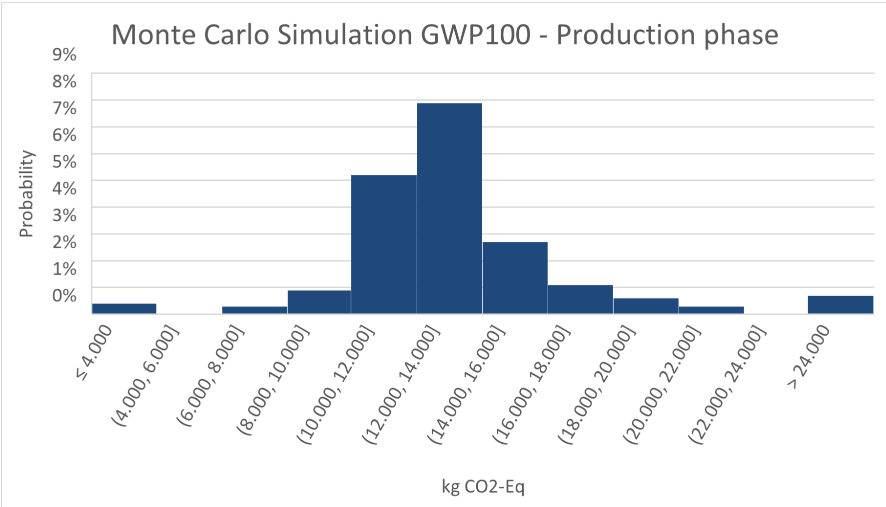


Figure 3.18: Monte Carlo Simulation - Production

Figure 3.19 shows the distribution between all the subsystems in terms of impact in the GWP100, and Table 3.3 shows the value for each subsystem. It clearly shows that the cryostat dominates embodied impact. This subsystem impacts 51% of the total foot print.

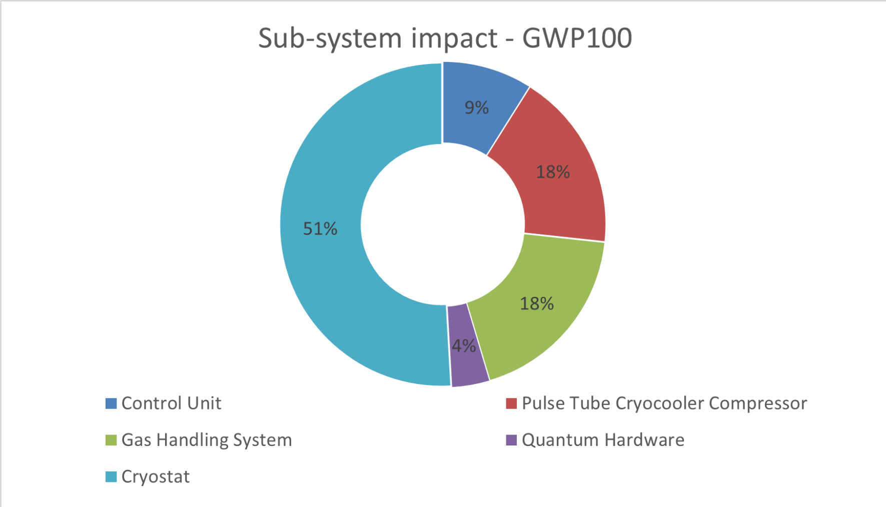


Figure 3.19: Subsystem percentage of impact

| **Main subsystems** | **Global Warning Potential (GWP100)** [kg $CO_2$-eq] |
|---|---:|
| Control Unit | 857.5 |
| Pulse Tube Cryocooler Compressor | 1704,6 |
| Gas Handling System | 1790.6 |
| Quantum Hardware | 357.4 |
| Cryostat | 4881.3 |
| **Total** | **9591.5** |

Table 3.3: Carbon footprint of main components of the SQC for the production

### Subsystems Analysis

The following graph includes a cut-off of 1%. It means that each element under 1% is group under the "Rest" category. The 100% value is based on the value of each main subsystem; see Table 3.3.

**Cryostat** : Figure 3.20 shows that the cryostat could be almost approximated by two main components :

1. The structure with 2670 kg $CO_2$-eq (55%)
2. The shields with 2090 kg $CO_2$-eq (43%)

The impact of the other components represents less than 2% of the overall impacts, which corresponds to 140 kg $CO_2$-eq.

As expected, the substantial structure surrounding the cryostat, made from alloy steel, accounts for 55% of the impact. These types of structures are similar

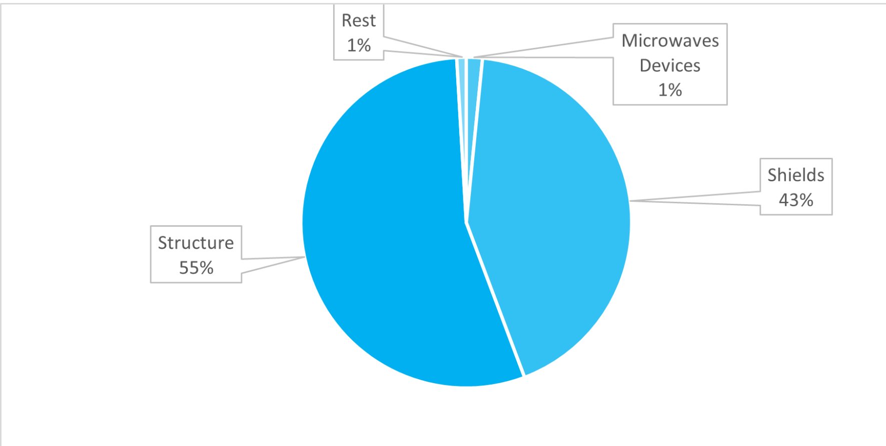


Figure 3.20: Cryostat percentage of impact of each subsystem

to those used in industrial settings to support heavy motors or large operational production lines. Due to their widespread use, such structures have already undergone considerable optimisation for the requirements of the SQC. It can be considered that these structures are already close to their optimum in terms of environmental footprint. While there is always potential to reduce the footprint further by improving production techniques or reducing transport, following the Pareto principle, such reductions would require significant development efforts for relatively small gains.

Within the cryostat, the gold coated flanges stand out as the most impactful components regarding the GWP impact. Comparatively, 130 kg of alloy steel results in an impact of 880 kg $CO_2$-eq, whereas 25 g of gold results in an impact of 3300 kg $CO_2$-eq. When normalised to 1 g, gold has an impact of 132 kg $CO_2$-eq/g, while steel has an impact of 0.007 kg $CO_2$-eq/g. The copper used in producing these flanges has an almost equivalent $CO_2$ intensity per gram to the alloy steel. Given that copper comprises almost half the weight of steel, it is logical to observe approximately half the impact.

The other half of the cryostat's impact arises from the shields (43% of the cryostat). These also contain gold, contributing similarly to the impact observed in the flanges. In the Shields, gold production accounts for 41% of the total impact of this sub-subsystem (it corresponds to 1990 kg $CO_2$-eq). As anticipated, gold is the primary component concerning impact. Each gram of production has a significant influence on the results. Therefore, to ensure the accuracy of the LCA, the first aspect to verify for further analysis is the weight of gold.

To further elaborate, the use of gold in such quantities significantly drives up the global warming potential due to the intensive energy and environmental costs associated with gold mining and processing. Furthermore, alloy steel, while contributing considerably due to its large mass, benefits from well-established manufacturing and recycling processes that mitigate some of its environmental impacts. Copper, often used for its excellent thermal and electrical conductivity, also adds to the environmental burden, though to a lesser extent than gold.

The critical takeaway here is that while bulk materials like steel and copper have substantial impacts primarily due to their sheer volumes, high-impact materials such as gold, even in small quantities, can disproportionately affect the overall environmental footprint. It will be proved by the GSA in the section below. Therefore, any strategies aimed at reducing the embodied environmental impacts of such systems must consider both the reduction in the use of high-impact materials and the optimisation of bulk material usage.

**Gas Handling System** : Figure 3.21 shows that the GHS subsystem has two main components regarding the impacts :

1. The Structure with 448 kg $CO_2$-eq (25%)
2. The Mixture Tank with 415 kg $CO_2$-eq (23%)

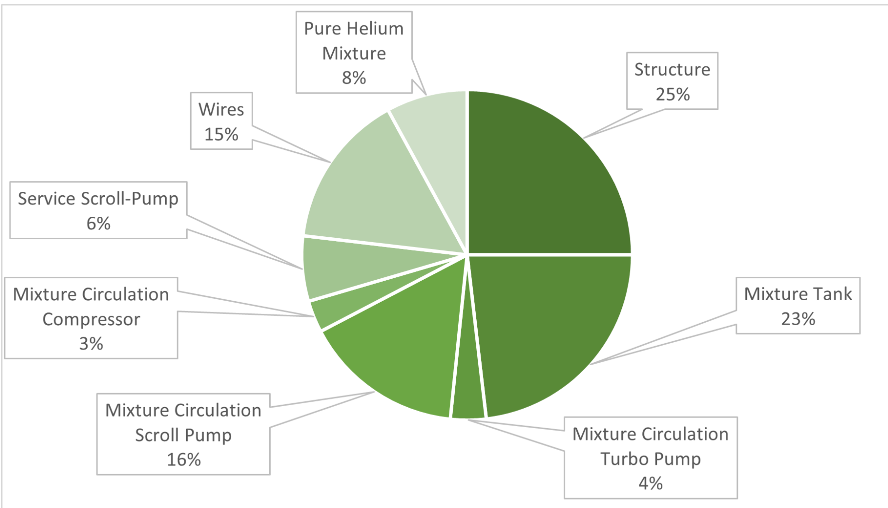


Figure 3.21: Gas Handling System percentage of impact of each subsystem

This subsystem exhibits more diversity concerning the variety of subsystem impacts. Firstly, it is important to note that this subsystem has been significantly simplified due to its complexity and the lack of detailed information. As explained in Section 3.3, each pump has been modelled in the Activity Browser with a scaling factor based on the power (Annex B). Figure 3.21 shows the distribution among each sub-subsystem.

The primary component is the structure, contributing 25% of the total impact, equivalent to 448 kg $CO_2$-eq. This is already quite distant from the impact of the cryostat's structure, six times less. This structure, looking like a rack cabinet or office cabinet, benefits from a well-established manufacturing process. Due to the weight it needs to support, this level of impact is expected.

The second major component is the mixture tank. This tank consists of two large alloy steel cylinders with a selective coating to withstand pressure and the gases it contains. The tank's weight is almost equivalent to the structure's weight, given the volume of gas it needs to retain within the system.

Regarding gases, it is surprising that helium does not emerge as a significant contributor to the overall environmental impact. Based on our research and discussions with the Gehring Laboratory [37], it is clear that helium represents a substantial cost within this subsystem. Initially, before modelling, the assumption was that helium would account for the most significant impact in the production phase. However, this expectation was not reflected in the results, which can be attributed to the specific activity used in the model. The "market for helium" activity in the EcoInvent database includes the transport and production of pure helium. This activity utilises a dataset representing the purification of helium, from crude to Grade-A helium, and its subsequent liquefaction. The technology used for helium purification is pressure swing adsorption (PSA) combined with a liquefaction unit [78].

However, it is important to note that this activity may underestimate the actual impacts associated with helium production. Databases often rely on generalised or averaged data, which might not capture the specificities of helium production. One example is the absence of the "used charcoal" exchange in the dataset. "Used charcoal" is a significant by-product in the helium purification process, particularly in PSA technology. Charcoal plays a role in adsorbing impurities from the crude helium, and its disposal or regeneration has environmental implications. The omission of this material means that the dataset does not fully capture the environmental load, leading to an underestimation of the impact associated with helium production.

Moreover, the dataset does not differentiate between Helium-4 (He-4) and Helium-3 (He-3), which further complicates the assessment. Helium-3, a rare isotope essential for dilution refrigerators, as explained in Section 1.4.1, is produced through various methods. Below is a brief description of each method and the environmental impact that should also be taken into account [79, 80]:

- **Decay of Tritium**:
  - *Process*: The most common method of obtaining Helium-3 is through the radioactive decay of tritium (hydrogen-3). Tritium is produced in nuclear reactors, and over time it decays into Helium-3.
  - *Environmental Impact*: This method is energy-intensive and involves handling radioactive materials, which has environmental and safety considerations.
- **Extraction from Natural Gas**:
  - *Process*: Helium-3 can be found in small quantities in natural gas reserves, typically alongside Helium-4. The extraction process involves isolating He-3 from these reserves. Unfortunately no activity in the EcoInvent database.
  - *Environmental Impact*: The environmental impact includes the energy required for extraction, transport and the potential for methane emissions during the process.
- **Nuclear Fusion Byproduct**:
  - *Process*: In some experimental nuclear fusion reactions, Helium-3 can be produced as a byproduct. However, this is not yet a commercially viable method.
  - *Environmental Impact*: Currently, the impact is theoretical, but large-scale fusion could involve significant energy consumption and waste management issues.
- **Collection from the Moon**:
  - *Process*: Helium-3 is thought to be present in the lunar regolith (moon soil) due to solar wind implantation. Future space missions could potentially harvest He-3 from the Moon.
  - *Environmental Impact*: The impact would be immense, involving space travel, lunar mining, and significant energy expenditure, but this remains speculative at this stage.

Each of these methods has a significantly higher environmental impact compared to the production of Helium-4. If the LCA model does not specifically account for He-3 and instead generalises its impact as He-4, this leads to a considerable underestimation of the true environmental footprint. This oversight underscores the importance of using detailed and specific datasets when evaluating the environmental impacts of advanced technologies that rely on rare materials like Helium-3.

To summarise, specialised materials and gases like helium require more specific LCI datasets to ensure accurate impact assessment. Further investigation and improved data collection methods are necessary to refine these assessments and provide a more accurate representation of their environmental impacts.

**Pulse Tube Cryocooler Compressor** : Figure 3.22 shows that the component with the biggest impact in the Pulse Tube Cyocooler Compressor subsystem is the compressor. It corresponds to more than 1120 kg $CO_2$-eq.

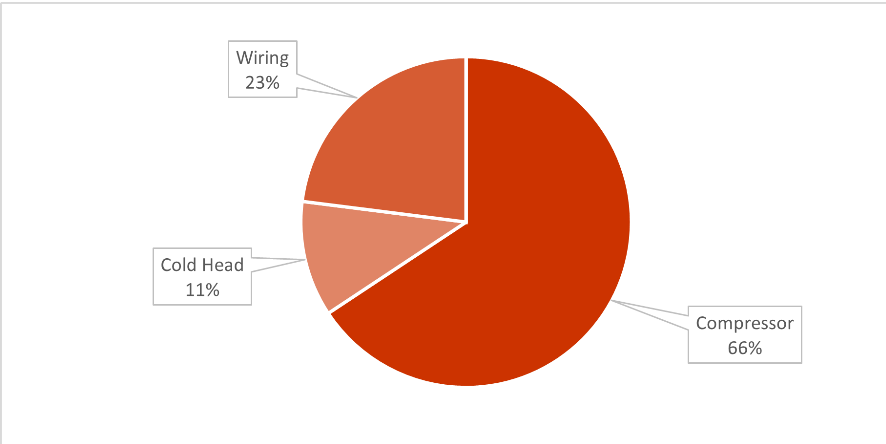


Figure 3.22: Pulse Tube Cryocooler Compressor percentage of impact of each subsystem

As expected, the compressor has the most significant impact, being the primary component in terms of weight and complexity within this subsystem. Although specific documentation or detailed information about its internal components was not found, insights from our visit to the Ghering Lab and discussions there made it clear that this compressor is a critical factor for the dilution refrigerator. As with other pumps and compressors, the assumptions and factors used to design this pump should be highlighted as the points with the greatest influence on the final result for production.

The compressor, manufactured by Cryomech, is supplied with wires that also contribute significantly to the subsystem's impact due to their length and alloy steel composition. The length of these wires can vary depending on the system's position and the requirement to place the compressor in a separate room to avoid frequency issues or vibration influences. For comparison, the structure of the control unit accounts for 373 kg $CO_2$-eq, whereas the wires used involve 392 kg $CO_2$-eq in this case, with potential increases depending on the wire length.

The Cold Head could have a more significant impact if specific materials were used. In our case, the assumption of alloy steel seems logical based on discussions with the Ghering Lab and observations. The technology might also include hidden materials such as gold or other impactful substances, which could increase the footprint. Even though the pulse tube cryocooler corresponds to only 18% of the production impact, the power of the compressor (9.1kW) indicates that it will overcome the other subsystems in the use phase. It will be discussed in Section 3.4.3.

**Control unit** : As for the other Figure 3.23 shows the distribution of the impact. The three components with the biggest impact are:

1. The Structure with 373 kg $CO_2$-eq (43%)
2. The Main Board with 222 kg $CO_2$-eq (26%)
3. The Control Panel and Backside with 188 kg $CO_2$-eq (22%)

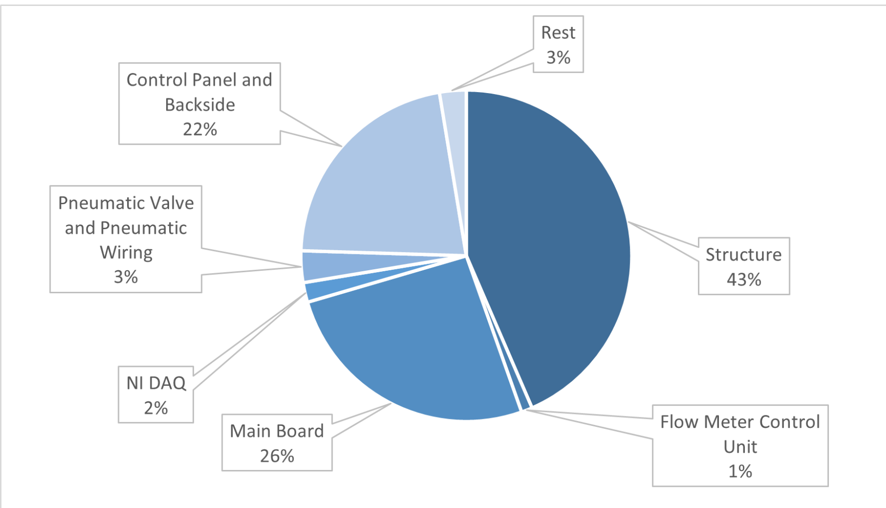


Figure 3.23: Control unit percentage of impact of each subsystem

One more time, the structure is highlighted in the main component. As previously explained, the structure's key factor is the weight due to volume. This control unit looks like a rack cabinet or another desk cabinet. Being smaller than other subsystems, it logically has a smaller impact in terms of footprint.

The next two significant impacts come from the integrated circuits (ICs) component, which is highlighted for the first time in the entire system. These ICs are impactful due to their size and the complex processes involved in their production. The most significant impact comes from the activities "market for integrated circuit production, memory type" and "market for integrated circuit production, logic type." These datasets include all the processes required to produce a logic type microchip. Included are 'die separation,' 'encapsulation,' 'die attachment,' 'lead bonding,' 'plating,' and 'marking.' These operations are represented by the material input of glass epoxy, metals, epoxy resin, doped silicon, glue, gold (wires), etc., and the assembly process energy used. Neither direct air emissions nor any waste are accounted for in this packaging dataset. Logic type circuits perform specified logical operations on incoming data, and memory type circuits store and return data in the same form in which it is entered.

In terms of impact, these and their raw materials significantly influence the overall environmental footprint, as will be explained in the section below with the sensitivity analysis.

**Quantum Hardware** : For the last subsystem, Quantum Hardware, Figure 3.24 shows the distribution of the impact. The biggest component in terms of impact is the workstation. It corresponds to more than 235 kg $CO_2$-eq.

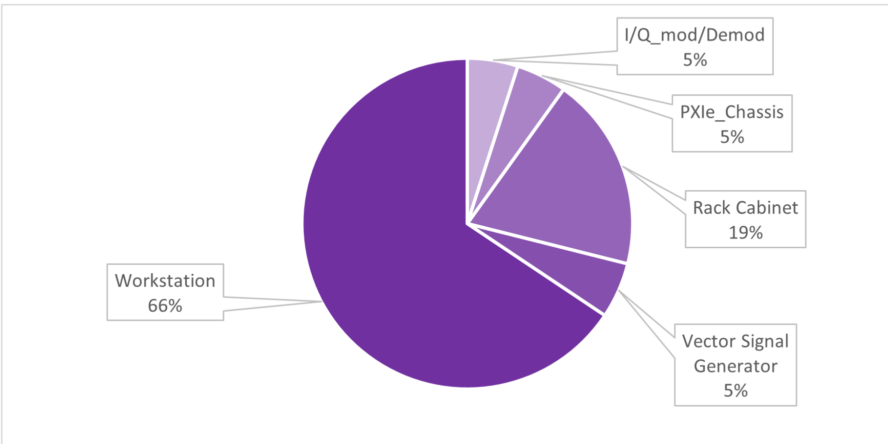


Figure 3.24: Quantum Hardware percentage of impact of each subsystem

For the first time, the structure does not appear to be the most impactful sub-subsystem. The structure accounts for only 19% of the impact in this system. It is, once again, a classic rack cabinet frequently used in various applications. The other sub-subsystems each contribute around 5% to the overall impact. These utility devices are common in industrial and electrical/scientific laboratories.

The most impactful part of the quantum hardware subsystem is something well known and well studied in recent years. Indeed, the workstation, resembling a supercomputer, is the most impactful part of this system. The workstation is required to generate and mix the signals to send to the cryostat, where computation is carried out on the quantum chip. It also needs to transform the return signals and display them for the user. The assumption was made to consider only a workstation for physical access to the superconducting quantum computer. However, in many applications, remote access is available. In our application, the workstation accounts for 66% of the GWP impact with 235 kg $CO_2$-eq, but this depends on the components inside the workstation. Including online access would further increase this impact due to the need for servers. This impact seems to be consistent with the example taken earlier, with the classic computer. But remembering that it's only in the production phase, so the workstation differs from conventional computers, and even more in the use phase.

**Type of Activities Distribution**

One of the goals of this study is to determine which types of activities have the most significant environmental footprint for the SQC. This thesis was initiated with questions about quantum technologies and whether they are more impactful than traditional integrated circuits.

To do so, three categories were created : (i) structure; (ii) electronic & quantum device; and (iii) refrigerator device in the production phase. For this comparison, activities describing structural elements, such as cabinets and supports, are grouped under the structure category. Activities related to refrigerator devices, such as compressors, pumps, pneumatic wires, and valves, are grouped under the Refrigerator Device category. Lastly, all remaining activities, including mounted boards, electronic wires, and workstations, are classified under the Electronic & Quantum Device category.

Figure 3.25 illustrates that the refrigerator device category has the largest impact, representing 5191.5 kg $CO_2$-eq (54% of the total system). The second largest category is the structure, with 3559 kg $CO_2$-eq (37%), followed by the electronic

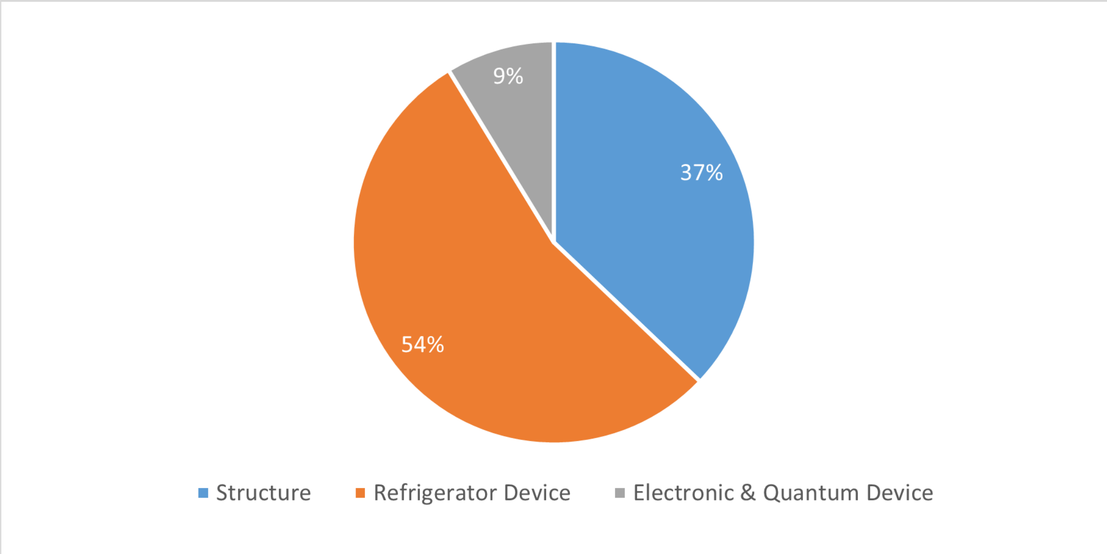


Figure 3.25: Percentage of Impact of Each Type of Activities Distribution - Production Phase

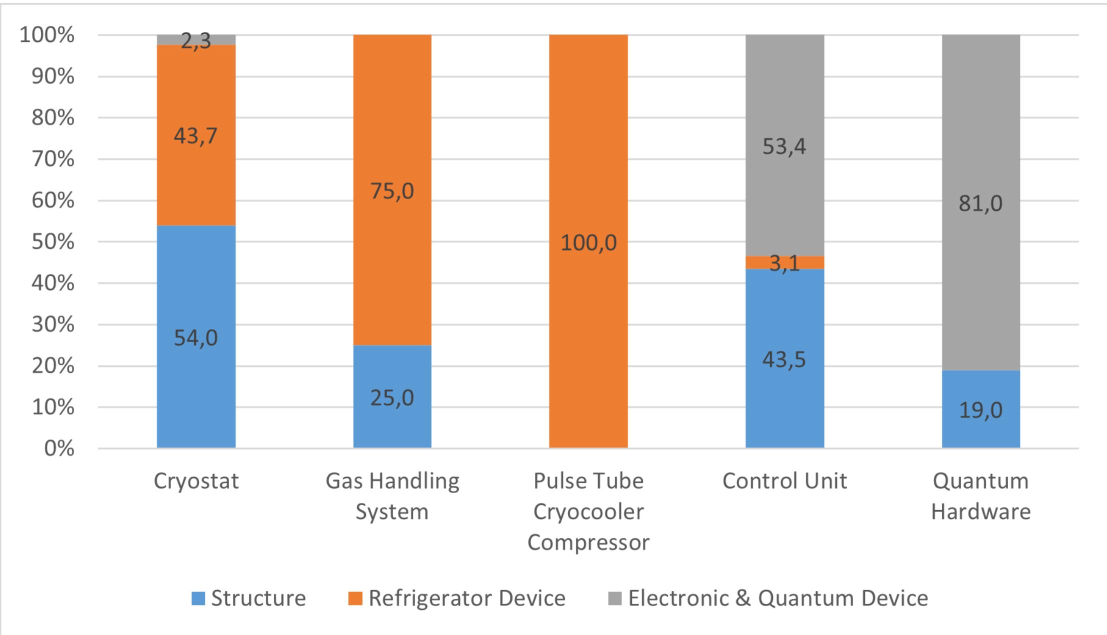


Figure 3.26: Percentage of Each Type of Activities Distribution in Each subsystem

& quantum device category 841 kg $CO_2$-eq. Figure 3.26 shows the distribution of each type of activity within each subsystem. The activities in Activity Browser considered for each category are listed in Appendix C. For instance, in the case of the pulse tube cryocooler compressor, the assumption was made that all components within this subsystem were solely for the cooling system, thus it is 100% in Refrigerator Device type. However, in reality, electronic devices are also an integral part of its operation, and to be truly rigorous, each component should be separated and classified by type. Here, the choice has been made to consider everything in the Refrigerator Device category. Changing this breakdown will inevitably alter the results obtained. This graph, Figure 3.26, helps to understand the hypothesis and to see how the types of activity are distributed in each sub-system. This distribution stays the same for the use phase.

The assumptions made during this analysis are critical components. Once these assumptions are clearly understood, the results may be more surprising than expected. The initial expectation was that electronic components would significantly influence the environmental footprint, because SQC was at first expected to be only a computer with a lot of ICs inside "the box" and with a bigger cooling system. However, Figure 3.25 presents a different perspective. The electronic & quantum device category accounts for only 9% of the total production impact in terms of kg $CO_2$-eq, whereas the refrigerator device category is the most impactful in terms of production.

Even though these subsystems are based on well-known and developed technologies, they are at the forefront of technological innovation. As previously explained, the dilution refrigerator requires numerous pumps and top compressors to operate, in addition to pure helium, all of which have a significant environmental footprint. This is corroborated by the data in Table 3.4, which will be analysed in Section 3.4.2.

#### Sensitivity Analysis

Sensitivity analysis is performed to understand how changes in key parameters affect the overall results of the LCA. This analysis helps identify which parameters have the most significant impact on the results and assess the robustness of the conclusions [81].

Global sensitivity analysis (GSA) is a method that works with :

1. **Input Parameters:** The GSA considers various input parameters used in the LCA model. These could be quantities of materials, energy consumption values, emission factors, etc.

2. **Sampling and Simulation:** The Activity Browser uses Monte Carlo simulations to vary these input parameters across their possible ranges. Each simulation run uses a different set of input values sampled from specified distributions.

3. **Output Analysis:** The results of these simulations are analysed to determine the sensitivity of the impact category results to changes in each input parameter.

The results of the sensitivity analysis are summarised in Table 3.4, the cut-off is 20% to make it clearer, and the "T:" or "B:" means this is a technospehre activity or a biosphere activity. Figure 3.18 illustrates the Monte Carlo simulation for the production.

In GSA results, "delta" quantifies the sensitivity of an output to changes in input parameters. It is expressed as a percentage to facilitate comparison across different parameters with varying scales and units. A higher percentage delta means that the output is more sensitive to changes in that particular input parameter. For example, if the delta for the electricity emission factor is 20%, it implies that a 10% change in the emission factor will result in a 2% change in the GWP result. The change in the output is proportional to the change in the input parameter, not necessarily the same percentage.

Now, let's interpret those results summarised in Table 3.4, it list the technosphere activities that have the most influence on the results. The refrigerator device activities are the most represented activities in the list. The activity "T:electricity, medium voltage FROM market group for electricity, medium voltage [GLO] TO natural gas liquids production (helium, crude) [GLO]" refers to the electricity consumed in helium production. This activity has a delta of 33.20%, the highest among all activities. Additionally, three more activities related directly to Refrigerator Devices and their compressors, each with a delta of around 23%, further underscore that this category has an important influence on results in terms of the environmental footprint. So even small changes in this type of activity would have a massive impact on the overall result.

Another point to focus on is the fourth line in Table 3.4, which lists the activity "T: electricity, medium voltage FROM market group for electricity, medium voltage [RLA] TO gold refinery operation (gold) [RoW]". This entry highlights the significant impact of electricity consumption on the production of gold, with a 27.94% delta. Gold is a key material in SQC, and even a minor variation of 10% of the weight (in grams) can lead to a 2.8% change in the final result.

Overall, the most impactful activities identified in Table 3.4 are related to the energy consumption associated with production processes. This indicates that the geographical locations where raw materials are extracted and processed can greatly influence the final environmental impact. Improved knowledge about the specific origins of components in each subsystem could significantly affect the LCA outcomes. Additionally, the energy mix used during production is a crucial factor to consider, highlighting an area for potential improvement in further analyses. However, this improvement will still quite small relative to the use phase.

| GSA name | delta |
|---|---|
| T: electricity, medium voltage FROM market group for electricity, medium voltage [GLO] TO natural gas liquids production (helium, crude) [GLO] | 33,20% |
| T: explosive, tovex FROM market for explosive, tovex [GLO] TO blasting (blasting) [RoW] | 28,12% |
| T: hard coal FROM market for hard coal [CN] TO heat and power co-generation, hard coal (electricity, high voltage) [RoW] | 28,05% |
| T: electricity, medium voltage FROM market group for electricity, medium voltage [RLA] TO gold refinery operation (gold) [RoW] | 27,94% |
| T: electricity, high voltage FROM electricity production, hard coal [CN-AH] TO electricity production, coal, aluminium industry (electricity, high voltage, aluminium industry) [CN] | 26,72% |
| T: heat, district or industrial, other than natural gas FROM market for heat, district or industrial, other than natural gas [RoW] TO hard coal mine operation and hard coal preparation (hard coal) [CN] | 25,80% |
| T: electricity, medium voltage FROM market group for electricity, medium voltage [RAS] TO gold mine operation and gold production, unrefined (gold, unrefined) [RoW] | 24,55% |
| T: electricity, medium voltage FROM market group for electricity, medium voltage [RAS] TO hot rolling, steel (hot rolling, steel) [RoW] | 24,32% |
| T: cast iron FROM market for cast iron [GLO] TO air compressor production, screw-type compressor, 4kW (air compressor, screw-type compressor, 4kW) [RER] | 23,57% |
| T: heat, district or industrial, other than natural gas FROM market for heat, district or industrial, other than natural gas [RoW] TO smelting of copper concentrate, sulfide ore (copper, anode) [RoW] | 23,54% |
| T: steel, chromium steel 18/8, hot rolled FROM market for steel, chromium steel 18/8, hot rolled [GLO] TO air compressor production, screw-type compressor, 4kW (air compressor, screw-type compressor, 4kW) [RER] | 23,48% |
| T: heat, district or industrial, other than natural gas FROM market for heat, district or industrial, other than natural gas [RoW] TO sheet rolling, steel (sheet rolling, steel) [RoW] | 23,34% |
| T: electricity, medium voltage FROM market group for electricity, medium voltage [RME] TO steel production, converter, low-alloyed (steel, low-alloyed) [RoW] | 23,32% |
| T: electricity, medium voltage FROM market group for electricity, medium voltage [RLA] TO cast iron production (cast iron) [RoW] | 23,11% |
| T: electricity, medium voltage FROM market group for electricity, medium voltage [RAS] TO cast iron production (cast iron) [RoW] | 22,71% |
| T: steel, unalloyed FROM market for steel, unalloyed [GLO] TO sheet rolling, steel (sheet rolling, steel) [RoW] | 22,14% |
| T: heat, district or industrial, other than natural gas FROM market group for heat, district or industrial, other than natural gas [GLO] TO cobalt production (electrolyte, copper-rich) [GLO] | 22,14% |
| T: aluminium, wrought alloy FROM market for aluminium, wrought alloy [GLO] TO explosive production, tovex (explosive, tovex) [RoW] | 21,89% |
| T: electricity, medium voltage FROM market for electricity, medium voltage [RU] TO explosive production, tovex (explosive, tovex) [RoW] | 21,74% |
| T: diesel, burned in building machine FROM market for diesel, burned in building machine [GLO] TO gold production (gold) [AU] | 21,63% |
| T: electricity, medium voltage FROM market for electricity, medium voltage [AU] TO hot rolling, steel (hot rolling, steel) [RoW] | 21,62% |
| T: copper concentrate, sulfide ore FROM market for copper concentrate, sulfide ore [GLO] TO smelting of copper concentrate, sulfide ore (copper, anode) [RoW] | 21,53% |
| T: heat, district or industrial, other than natural gas FROM market group for heat, district or industrial, other than natural gas [GLO] TO integrated circuit production, logic type (integrated circuit, logic type) [GLO] | 21,50% |
| T: diesel, burned in diesel-electric generating set, 10MW FROM market for diesel, burned in diesel-electric generating set, 10MW [GLO] TO cobalt production (electrolyte, copper-rich) [GLO] | 21,46% |
| B: Carbon dioxide, fossil // ferrochromium production, high-carbon, 68% Cr (ferrochromium, high-carbon, 68% Cr) [RoW] | 20,60% |
| T: blasting FROM market for blasting [GLO] TO hard coal mine operation and hard coal preparation (hard coal) [CN] | 20,38% |
| T: diesel, burned in building machine FROM market for diesel, burned in building machine [GLO] TO cobalt production (electrolyte, copper-rich) [GLO] | 20,22% |
| T: electricity, medium voltage FROM market group for electricity, medium voltage [CN] TO steel production, converter, low-alloyed (steel, low-alloyed) [RoW] | 20,02% |

Table 3.4: Sensitivity analysis results showing the delta values for the most impactful input parameters

### 3.4.3 Use Phase

This section will focus on LCIA results for the use phase of the SQC. It will focus on a comparison between two scenarios, one in the Belgium mix of energy and one in the GLO mix of energy.

Figures 3.27 and 3.28 show the Monte Carlo simulations for the two scenarios. The same parameters used for the production phase were used for this simulation (200 runs, technoshepre, and biosphere activity variations).

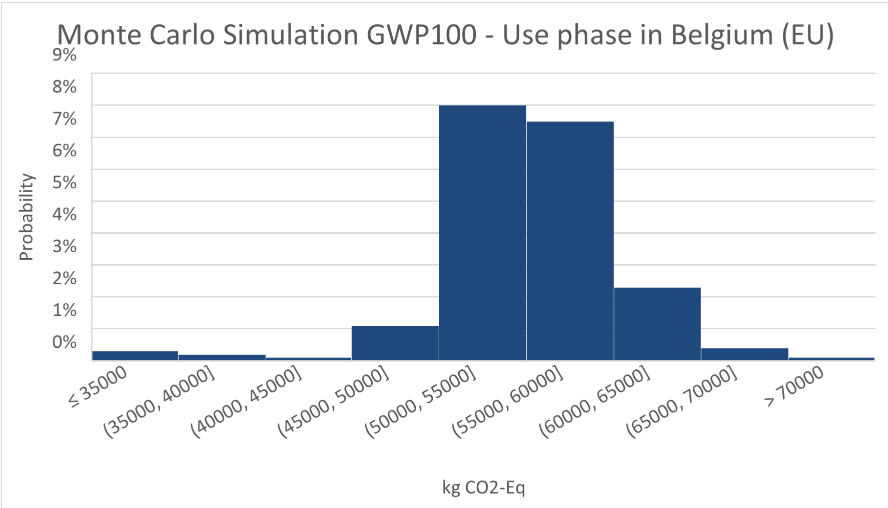


Figure 3.27: Monte Carlo Simulation - Use phase in Belgium

It shows two Gaussian distributions: in the case of the functional unit, there is a peak between 50,000 and 60,000 kg $CO_2$-eq, while in the GLO scenario, there is a double peak between 155,000 and 165,000 kg $CO_2$-eq. One of the major impacts seems to be the SQC's energy consumption. It is therefore important to discuss this in order to provide some nuances and explanations for these results.

First of all, since the tasks performed by the computer are not known in advance, it is difficult to calculate the average power consumption of the various subsystems. Indeed, if a heavy task is performed or if more qubits are encapsulated in the mixing chamber, the cooling power will be much higher to counterbalance the thermal interactions of these elements.

Thus, it is the nominal power that has been evaluated for all results, which may raise energy consumption a little in the case of a simple application. However, in

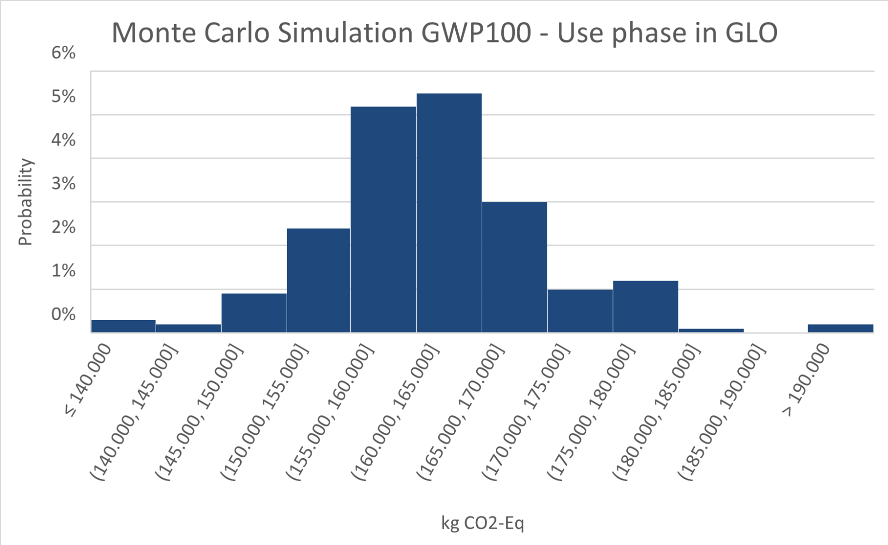


Figure 3.28: Monte Carlo Simulation - Use phase in GLO

| | Use Phase, GWP100 [kg CO2-eq] | |
|---|---|---|
| **Main Components** | Belgium (EU) | GLO |
| Quantum Hardware | 7316.7 | 26178.2 |
| Control Unit | 4877.8 | 17452.1 |
| Pulse Tube Cryocooler | 19299.1 | 69049.6 |
| Gas Handling Station | 7804.6 | 27923.7 |
| Cryostat | 0.0 | 0.0 |
| **Total** | **39298.1** | **140603.6** |

Table 3.5: Carbon footprint of main components of the SQC for the use phase.

the future, our assumption is that SQCs will probably be used remotely by users, and the server will try to optimise requests by allocating all qubits to different users if necessary. This will push performance close to nominal power.

### Subsystems Analysis

Examining these two scenarios in more detail, the results are illustrated in Figure 3.29, which shows the percentage impact in terms of the environmental footprint for each subsystem. Table 3.5 presents the corresponding values in terms of global warming potential over 100 years (GWP100) for each subsystem.

Figures 3.30 and 3.31 display the distribution of the use phase impacts across each subsystem compared to the production phase in both the EU and GLO scenarios. These figures provide a detailed comparison of the use phase impacts

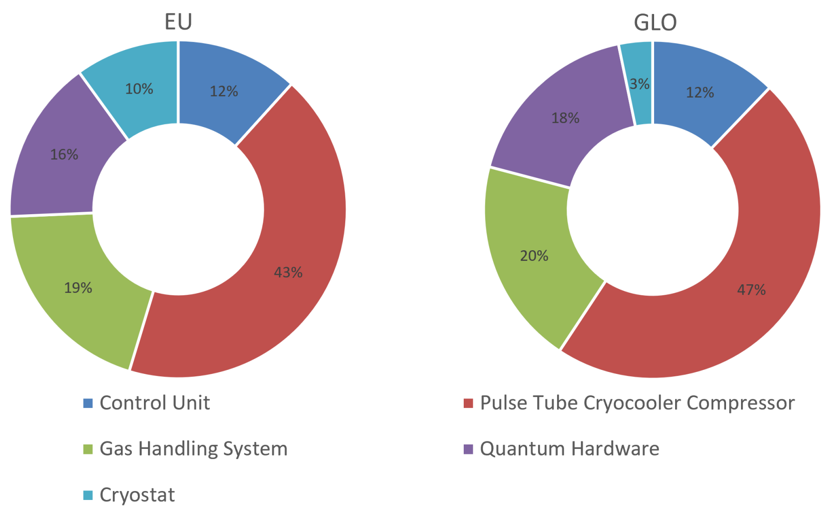


Figure 3.29: subsystem percentage of impact in the Belgium (EU) scenario and GLO scenario

in relation to the production phase, offering insights into how each subsystem's operational activities contribute to the total GWP100 emissions.

As with the production phase, Table 3.5 and Figure 3.29 depict the distribution of environmental impacts across each subsystem in terms of footprint. A significant difference is observed between Figure 3.19 and Figure 3.29, where the Cryostat's contribution in the production phase was 51% it decreased to 10% in the EU case and just 3% in the GLO scenario. This reduction is due to the assumptions made regarding the cryostat.

In this study, it is assumed that the cryostat does not consume energy during its operation. It is portrayed as a large, insulated container where the vacuum is maintained and all external energy and material flows pass through without additional consumption by the cryostat itself. While, in terms of thermal energy, the cryostat does indeed engage in heat exchange to cool its interior, it is designed to minimise energy loss (see Section 3.3.1). Therefore, it seems reasonable to exclude its energy consumption from the use phase in this analysis. It is also shown in Figure 3.30 and Figure 3.31.

Unlike the Cryostat, the Pulse Tube Cryocooler Compressor shows a significant increase in environmental impact, rising from 18% in the baseline scenario to 43% in the EU and 47% in the GLO scenarios. This is primarily due to the high energy

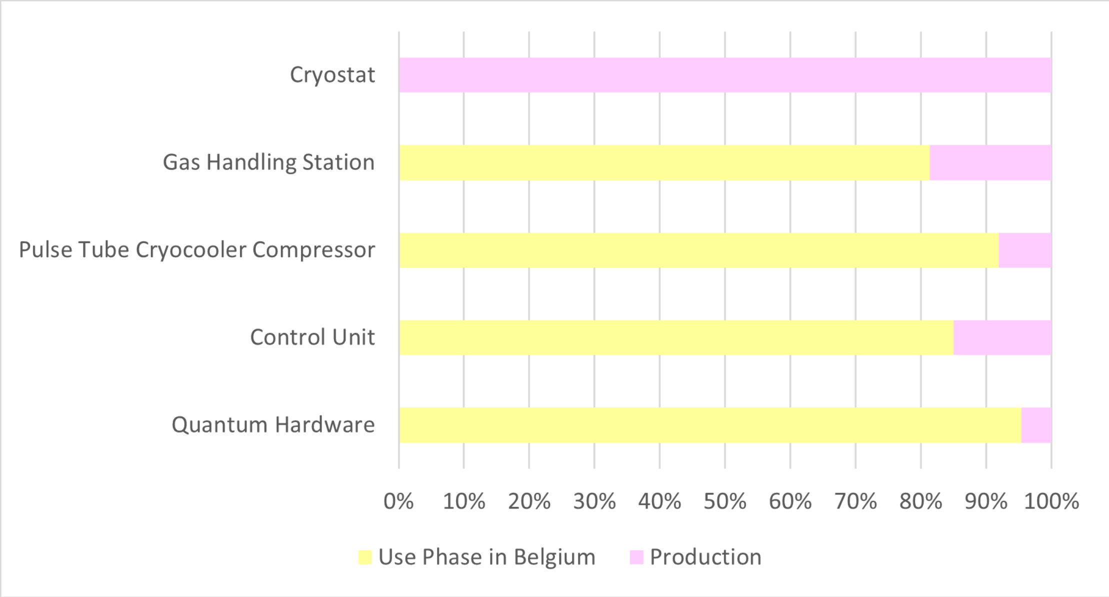


Figure 3.30: Use phase in Belgium and the production pourcentage of impact for each subsystem

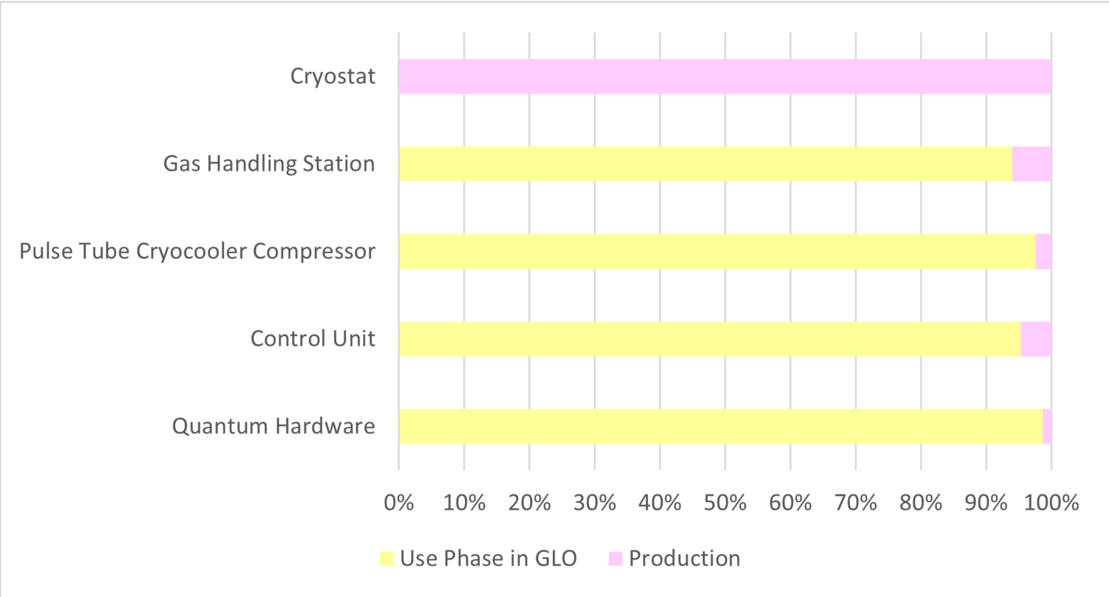


Figure 3.31: Use phase in GLO and the production pourcentage of impact for each subsystem

consumption of the compressor, which is a crucial component in this subsystem. As explained in Section 3.3.3, the compressor has a power of 9.1 kW.

To put this into perspective, the energy consumption of the pulse tube cryocooler compressor can be compared to that of common household devices. For instance, a typical residential air conditioning unit might have a power output of around 3.5 kW, meaning the compressor used in this subsystem has a power output approximately three times bigger [82]. Similarly, compared to an average electric vehicle charging at 7.2 kW, the compressor's energy demand is significantly higher, highlighting its substantial contribution to the overall energy footprint of the superconducting quantum computer [83].

Behind this component, the GHS remains almost unchanged, at approximately 19%, similar to previous levels. The control unit followed the pattern of the PT, with a slight increase of 4% in each scenario.

The final component of the subsystem is the quantum hardware, which shows a significant increase in terms of impact, with nearly a 15% rise, making it the third most influential subsystem in terms of global impact. This increase is attributed to the high-tech systems used, such as the PXIe modules with a power rating of 1.3 kW and the workstation with a power rating of 1.4 kW. Adding these together (addind the other sub-subsystem) results in a total power of 3.4 kW for this subsystem. Consequently, the quantum hardware is comparable to the GHS in terms of power and impact during the use phase. See Figure 3.29.

### Type of Activities Distribution

Based on the attribution detailed in Section 3.4.2, Figure 3.32 illustrates the percentage impact of each type of activity during the use phase for both the Belgium and Global (GLO) scenarios. Since the structure does not consume energy during its operation, its emissions remain constant at 3559 kg $CO_2$-eq across all scenarios.

For the refrigerator device, the environmental impact is 32 279 kg $CO_2$-eq in the EU scenario and 102 179 kg $CO_2$-eq in the GLO scenario.

Finally, the Electronic & Quantum Device category has an impact of 13 052 kg $CO_2$-eq in the EU scenario and 44 442 kg $CO_2$-eq in the GLO scenario.

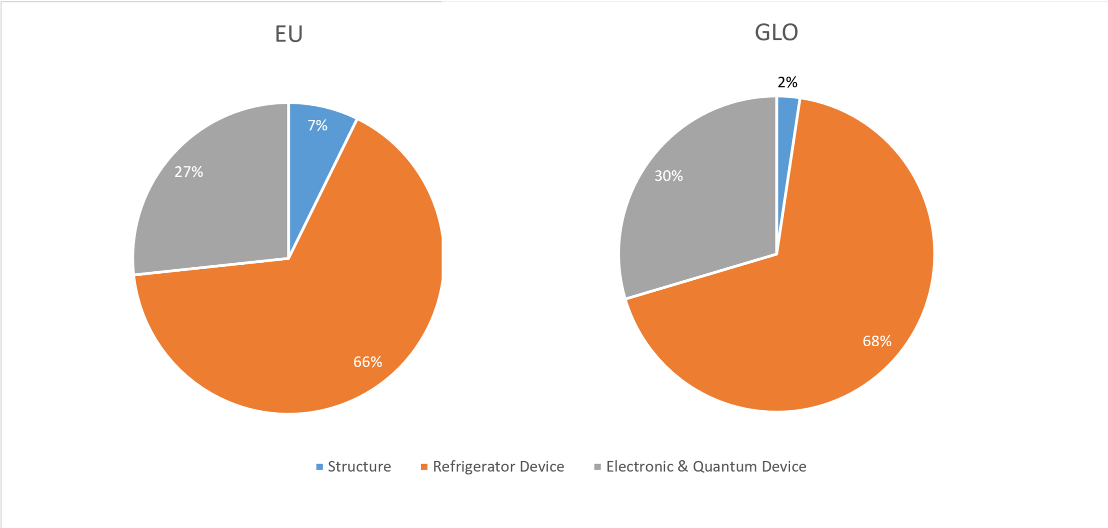


Figure 3.32: Percentage of impact of each type of activities distribution during the use phase for the lifetime considered in the FU - Belgium and GLO Cases

As anticipated, research by Martin M. indicates that the power consumption associated with the dilution defrigerator activities surpasses the impact of the other two categories, accounting for approximately 67% of the total impact, as illustrated in Figure 3.32 [35]. The electronic & quantum devices contribute around 28%, highlighting once again the significance of the energy mix employed. Indeed, in the EU case, the residual impact of the structure remains non-negligible at 7%, compared to just 2% for the structure type in the GLO case. As shown in Figure 3.30, nearly four out of five subsystems still exhibit a production impact of 10%. In contrast, for the GLO case (Figure 3.31), the assumption that production impact is negligible is valid, as all subsystems (excluding the Cryostat) have a residual production impact of less than 6%. This discrepancy is attributed to the energy mix used.

To further analyse the use phase, a detailed inventory of the consumption for each item within each subsystem would be beneficial. This detailed information could help identify the most impactful subsystem, thereby directing research or optimisation efforts towards it. Additionally, improving the accuracy of power consumption data by considering the maximum power demands throughout the entire application would yield more precise results for the LCA.

### Sensitivity Analysis

Table 3.6 and Table 3.7 present the output results of the GSA method for the use phase in the functional unit and the GLO scenario.

As explained in Section 3.4.2, the notation "T:" or "B:" indicates whether an activity is a technosphere or biosphere activity, respectively. The "delta" value quantifies the sensitivity of an output to changes in input parameters. In this analysis, a cut-off of 15% was applied.

This sensitivity analysis reveals some surprising results, as shown in Table 3.6 for the EU case and Table 3.7 for the GLO case. The two highest deltas are associated with the same technosphere variation, "T: natural gas, high pressure," but are related to different uses. For the EU case, this gas is linked to petroleum and gas production from Russia, whereas in the GLO case, it is sourced from the US and used in steel production. Logically, nearly all technosphere or biosphere entries with a delta greater than 15% are related to electricity use or production.

Surprisingly, gold remains a significant factor in the sensitivity analysis. In both scenarios (second in Belgium and six in GLO), gold has a notable influence: in the EU case due to the electricity required for gold mining and production, and in the GLO case due to gold refinery operations. These technosphere entries have deltas of 20.42% and 19.94%, respectively, indicating a strong influence related to the production phase.

Although the two tables may appear similar in some aspects, they once again highlight the impact of the energy mix used. In the GLO table, most energy-related production is associated with gas or hard coal electricity generation. In contrast, the EU table, particularly for Belgium, also includes gas but features significant contributions from photovoltaic production, reflecting the ongoing energy transition in Belgium. The technosphere entry "T: photovoltaic slanted-roof installation, 3 kWp, single-Si, panel, mounted, on roof [GLO] TO electricity production, photovoltaic, 3 kWp slanted-roof installation, single-Si, panel, mounted (electricity, low voltage) [BE]" shows a delta of 15.44%, underscoring the importance of examining this aspect in further use phase analysis. This difference can be illustrated more visually with the following Figure 4.7 in Appendix E, this figure also shows the importance of nuclear energy in the Belgian energy mix.

| GSA name | delta |
|---|---|
| T: natural gas, high pressure FROM petroleum and gas production, onshore [RU] TO transport, pipeline, onshore, long distance, natural gas (transport, pipeline, onshore, long distance, natural gas) [RU] | 21,57% |
| T: electricity, medium voltage FROM market group for electricity, medium voltage [RAS] TO gold mine operation and gold production, unrefined (gold, unrefined) [RoW] | 20,42% |
| B: Carbon dioxide, fossil // sweet gas, burned in gas turbine (sweet gas, burned in gas turbine) [GLO] | 19,14% |
| T: ferrochromium, high-carbon, 68% Cr FROM market for ferrochromium, high-carbon, 68% Cr [GLO] TO steel production, electric, chromium steel 18/8 (steel, chromium steel 18/8) [RoW] | 18,98% |
| T: natural gas, high pressure FROM petroleum and gas production, onshore [RU] TO natural gas, high pressure, import from RU (natural gas, high pressure) [BE] | 18,12% |
| B: Carbon dioxide, fossil // electricity production, natural gas, combined cycle power plant (electricity, high voltage) [BE] | 18,11% |
| T: distribution network, electricity, low voltage FROM market for distribution network, electricity, low voltage [GLO] TO market for electricity, low voltage (electricity, low voltage) [BE] | 17,76% |
| B: Carbon dioxide, fossil // heat and power co-generation, natural gas, combined cycle power plant, 400MW electrical (electricity, high voltage) [BE] | 17,55% |
| T: sweet gas, burned in gas turbine FROM market for sweet gas, burned in gas turbine [GLO] TO petroleum and gas production, onshore (natural gas, high pressure) [RU] | 17,47% |
| B: Carbon dioxide, fossil // heat and power co-generation, natural gas, conventional power plant, 100MW electrical (electricity, high voltage) [BE] | 16,66% |
| T: natural gas, high pressure FROM evaporation of natural gas, import from QA [Europe without Switzerland] TO natural gas, high pressure, import from QA (natural gas, high pressure) [BE] | 16,23% |
| T: multi-Si wafer FROM market for multi-Si wafer [GLO] TO photovoltaic cell production, multi-Si wafer (photovoltaic cell, multi-Si wafer) [RoW] | 15,76% |
| B: Methane, fossil // natural gas venting from petroleum/natural gas production (natural gas, vented) [GLO] | 15,63% |
| T: natural gas, burned in gas turbine FROM natural gas, burned in gas turbine [RU] TO natural gas, high pressure, import from RU (natural gas, high pressure) [BE] | 15,62% |
| T: photovoltaic slanted-roof installation, 3kWp, single-Si, panel, mounted, on roof FROM market for photovoltaic slanted-roof installation, 3kWp, single-Si, panel, mounted, on roof [GLO] TO electricity production, photovoltaic, 3kWp slanted-roof installation, single-Si, panel, mounted (electricity, low voltage) [BE] | 15,44% |
| T: natural gas, vented FROM market for natural gas, vented [GLO] TO petroleum and gas production, onshore (natural gas, high pressure) [RU] | 15,10% |
| T: electricity, medium voltage FROM market group for electricity, medium voltage [IN] TO ferrochromium production, high-carbon, 68% Cr (ferrochromium, high-carbon, 68% Cr) [RoW] | 15,02% |

Table 3.6: Sensitivity analysis results showing the delta values for the most impactful input parameters for EU



| GSA name | delta |
|---|---|
| T: natural gas, high pressure FROM market for natural gas, high pressure [US] TO steel production, electric, chromium steel 18/8 (steel, chromium steel 18/8) [RoW] | 25,22% |
| T: electricity, medium voltage FROM market group for electricity, medium voltage [RAS] TO steel production, electric, chromium steel 18/8 (steel, chromium steel 18/8) [RoW] | 21,03% |
| B: Carbon dioxide, fossil // electricity production, natural gas, combined cycle power plant (electricity, high voltage) [US-SERC] | 20,81% |
| T: hard coal FROM market for hard coal [CN] TO electricity production, hard coal, at coal mine power plant (electricity, high voltage, for internal use in coal mining) [CN] | 20,74% |
| B: Carbon dioxide, fossil // electricity production, oil (electricity, high voltage) [RoW] | 20,46% |
| T: gold, unrefined FROM market for gold, unrefined [GLO] TO gold refinery operation (gold) [RoW] | 19,94% |
| T: hard coal FROM market for hard coal [CN] TO steel production, electric, chromium steel 18/8 (steel, chromium steel 18/8) [RoW] | 19,92% |
| B: Carbon dioxide, fossil // electricity production, hard coal (electricity, high voltage) [CN-XJ] | 19,12% |
| T: ferronickel FROM market for ferronickel [GLO] TO steel production, electric, chromium steel 18/8 (steel, chromium steel 18/8) [RoW] | 19,00% |
| B: Methane, fossil // hard coal mine operation and hard coal preparation (hard coal) [CN] | 18,80% |
| B: Carbon dioxide, fossil // electricity production, hard coal (electricity, high voltage) [RoW] | 18,53% |
| B: Carbon dioxide, fossil // electricity production, hard coal, conventional (electricity, high voltage) [ZA] | 17,79% |
| B: Carbon dioxide, fossil // electricity production, hard coal (electricity, high voltage) [CN-SA] | 17,18% |
| T: electricity, medium voltage FROM market for electricity, medium voltage [AU] TO gold mine operation and gold production, unrefined (gold, unrefined) [RoW] | 17,13% |
| B: Methane, fossil // natural gas venting from petroleum/natural gas production (natural gas, vented) [GLO] | 16,67% |
| T: hard coal FROM market for hard coal [CN] TO electricity production, hard coal (electricity, high voltage) [CN-GD] | 16,52% |
| T: electricity, medium voltage FROM market group for electricity, medium voltage [IN] TO ferrochromium production, high-carbon, 68% Cr (ferrochromium, high-carbon, 68% Cr) [RoW] | 15,02% |

Table 3.7: Sensitivity analysis results showing the delta values for the most impactful input parameters for GLO

### 3.4.4 Future Improvements

Although this study provides a significant insight into the environmental impact of the system under consideration, there is still considerable scope for improvement to enhance its precision and relevance.

Firstly, further refinement could be achieved by conducting a more detailed analysis of certain subsystems. Several assumptions were made to avoid the need for an exhaustive analysis of individual components. Instead, activities from the Activity Browser were selected that best approximated the components, or they were dimensioned from scratch, which inevitably introduces a degree of approximation. It is important to note that there is limited documentation available for the bill of materials for such a system, as these details are still highly protected due to their technical complexity. However, this situation is likely to change in the future, allowing for re-evaluation or continuation of this work.

Furthermore, the dataset used in this study was EcoInvent. As explained in Section 2.2.1, there are many other datasets available. It would be beneficial to use an alternative dataset incorporating the same activities employed in this study. This approach would strengthen our analyses and provide a more nuanced understanding of the results. Additionally, there are discussions regarding the need for the evolution of these datasets [84].

Another critical aspect to consider is the power phase, which was developed based on certain hypotheses that could significantly alter the final result, particularly in relation to the energy mix. The assumptions regarding the power consumption and the energy sources used are key factors that influence the overall environmental impact. Therefore, a more detailed examination of the power phase, considering different energy scenarios, could provide a clearer picture of the potential environmental impacts and help identify areas for optimisation.

# Chapter 4

# Conclusion

Quantum computers are in full swing at the moment, and it's a race against time for every state to get their hands on one as quickly as possible. Although the race for technology is often a good thing in evolution, the ecological aspect is all too often put aside in the first instance. Indeed, you can already find hundreds of documents online talking about the technological prowess of these new computers, but none of them mention the ecological impact that this kind of technology could have, and more specifically, in terms of greenhouse gases.

Therefore, the aim of this work is to analyse the GWP impact involved in manufacturing a quantum computer, in this case a superconductor, as well as its energy consumption over 5 years.

The results of this work showed that this technology had a rather high ecological footprint. Indeed, it was observed that over five years, combining the production of the quantum computer and its energy consumption, the carbon footprint is around 50,000 kg $CO_2$-eq for a Belgian energy mix and 150,000 kg $CO_2$-eq for a global energy mix. It's important to note that carbon impacts are much greater during the use phase ($\tilde{8}0\%$) than during the production phase ($\tilde{2}0\%$). These results were obtained by applying a life cycle assessment to each subsystem of the quantum computer. It was then observed that the subsystem with the heaviest ecological impact during the production phase is the cryostat, mainly due to the use of gold, and the subsystem with the greatest ecological impact during the use phase (five years) is the pulse tube cryocooler compressors, which are essential for cooling the cryostat. In fact, the components responsible for cooling the cryostat are accountable for two-thirds of the carbon impact.

However, given the complexity of a superconducting quantum computer with its many underlying components, the still very secret aspect of this technology, and a one-year period to carry out this life-cycle analysis, a coarse-grain methodology was chosen for this work, and this implies certain limitations. Indeed, not all components were dismantled down to the last bolt for the analysis of the production phase, and assumptions were often made in order to simplify these components. The main idea was to gain an overview of the ecological impacts of the various subsystems as well as the types of activity with the highest carbon footprint.

Finally, in terms of improvements, it would be interesting to complete the LCI of this study by further refining some of the more problematic subsystems or by making other LCIs based on other databases in order to make comparisons. Furthermore, applying more uncertainties to the different activities could also be a good improvement to the LCA analysis.

# Appendices

## A Quantum gates

| **Single-Qubit Gates** | | | |
|---|---|---|---|
| Name | Symbol | Matrix Representation | Description |
| Pauli-X Gate (NOT Gate) | X | $\begin{pmatrix} 0 & 1 \\ 1 & 0 \end{pmatrix}$ | The Pauli-X gate flips the state of a qubit, converting $\|0\rangle$ to $\|1\rangle$ and $\|1\rangle$ to $\|0\rangle$. |
| Pauli-Y Gate | Y | $\begin{pmatrix} 0 & -i \\ i & 0 \end{pmatrix}$ | The Pauli-Y gate combines a bit-flip with a phase flip, adding a complex phase factor. |
| Pauli-Z Gate (Phase Flip) | Z | $\begin{pmatrix} 1 & 0 \\ 0 & -1 \end{pmatrix}$ | The Pauli-Z gate flips the phase of the $\|1\rangle$ state, converting $\|1\rangle$ to $-\|1\rangle$. |
| Hadamard Gate | H | $\frac{1}{\sqrt{2}}\begin{pmatrix} 1 & 1 \\ 1 & -1 \end{pmatrix}$ | The Hadamard gate creates a superposition state from a basis state, converting $\|0\rangle$ to $\frac{1}{\sqrt{2}}(\|0\rangle + \|1\rangle)$ and $\|1\rangle$ to $\frac{1}{\sqrt{2}}(\|0\rangle - \|1\rangle)$. |
| Phase Gate | S | $\begin{pmatrix} 1 & 0 \\ 0 & i \end{pmatrix}$ | The phase gate applies a phase shift of $\frac{\pi}{2}$ to the $\|1\rangle$ state, converting $\|1\rangle$ to $i\|1\rangle$. |
| T Gate | T | $\begin{pmatrix} 1 & 0 \\ 0 & e^{\frac{i\pi}{4}} \end{pmatrix}$ | The T gate, also known as the $\frac{\pi}{8}$ gate, applies a phase shift of $\frac{\pi}{4}$ to the $\|1\rangle$ state. |

Table 4.1: Single-Qubit Gates

| Two-Qubit Gates | | | |
|---|---|---|---|
| Name | Symbol | Matrix Representation | Description |
| Controlled-NOT Gate (CNOT Gate) | CNOT | $\begin{pmatrix} 1 & 0 & 0 & 0 \\ 0 & 1 & 0 & 0 \\ 0 & 0 & 0 & 1 \\ 0 & 0 & 1 & 0 \end{pmatrix}$ | The CNOT gate flips the state of the target qubit if the control qubit is in the 1⟩ state. It is crucial for creating entanglement. |
| Controlled-Z Gate (CZ Gate) | CZ | $\begin{pmatrix} 1 & 0 & 0 & 0 \\ 0 & 1 & 0 & 0 \\ 0 & 0 & 1 & 0 \\ 0 & 0 & 0 & -1 \end{pmatrix}$ | The CZ gate applies a phase flip to the target qubit if the control qubit is in the 1⟩ state. |
| SWAP Gate | SWAP | $\begin{pmatrix} 1 & 0 & 0 & 0 \\ 0 & 0 & 1 & 0 \\ 0 & 1 & 0 & 0 \\ 0 & 0 & 0 & 1 \end{pmatrix}$ | The SWAP gate exchanges the states of two qubits. |

Table 4.2: Two-Qubit Gates

| Multi-Qubit Gates | | | |
|---|---|---|---|
| Name | Symbol | Matrix Representation | Description |
| Toffoli Gate (CCNOT Gate) | Toffoli | $\begin{pmatrix} 1 & 0 & 0 & 0 & 0 & 0 & 0 & 0 \\ 0 & 1 & 0 & 0 & 0 & 0 & 0 & 0 \\ 0 & 0 & 1 & 0 & 0 & 0 & 0 & 0 \\ 0 & 0 & 0 & 1 & 0 & 0 & 0 & 0 \\ 0 & 0 & 0 & 0 & 1 & 0 & 0 & 0 \\ 0 & 0 & 0 & 0 & 0 & 1 & 0 & 0 \\ 0 & 0 & 0 & 0 & 0 & 0 & 0 & 1 \\ 0 & 0 & 0 & 0 & 0 & 0 & 1 & 0 \end{pmatrix}$ | The Toffoli gate flips the state of a target qubit if both control qubits are in the 1⟩ state. It is a universal gate for reversible classical computation. |
| Fredkin Gate (CSWAP Gate) | Fredkin | $\begin{pmatrix} 1 & 0 & 0 & 0 & 0 & 0 & 0 & 0 \\ 0 & 1 & 0 & 0 & 0 & 0 & 0 & 0 \\ 0 & 0 & 1 & 0 & 0 & 0 & 0 & 0 \\ 0 & 0 & 0 & 1 & 0 & 0 & 0 & 0 \\ 0 & 0 & 0 & 0 & 1 & 0 & 0 & 0 \\ 0 & 0 & 0 & 0 & 0 & 0 & 1 & 0 \\ 0 & 0 & 0 & 0 & 0 & 1 & 0 & 0 \\ 0 & 0 & 0 & 0 & 0 & 0 & 0 & 1 \end{pmatrix}$ | The Fredkin gate swaps the states of two target qubits if the control qubit is in the 1⟩ state. |

Table 4.3: Multi-Qubit Gates

# B References, Hypothesis and Activities for Each Sub-System

Find under this all the assumptions and the reference used. We also include all the activities used in Activity Browser.

## B.1 Cryostat

- Holding structure
  - **References** : Based on the information given in the User Manual [70] and information taken in the Gehring's Lab (UCLvouain)
  - **Materials** : Chromium steel
  - **Hypothesis & Activities** : The total volume is plus or minus $150000cm^3$ considering dimension on 3.5. This is not a plain structure, so removing +/- 2/3 of the surface, we finally get $50000cm^3$ and considering the volumic mass of $7.14g/cm^3$, the mass is then +/- 130kg which correlate the mass given in the manual.

    chromium steel : 130kg.
- Flanges and support
  - **References** : [69]
  - **Materials** : Copper and gold
  - **Hypothesis & Activities** : There are 5 flanges, each made of copper and gold coated. The gold coating is 1ţm thick.

    market for copper-rich materials : $6283cm^3$ –> +/- 50kg

    market for gold : $13194cm^2$ –> +/- 25g
- Shields
  - **References** : [85] [70]
  - **Materials** : Steel, gold and Mu-Metal
  - **Hypothesis & Activities** :

    Market for gold : 0.04kg of gold. Sheet rolling copper and steel : 77kg + 150kg
- Wiring
  - **References** : [**noauthor_coaxial_202**] [86]

- **Materials** : CuNi, NbTi and Copper
- **Hypothesis & Activities** : Wire drawing, copper : 10kg. 10g of NbTi alliage, 4.6g of ferrobium and 5.4g of niobioum. 3g of CuNi alloy, 2.1g of copper-rich material and 0.9g nickel-rich material.

- Dilution Refrigirator Components
  - **References** : [87]
  - **Materials** : Copper
  - **Hypothesis & Activities** : 5kg of copper-rich material and 20g of silver.

- Microwaves Devices
  - **References** : [88] [89]
  - **Materials** : Copper
  - **Hypothesis & Activities** : 5kg of copper-rich material and 1g of gold.

## B.2 Gas Handling System

- Structure (Cabinet and support plate)
  - **References**: [69] [90]
  - **Materials** : Extruded steel
  - **Hypothesis & Activities** : Dimensions 90x75x215 $cm^3$ [69], based on this we find some references [90] to find the weight and materials used.
    * market for steel, chronium steel 18/8, hot rolled : based on internet reference, classic cabinet are made of steel. For 270kg charge, a cabinet of 44kg is needed [90], here we suppose this more heavy with 60kg of steel.
    * market for metal working, average for steel product manufacturing : 60kg, metal working to do a cabinet.

- Mixture tank
  - **References**: WGA232-50-20, two times 50L [91][69]
  - **Materials** : 34CrMo4, Helium 99,99%
  - **Hypothesis** : We consider the tank in full steel with a selective coat on the out-side of the tanks. We known that we have 50L of He gas in it so it's around 11 kg He.

    - ∗ market for steel, chronium steel 18/8, hot rolled : 56 kg,based on [91]. There no activity more similar to our steel.
    - ∗ market for metal working, average for steel product manufacturing : 56kg, metal working to do a cabinet.
    - ∗ market for selective coat, stainless steel sheet, black chrome : 0.183 $m^2$, the external sides of the tanks have been treated. We have the radius and the height so we found the surface.
    - ∗ market for helium : 11.241 kg, we know there is 50L of He in the system and we know the density of the He.

- Mixture circulation turbo pump
  - **References**: Pfeiffer HiPace 400 [69] [92]
  - **Materials** : /
  - **Hypothesis & Activities** :
    - ∗ air compressor, screw-type compressor, 4kW : This activity covers the manufacture of a screw-type air compressor, wich correspond to the type of the pump. Based on the weight the reference compressor and ours we apply a coefficient to the unit, reference weight 140kg, ours 10.6kg so coefficient of 0.0757 unit.

- Mixture circulation scroll pump
  - **References**: Edwards XDS35i [69] [93]
  - **Materials** : /
  - **Hypothesis & Activities** :
    - ∗ air compressor, screw-type compressor, 4kW : This activity covers the manufacture of a screw-type air compressor, wich correspond to the type of the pump. Based on the weight the reference compressor and ours we apply a coefficient to the unit, reference weight 140kg, ours 48kg so coefficient of 0.342 unit.

- Mixture circulation compressor
  - **References**: Agilent IDP-3 [69] [94]
  - **Materials** : /
  - **Hypothesis & Activities** :

    * air compressor, screw-type compressor, 4kW : This activity covers the manufacture of a screw-type air compressor, wich correspond to the type of the pump. Based on the weight the reference compressor and ours we apply a coefficient to the unit, reference weight 140kg, ours 9.5kg so coefficient of 0.068 unit.

- Service scroll-pump
  - **References**: Agilent SH-110 [69] [95]
  - **Materials** : /
  - **Hypothesis & Activities** :
    * air compressor, screw-type compressor, 4kW : This activity covers the manufacture of a screw-type air compressor, wich correspond to the type of the pump. Based on the weight the reference compressor and ours we apply a coefficient to the unit, reference weight 140kg, ours 19.5kg so coefficient of 0.139 unit.
- Wires
  - **References**: Wires for gas [96]
  - **Materials** : Stainless Steel
  - **Hypothesis & Activities** :
    * market for chromium steel pipe : we estimate around 12 cables of a length around 1.8m (heigth of the cabinet 2.15m), with [97] we find a weight of 4.1kg for one cable. So total of 49.2kg of cables.

## B.3 Pulse Tube Cryocooler and Compressor

- Compressor
  - **References**: CP1110 [69] [70] [71]
  - **Materials** : /
  - **Hypothesis & Activities** :
    * air compressor, screw-type compressor, 4kW : This activity covers the manufacture of a screw-type air compressor, wich correspond to the type of the pump. Based on the weight the reference compressor and ours we apply a coefficient to the unit, reference weight 140kg, ours 190.5kg so coefficient of 1.36 unit.
- Cold head

- **References**: PT415 RM [69] [70] [71]
- **Materials** : Steel and copper
- **Hypothesis** : We don't have much information about the materials so we have fix that we have only steel and copper, 90% of steel and 10% of copper for the total weight of 25kg.
  - market for steel, chronium steel 18/8, hot rolled : 22.5 kg.
  - market for metal working, average for steel product manufacturing : 22.5kg, metal working to do the cold head.
  - market for metal working, average for copper product manufacturing : 2.5kg, copper metal working to do the cold head.
  - market for copper, cathode : 2.5kg, estimation of the copper we can see on the images.

- Wiring
  - **References**: [98]
  - **Materials** : Flexible steel line
  - **Hypothesis & Activities** :
    - market for chromium steel pipe : we a length of 20.1m and 3/4" corresponding to the inlet and outlet connection [98][71], with [97] we find 71kg of cable.

## B.4 Control Unit

Once the control unit (CU) is open we can describe those main elements (see Figure 3.13 and 3.12) and for every of the component we followed our methodology. We deleted the extension board because it an option and we try to stay general.

- Structure
  - **References**: Reference weight : **115kg** [70]
  - **Materials**: Steel
  - **Hypothesis & Activities** :
    - market for steel, chronium steel 18/8, hot rolled : based on internet reference, classic cabinet are made of steel. For 270kg charge, a cabinet of 44kg is needed [90], here we suppose this more heavy with 50kg of steel.
    - market for metal working, average for steel product manufacturing : 50kg, metal working to do a cabinet.

- Air Filters
  - **References**: Based on the catalog of air filters [99].
  - **Materials** : Poly-carbonate, Plastic (rubber joint), lubricating oil, Thin sheet of steel.
  - **Hypothesis & Activities** : Based on the catalog we found we can approximate the weight of every materials, with a max weight of 1,8kg.
    * market for poly-carbonate : 0.7kg, primary material.
    * market for steel, low-alloyed, hot rolled : 0.7kg, primary material.
    * market for synthetic rubber : 0.35kg, rubber joint.
    * market for lubricating oil : 0.05kg, used for lubrication the air.
- USB-Hub
  - **References**: [100]
  - **Materials** : PCB card, integrated circuit logic type, Poly-carbonate, resistor, capacitors.
  - **Hypothesis & Activities** :
    * market for printed wiring board, for surface mounting, Pb free surface : $0,012046m^2$, we estimate the full assembled flow meter unit is equal to 2.5 NI DAQ long so 158.5x76mm.
    * market for capacitor, for surface-mounting : 0.00086 kg, due the references we can estimate 10 units.
    * market for resistor, surface-mounted : 0,000098 kg, due the references we can estimate 10 units.
    * market for integrated circuit, logic type : 0.003 kg, we count 3 logic type component each 1g.
    * market for poly-carbonate : 0.025kg, for the box around 25g.
    * market for cable, data cable in infrastructure : 1.5m, in [69], we see a cable starting from the box going to the NI DAQ.
- Flow meter control unit
  - **References**: Based on [69], The Bronkhorst High-Tech model F-11B-2K0-ABD-33-V flow-meter unit, datasheet and information on their site. [101]
  - **Materials** : PCB card, Capacitor, Resistor, integrated circuit logic type, Stainless steel, polycarbonate.

- **Hypothesis & Activities** : The flow meter unit is composed by two printed board and the unit flow meter composed of Stainless steel, poly-carbonate.
  - market for printed wiring board, for surface mounting, Pb free surface : $0,004826m^2$, we estimate the full assembled flow meter unit is equal to one NI DAQ long so 63.5x76mm.
  - market for capacitor, for surface-mounting : 0.000344 kg, in [69] we have diagram of each electronic bloc, we count 4 capacitors, so with the weight given for one capacitor (see activity), we can found the weight for all.
  - market for resistor, surface-mounted : 0.0000392 kg, in [69] we have diagram of each electronic bloc, we count 4 resistor, so with the weight given for one capacitor (see activity), we can found the weight for all.
  - market for integrated circuit, logic type : 0.002 kg, we count 2 logic type component each 1g.
  - market for cable, data cable in infrastructure : 8m, one cable connected to the flow meter itself (made of 4 cables), one cable connected to the led panel (8-pin ribbon cable, unfortunately no 8-pin ribbon cable activity so we fix it equal to 4 cables). We have already take into account the cable going to the NI DAQ in the NI DAQ system. We average them to 1m each.
  - market for poly-carbonate : 0.3kg, based on the datasheet.
  - market for steel, chronium steel 18/8, hot rolled : 0.2kg, of steel.
  - market for metal working, average for steel product manufacturing : 0.2kg to make the flowmeter.

- 5V supplies
  - **References**: Datasheet LOGO!POWER 5V [102]
  - **Materials** : /
  - **Hypothesis & Activities** : Simens industries has already done a LCA on the component in the datasheet of the element. The Global warming potential [kg $CO_2$-eq] during manufacturing : **2.4 kg**.
    - Biosphere flows : carbon dioxide, fossil

- 24V supplies
  - **References**: Datasheet LOGO!POWER 24V [103]

- **Materials** : /
- **Hypothesis & Activities** : Simens industries has already done a LCA on the component in the datasheet of the element. The Global warming potential [kg $CO_2$-eq] during manufacturing : **3.9 kg**.
  - Biosphere flows : carbon dioxide, fossil

- Main circuit breaker
  - **References**: Schneider C60HD [104], we can see in [69].
  - **Materials** : Three mains components : strip made of steel, copper called bimetallic and the coil that stops short circuits.
  - **Hypothesis & Activities** : We know that it weight around 0.2 kg [105] and we had the hypothesis that the most of the impact come from the copper. So we consider a circuit breaker full of copper for 0.2 kg.
    - market for copper, cathode : 0.2 kg, copper production.
    - market for metal working, average for copper product manufacturing : 0.2kg, take into account the production of the circuit breaker.

- Main board
  - **References**: A lot of information find in [69]
  - **Materials** : Zener Diode, Resistor, Transistor, Capacitor, Ribbon cable, PCB card, cable and integrated circuit.
  - **Hypothesis** : There is four part in this main board, two lachting circuit, one off-chanel circuit and one digital I/O.
    - market for printed wiring board, for surface mounting, Pb free surface : $0, 1m^2$, we estimate the surface of board thanks to the NI DAQ dimensions know just under see in Figure 3.13. Dimensions : 260x390mm.
    - market for cable, ribbon cable, 20-pin, with plugs : 0.5 kg, 5 ribbon cable around 1m each, thank to the activity we know ribbon cable weight for 0.24m is 0.0242 kg so we know the weight for 5m
    - market for capacitor, for surface-mounting : 0.0124 kg, in [69] we have diagram of each electronic bloc, we count around 144 capacitor (8 I/O circuit, 64x2 lachting circuit, 16 for Off-chanel circuit) , so with the weight given for one capacitor (see activity), we can found the weight for all. Becare its for one lachting chanel, we have to multiply by 8.

    * market for resistor, surface-mounted : 0.0021 kg, in [69] we have diagram of each electronic bloc, we count around 256 resistor (16 I/O circuit, 88x2 lachting circuit, 64 for Off-chanel circuit), so with the weight given for one resistor (see activity), we can found the weight for all.
    * market for diode, glass-, for surface-mounting : 0.0024 kg, in [69] we have diagram of each electronic bloc, we count around 74 diode (6 I/O circuit, 32x2 lachting circuit, 4 for Off-chanel circuit), so with the weight given for one diode (see activity), we can found the weight for all.
    * market for integrated circuit, logic type : 0.12 kg, for all the logic integrated circuit as flip-flop, multiplexer, etc. We take all the weight of integrated circuit we have on the datasheet, we have averaged the weight for one unit at 1,2 g and we count 100 integrated circuit (4 I/O circuit, 40x2 lachting circuit, 16 for Off-chanel circuit).
    * market for cable, data cable in infrastructure : 50m, standard cable connected to the main board. There are 25 grey cables connected, made up of a red cable and a black cable, we estimate the length to 1m by cable in average.

- NI DAQ
  - **References**: NI USB-6008 [106]
  - **Materials** : Unknown
  - **Hypothesis & Activities** : It weight 84g, 54g without the connectors so we have already 20g of plastic around. This NI-DAQ offers basic functionality for applications such as simple data logging. So we know there is so logic type circuit and memory circuit to play with those data.
    * market for integrated circuit, logic type : 0.0054kg, we estimate the weight of the NI DAQ is 10% from the logic type circuit.
    * market for integrated circuit, memory type : 0.0054kg, we estimate the weight of the NI DAQ is 10% from the memory type circuit.
    * market for printed wiring board, for surface mounting, Pb free surface : $0.004m^2$, we know the dimensions but it can't be all full of printed wiring board so we fix 57x70mm.
    * market for poly-carbonate : 0.0578kg, for the box and the connectors (37.8g and 20g).
    * market for cable, data cable in infrastructure : 2.95m, standard cable connected to the main board. There is 13 cable of around 15cm and 1 cable going to connect to flow meter around 1m.

- Pneumatic valve and pneumatic wiring
  - **References**: Solenoid valve SY3000/5000 Base Mounted [107], wiring in Polymer plastic [108].
  - **Materials** : Plastic mix (for wiring) and steel low-alloyed.
  - **Hypothesis & Activities** :For 1m of plastic pipes the weight is 0.16kg [97]. We have 26 wiring output for pneumatic valve. We estimate an 1,5m average length for each. So 6,24kg of pipes.
    * market for extrusion, plastic pipes : 6.265 kg, 1kg of plastic give 0.996kg of pipes, we have 6.24kg.
    * market for synthetic rubber : 6.265kg, to produce the wire.
    * market for steel, low-alloyed, hot rolled : 1kg, thanks to the datasheet we can find 1kg if we consider that only steel.
    * market for metal working, average for steel product manufacturing : 1kg, to produce the pneumatic valve.
- Control panel backside
  - **References**: Figure 3.12
  - **Materials** : PCB card, resistor, diode, integrated circuit logic type, cable, pushing buttons.
  - **Hypothesis & Activities** : For the pushing buttons we find a kind similar pushing button with already a impact analyse contribution [109], of 5.26kg [$CO_2$-eq].
    * market for printed wiring board, for surface mounting, Pb free surface : $0.0127m^2$, we estimate the surface of board thanks to the Back of the push buttons we can see in Figure 3.12, they have a diameter of 16mm (online market [109]) and we can put 11 on the length, 4,5 on the width. Dimensions : 176x72mm.
    * market for resistor, surface-mounted : 0.00735 kg, in [69] we have diagram of one electronic bloc connected to eight valves, we count around 18 resistor (and there is 4 bloc of eight valves, so 18x4), and 3 for the connection on the remote part. Total of 75 resistor. With the weight given for one resistor (see activity), we can found the weight for all.
    * market for diode, glass-, for surface-mounting : 0.0011 kg, in [69] we have diagram of each electronic bloc, we count around 1 diode for each button and two for the remote system, so a total of 34 diodes. With the weight given for one diode (see activity), we can found the weight for all.

- * market for integrated circuit, logic type : 0.005 kg, for the logic integrated circuit we have only DIP component [110], 1.47g for eight poles. There four of them in the circuit.
- * market for cable, data cable in infrastructure : 30.6 m , standard cable connected to the main board. There are 34 grey cables connected, made up of 3 cables each, we estimate the length to 30cm by cable in average. We had already take into account the ribbon cable in the main board.
- * Biosphere flows : carbon dioxide, fossil. For the pushing buttons we have 34 of them. So as they are not same as ours we estimate 5kg [$CO_2$-eq] for a total of 170kg [$CO_2$-eq].

## B.5 Quantum Hardware

- Workstation
  - * **References** : [111]
  - * **Materials** : PCB card, aluminum, laptop
  - * **Hypothesis & Activities** :
    - · market for computer, laptop : 1 unit. This is an approximation of the whole workstation in terms of materials production, already including a screen
    - · market for aluminium : 5kg. For additional casing since it is not a laptop
    - · market for printed wiring board, for surface mounting, Pb free surface : $0.02cm^2$, for additional boards (estimation)
- Chassis with modules
  - * **References** : [73]
  - * **Materials** : PCB card, aluminum
  - * **Hypothesis & Activities** :
    - · market for printed wiring board, for surface mounting, Pb free surface : $0.001m^2$. This includes all the devices in the chassis.
    - · market for aluminium : 3kg.
- Rack cabinet
  - * **References** : [111]
  - * **Materials** : Steel
  - * **Hypothesis & Activities** :

    - Market for sheet rolling, steel : 177kg.
- Vector signal generator :
  - **References** : [111]
  - **Materials** : PCB card, aluminum
  - **Hypothesis & Activities** :
    - market for printed wiring board, for surface mounting, Pb free surface : $0.02m^2$.
    - market for aluminium : 3kg.
- I/Q Modulator/Demodulator : [111]
  - **References** :
  - **Materials** : PCB card, aluminum
  - **Hypothesis & Activities** :
    - market for printed wiring board, for surface mounting, Pb free surface : $0.0006m^2$.
    - market for aluminium : 3kg.

# C Table of Activities in Activity Browser for Type Activities Distribution

| **Structure** | **Activities name in AB** |
|---|---|
| Quantum Hardware | Rack_cabinet |
| Control Unit | CU_casing |
| GHS | GAS_Structure |
| Cryostat | Structure |

Table 4.4: Activity in AB for Structure Type

| **Refrigerator Device** | **Activities name in AB** |
|---|---|
| Control Unit | CU_PneumaticValve and CU_AirFilters |
| GHS | GAS_Wires |
| | GAS_Service_scroll_PUMP |
| | GAS_Mixture_circulation_turbo_pump |
| | GAS_Mixture_circulation_Scroll_PUMP |
| | GAS_Mixture_circulation_compressor |
| | GAS_Tanks |
| Cryostat | DR_comp |
| | Shields |
| Pulse Tube Cryocooler Compressor | PT_Cold_Head |
| | PT_Compressor |
| | PT_Wiring |

Table 4.5: Activity in AB for Refrigerator Device

| Electronic & Quantum Device | Activities name in AB |
|---|---|
| Quantum Hardware | I/Q_Mod/Demod |
| | PXIe_Chassis |
| | Vector_signal_generator |
| | Workstation |
| Control Unit | CU_USB_Hub |
| | CU_NIDAQ |
| | CU_FlowMeter |
| | CU_mainboard |
| | CU_control_Panel(back) |
| Cryostat | Microwaves_devices |

Table 4.6: Activity in AB for Electronic & Quantum Device

# D Monte Carlo Simulation

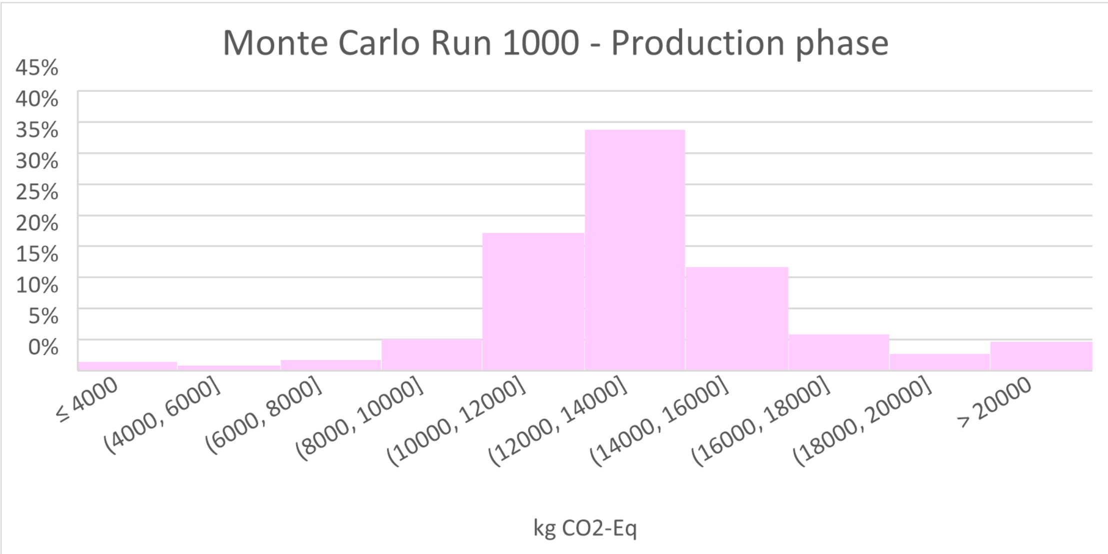


Figure 4.1: Monte Carlo Simulation 1000 runs for production phase

# E Results graphics

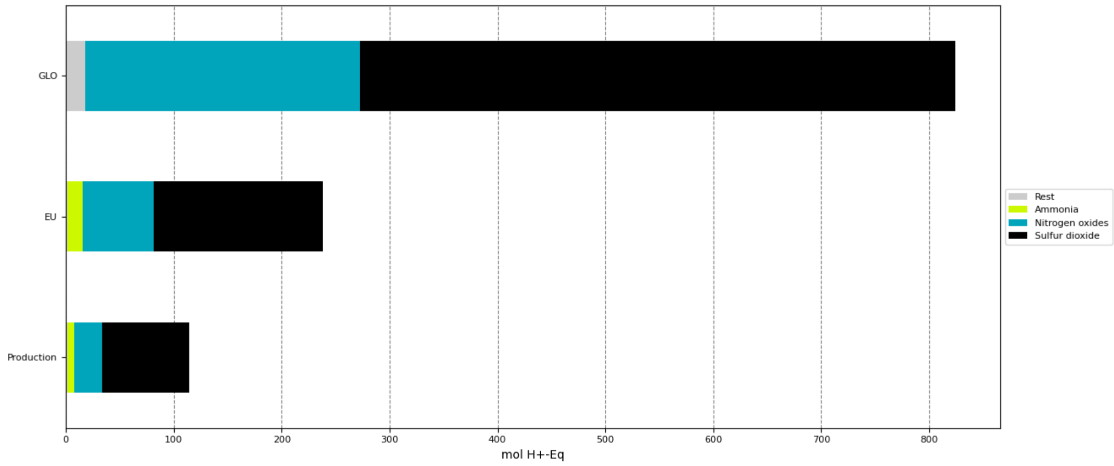


Figure 4.2: Acidification accumulated exceedance AE

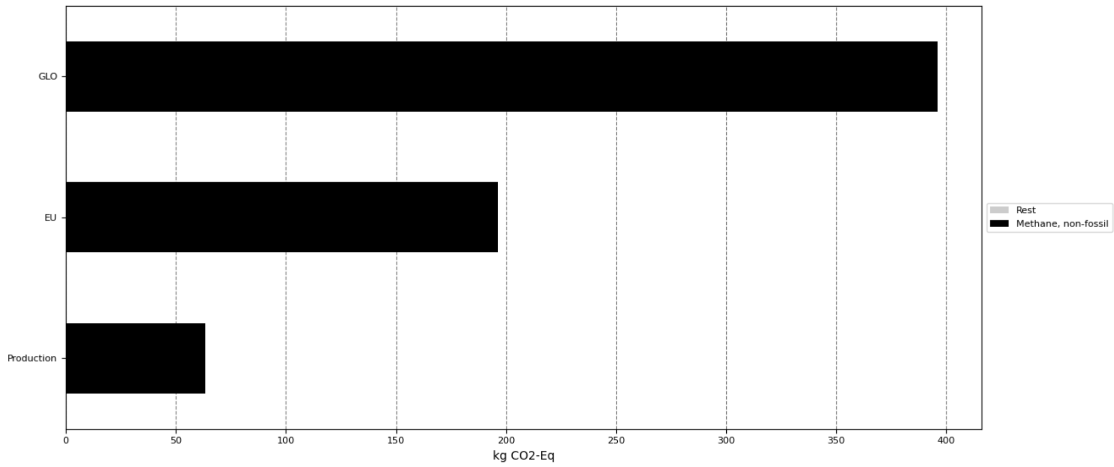


Figure 4.3: Climate change biogenic global warming potential GWP100

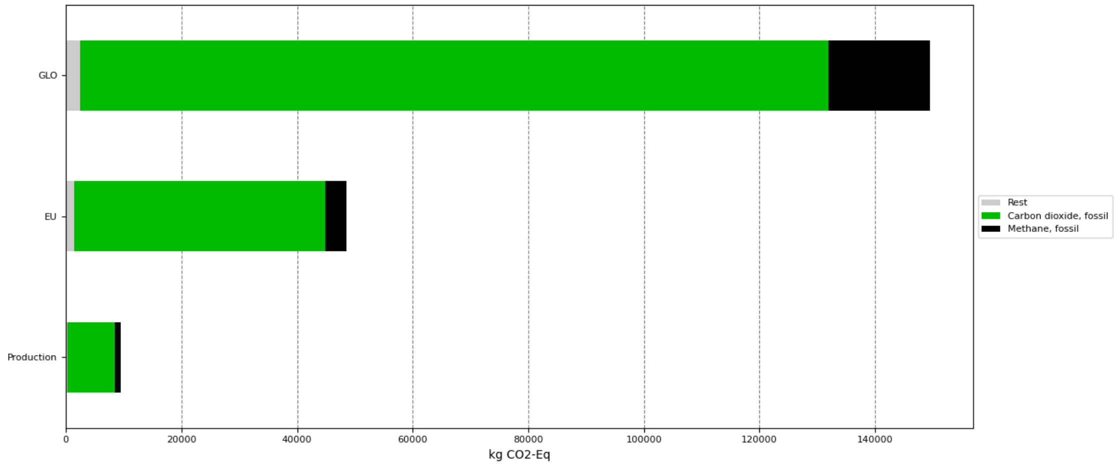


Figure 4.4: Climate change fossil global warming potential GWP100

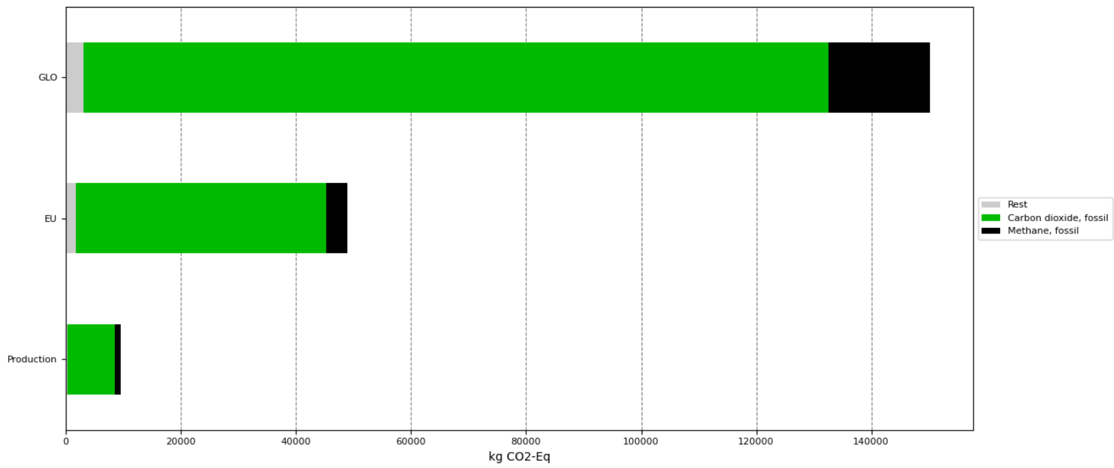


Figure 4.5: Climate change global warming potential GWP100

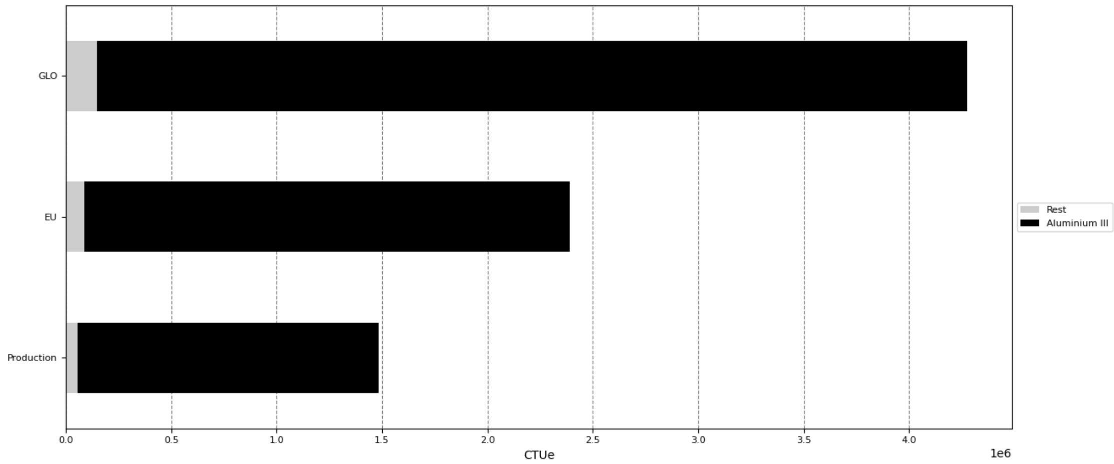


Figure 4.6: Ecotoxicity freshwater metals comparative toxic unit for ecosystems - CTUe

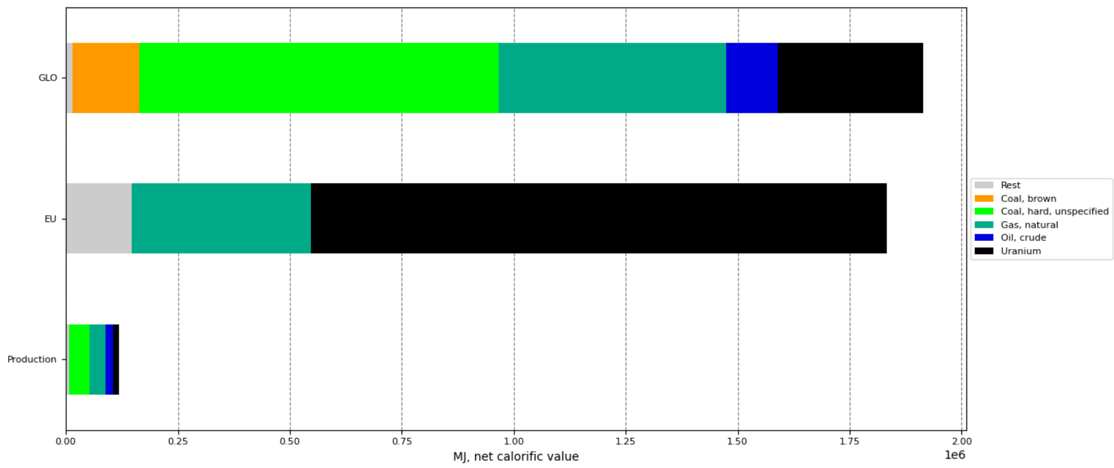


Figure 4.7: Energy resources non renewable abiotic depletion potential ADP fossil fuels MJ net calorific value

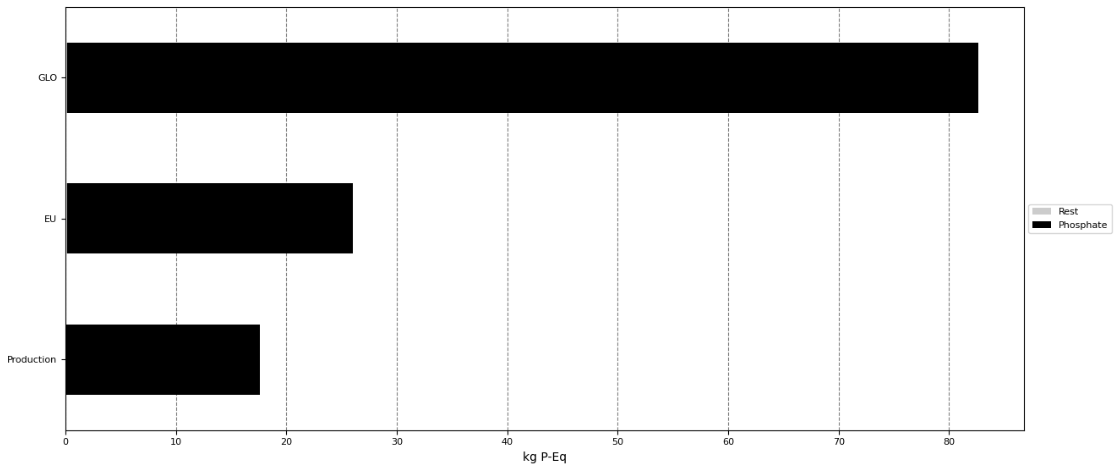


Figure 4.8: Eutrophication freshwater fraction of nutrients reaching freshwater end compartment kg P-Eq

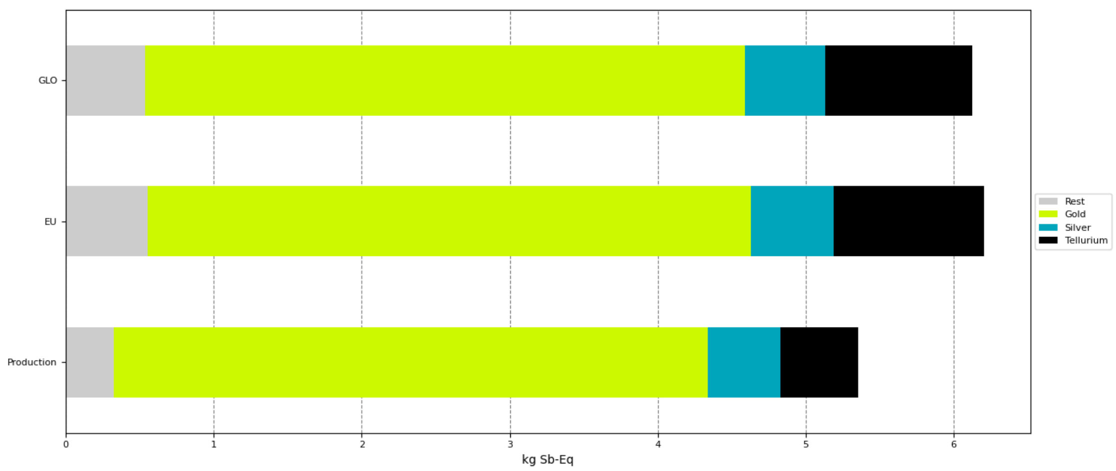


Figure 4.9: Material resources metalsminerals abiotic depletion potential ADP elements ultimate reserves kg Sb-Eq

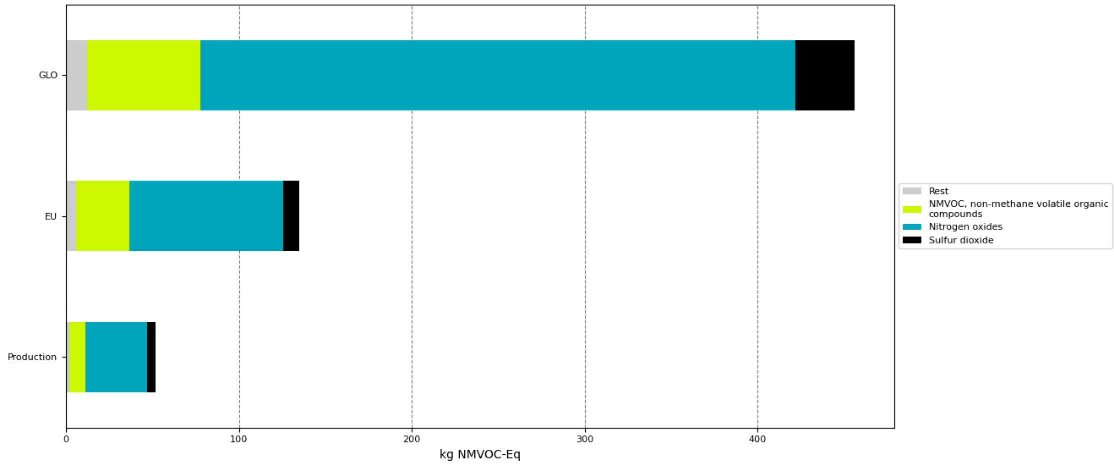


Figure 4.10: Photochemical oxidant formation human health tropospheric ozone concentration increase kg NMVOC-Eq

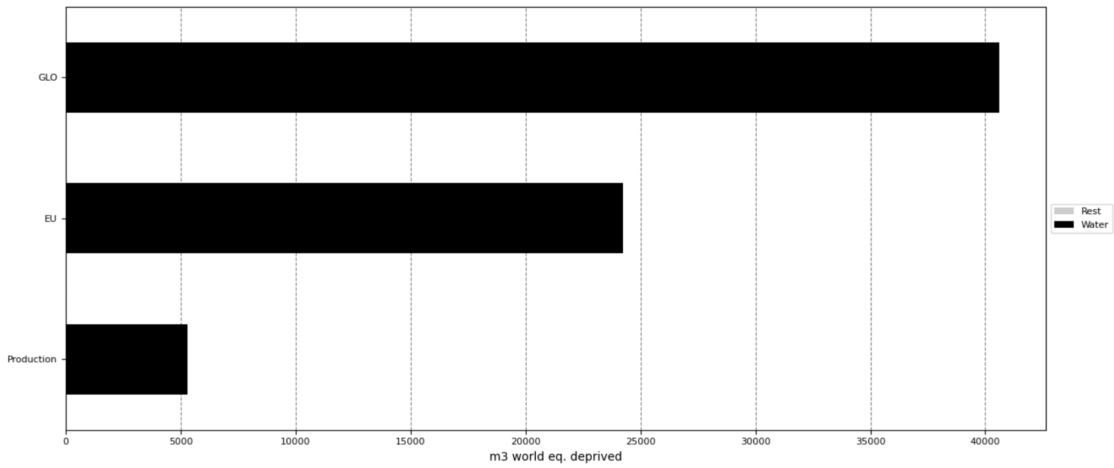


Figure 4.11: Water use user deprivation potential deprivation weighted water consumption m3 world Eq deprived

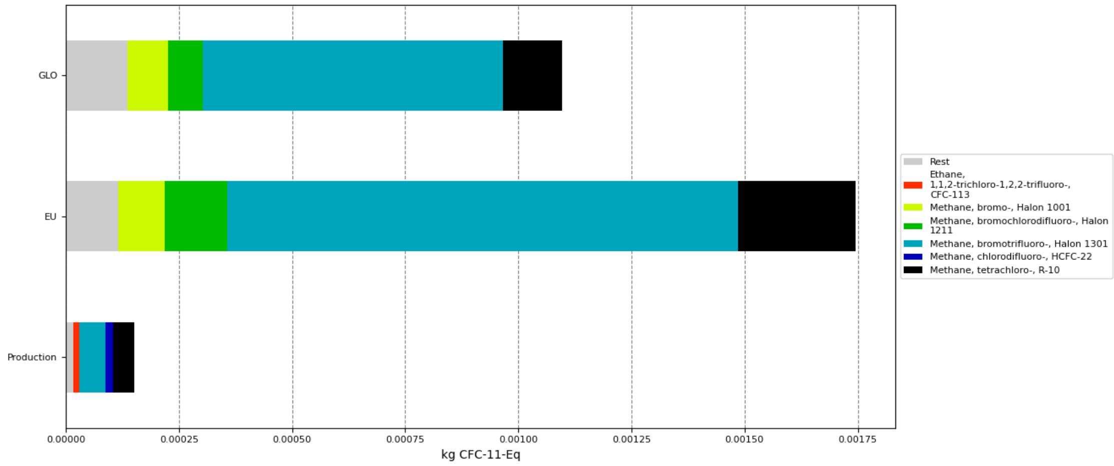


Figure 4.12: Ozone depletion ozone depletion potential ODP kg CFC-11-Eq

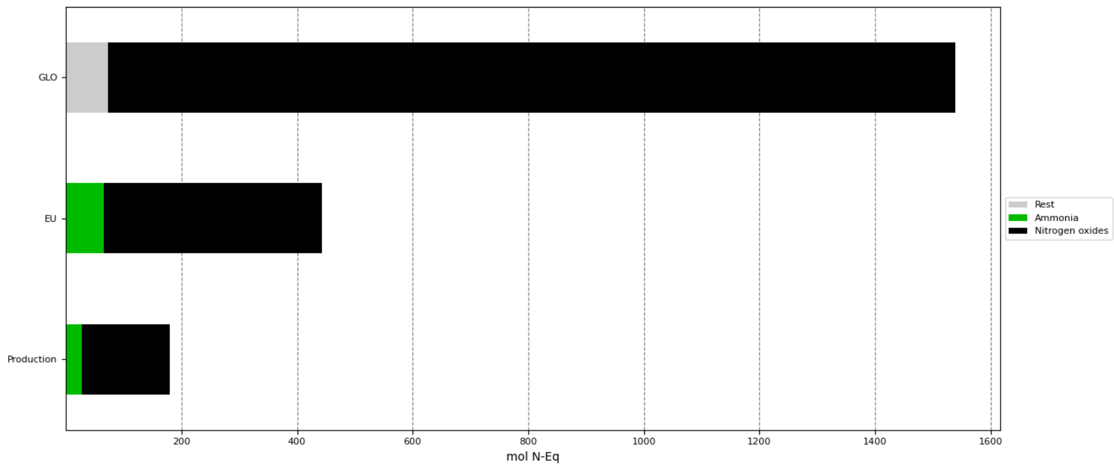


Figure 4.13: Eutrophication terrestrial accumulated exceedance AE mol N-Eq

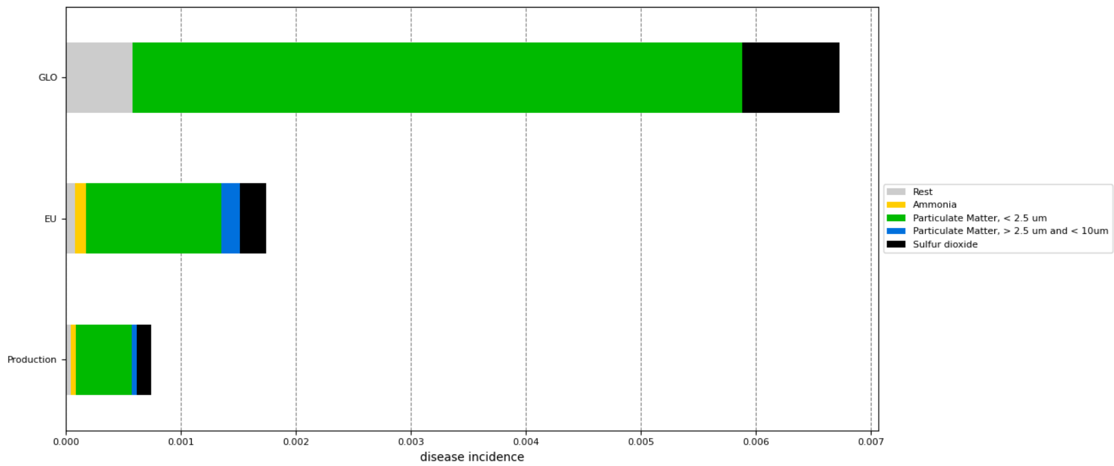


Figure 4.14: Particulate matter formation impact on human health disease incidence

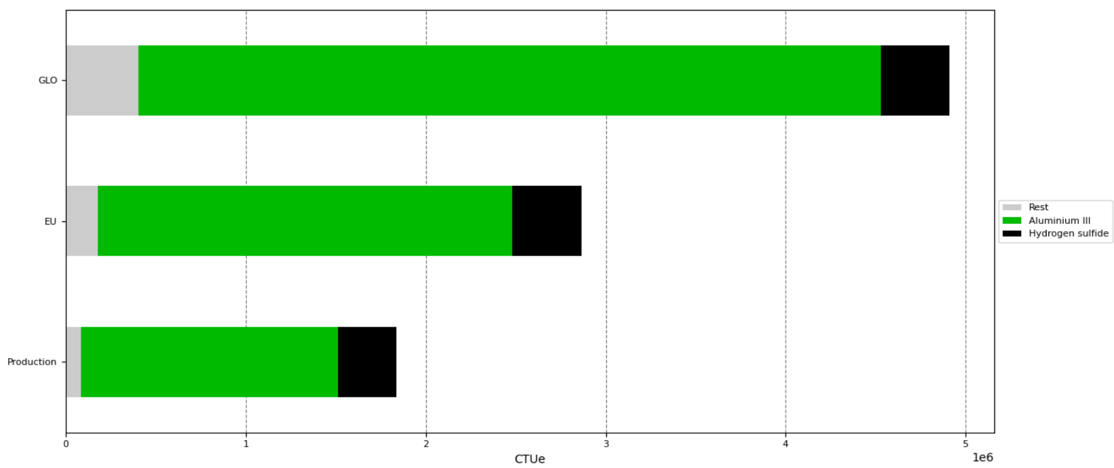


Figure 4.15: Ecotoxicity freshwater comparative toxic unit for ecosystems CTUe

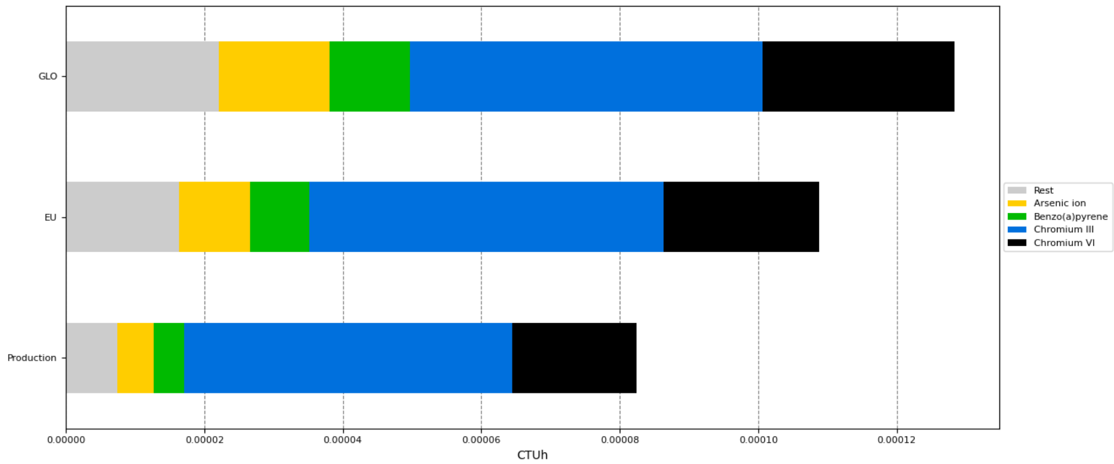


Figure 4.16: Human toxicity carcinogenic comparative toxic unit for human CTUh

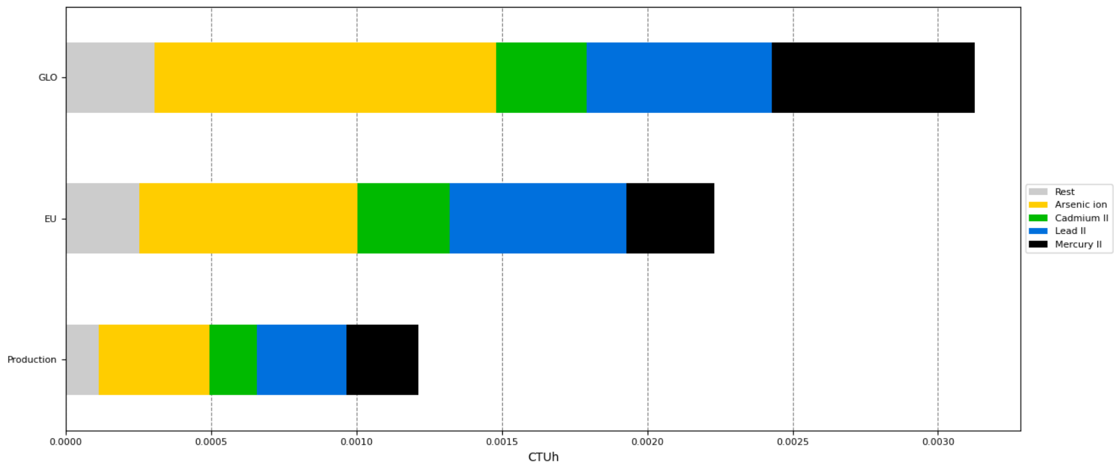


Figure 4.17: Human toxicity non carcinogenic comparative toxic unit for human CTUh

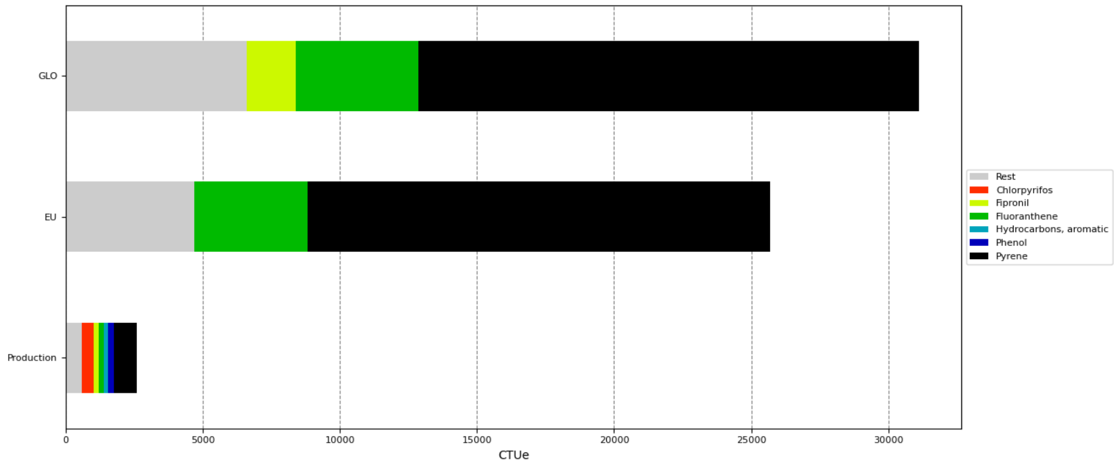


Figure 4.18: Ecotoxicity freshwater organics comparative toxic unit for ecosystems CTUe

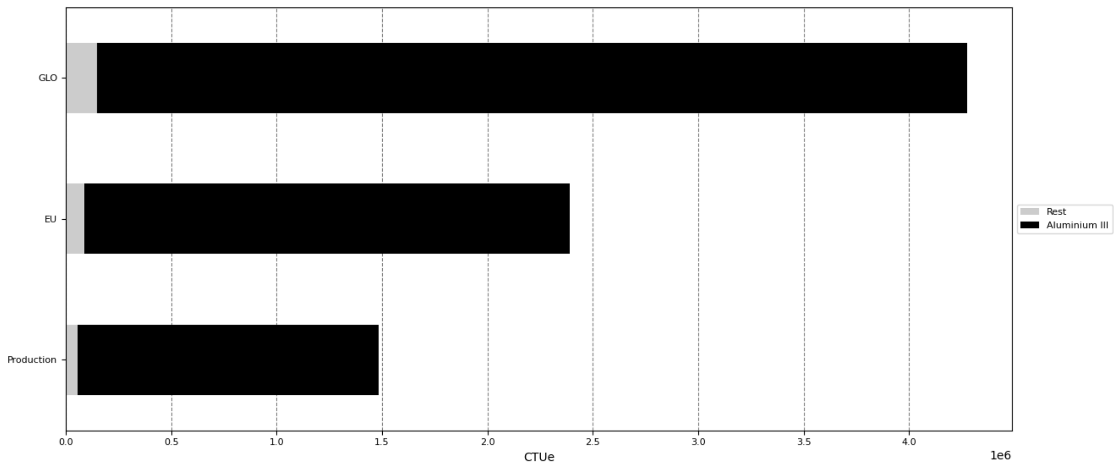


Figure 4.19: Ecotoxicity freshwater metals comparative toxic unit for ecosystems CTUe

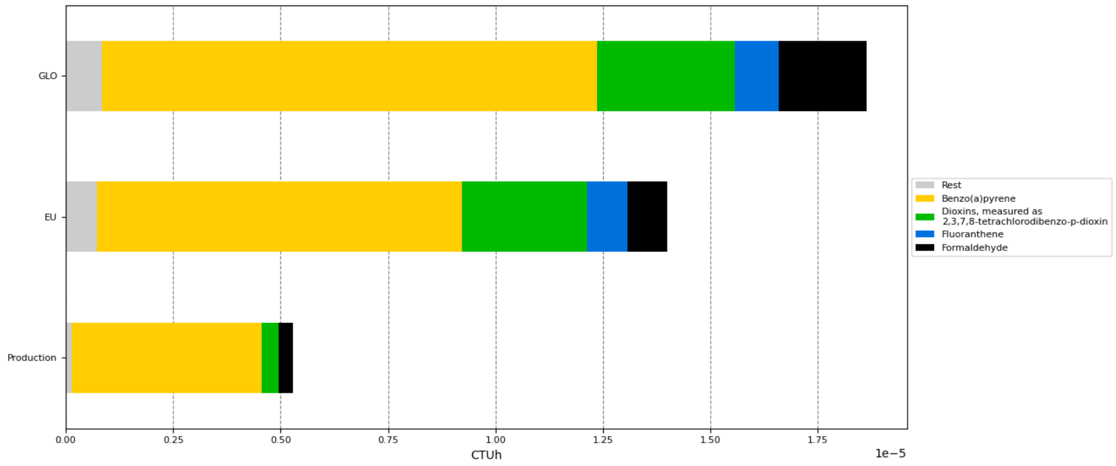


Figure 4.20: Human toxicity carcinogenic organics comparative toxic unit for human CTUh

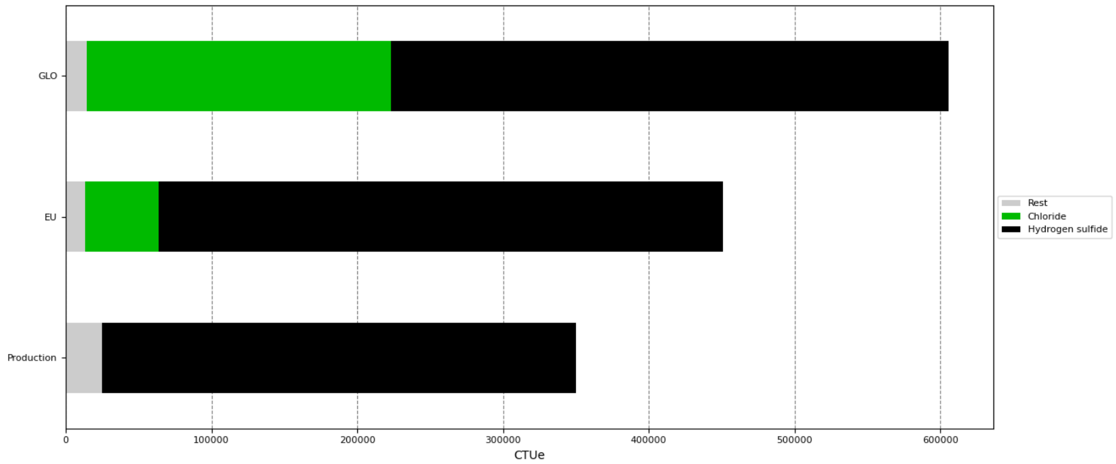


Figure 4.21: Ecotoxicity freshwater inorganics comparative toxic unit for ecosystems CTUe

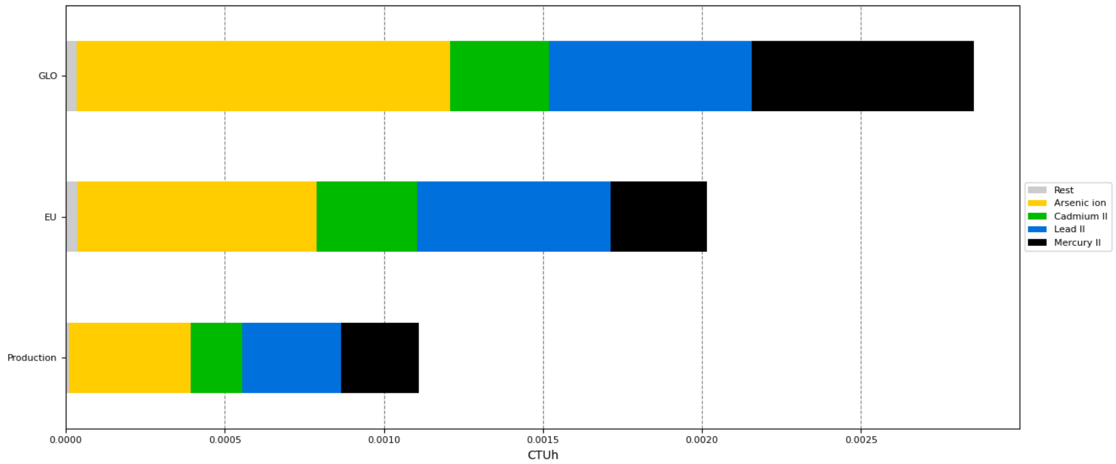


Figure 4.22: Human toxicity non carcinogenic metals comparative toxic unit for human CTUh

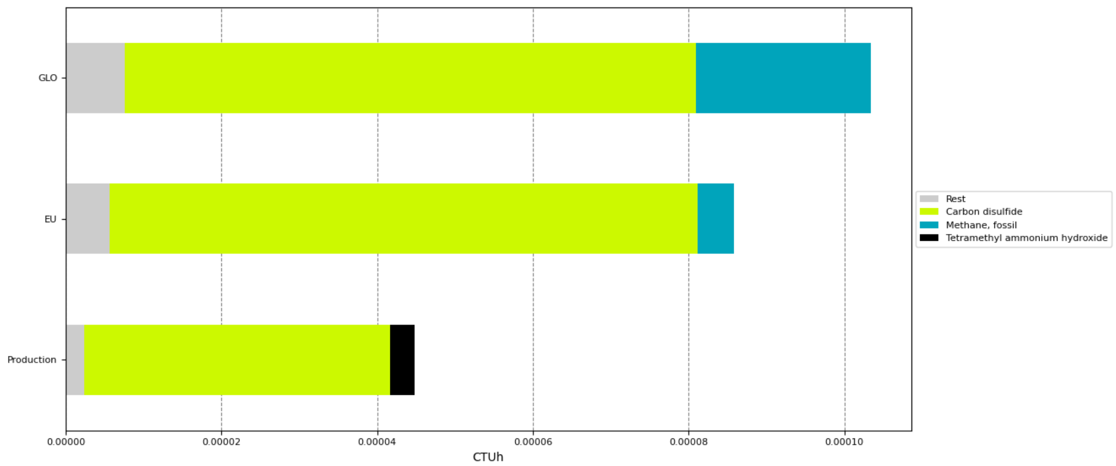


Figure 4.23: Human toxicity non carcinogenic organics comparative toxic unit for human CTUh

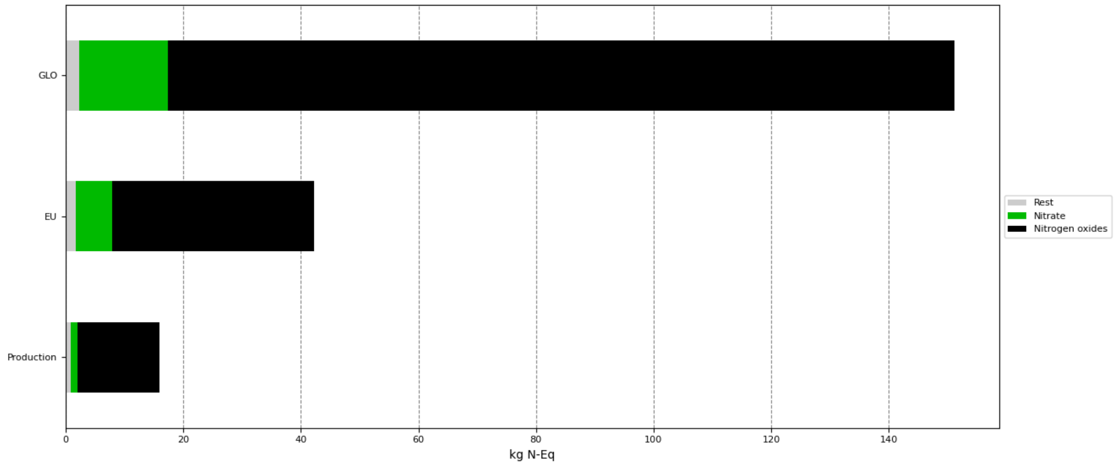


Figure 4.24: Eutrophication marine fraction of nutrients reaching marine end compartment kg N-Eq

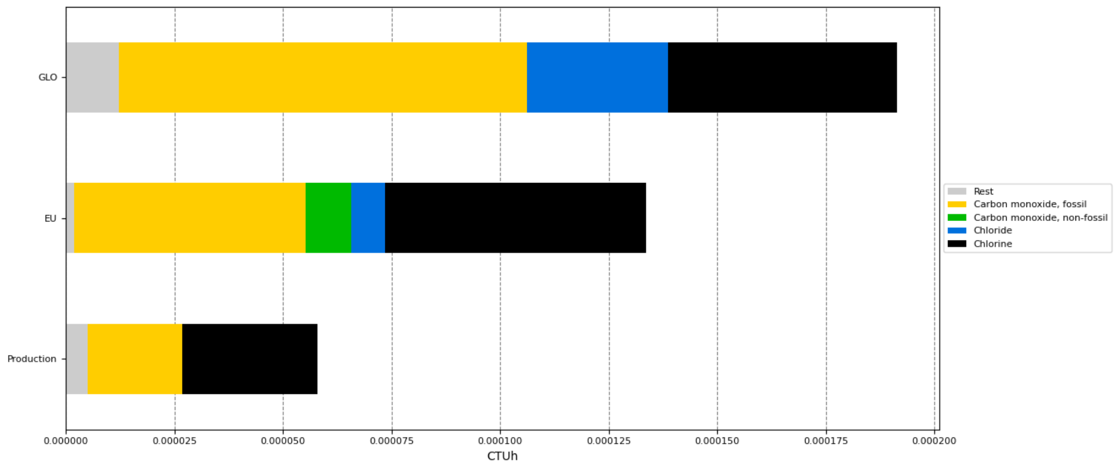


Figure 4.25: Human toxicity non carcinogenic inorganics comparative toxic unit for human CTUh

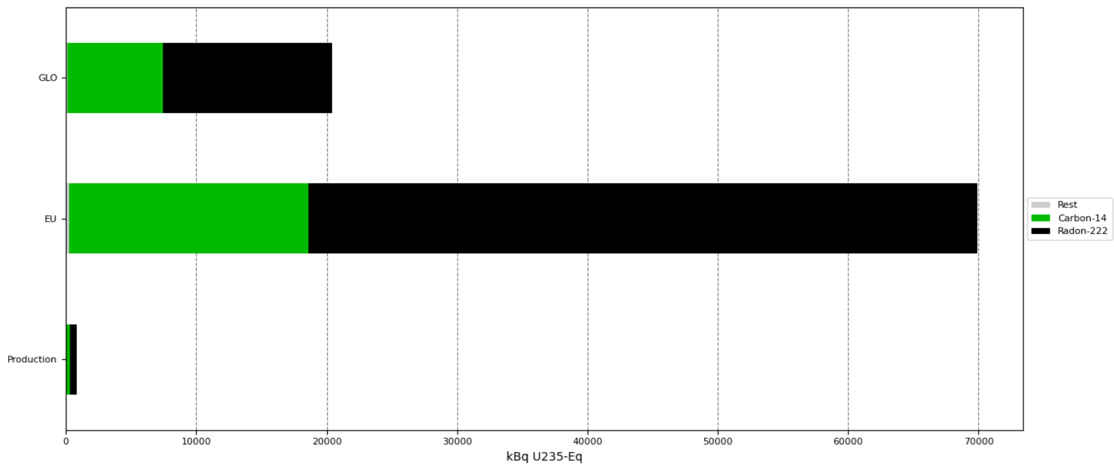


Figure 4.26: Ionising radiation human health human exposure efficiency relative to u235 in kBq U235-Eq

# Bibliography


[1] DeepL. *DeepL Translator*. Accessed: 2024-05-21. 2024. URL: https://www.deepl.com/translator.

[2] OpenAI. *ChatGPT*. Accessed: 2024-05-21. 2024. URL: https://www.openai.com/chatgpt.

[3] Tables Generator. *TablesGenerator.com: LaTeX Tables Generator*. Accessed: 2024-05-21. 2024. URL: https://www.tablesgenerator.com/latex_tables.

[4] Consesus. *Consensus AI-powered Academic Search Engine — consensus.app*. https://consensus.app/. [Accessed 28-07-2024].

[5] Arias et al. "Climate Change 2021: The Physical Science Basis. Contribution of Working Group I to the Sixth Assessment Report of the Intergovernmental Panel on Climate Change; Technical Summary". In: *The Intergovernmental Panel on Climate Change AR6*. Ed. by Masson-Delmotte et al. 2021. URL: https://elib.dlr.de/137584/.

[6] E.G. Rieffel and W.H. Polak. *Quantum Computing: A Gentle Introduction*. Scientific and Engineering Computation. MIT Press, 2011. ISBN: 9780262295062. URL: https://books.google.be/books?id=9Cs3AgAAQBAJ.

[7] Paul Benioff. "The computer as a physical system: A microscopic quantum mechanical Hamiltonian model of computers as represented by Turing machines". In: *Journal of Statistical Physics* 22.5 (May 1980), pp. 563–591. ISSN: 1572-9613. DOI: 10.1007/BF01011339. URL: https://doi.org/10.1007/BF01011339.

[8] Rolf Landauer. "Is Quantum Mechanics Useful?" In: *Ultimate Limits of Fabrication and Measurement*. Ed. by M. E. Welland and J. K. Gimzewski. Dordrecht: Springer Netherlands, 1995, pp. 237–240. ISBN: 978-94-011-0041-0. DOI: 10.1007/978-94-011-0041-0_33. URL: https://doi.org/10.1007/978-94-011-0041-0_33.

[9] P.W. Shor. "Algorithms for quantum computation: discrete logarithms and factoring". In: *Proceedings 35th Annual Symposium on Foundations of Computer Science*. 1994, pp. 124–134. DOI: 10.1109/SFCS.1994.365700.

[10] Peter W. Shor. "Scheme for reducing decoherence in quantum computer memory". In: *Phys. Rev. A* 52 (4 Oct. 1995), R2493–R2496. DOI: 10.1103/PhysRevA.52.R2493. URL: https://link.aps.org/doi/10.1103/PhysRevA.52.R2493.

[11] Lieven M. K. Vandersypen et al. "Experimental realization of Shors quantum factoring algorithm using nuclear magnetic resonance". In: *Nature* 414.6866 (Dec. 2001), pp. 883–887. ISSN: 1476-4687. DOI: 10.1038/414883a. URL: http://dx.doi.org/10.1038/414883a.

[12] Alex Serpo. *Light-based quantum circuit does basic maths*. 2007. URL: https://www.zdnet.com/article/light-based-quantum-circuit-does-basic-maths/.

[13] Arute et al. "Quantum supremacy using a programmable superconducting processor". In: *Nature* 574.7779 (Oct. 2019), pp. 505–510. ISSN: 1476-4687. DOI: 10.1038/s41586-019-1666-5. URL: https://doi.org/10.1038/s41586-019-1666-5.

[14] John Preskill. "Quantum Computing in the NISQ era and beyond". In: *Quantum* 2 (Aug. 2018), p. 79. ISSN: 2521-327X. DOI: 10.22331/q-2018-08-06-79. URL: https://doi.org/10.22331/q-2018-08-06-79.

[15] Wikipedia contributors. *Quantum mechanics — Wikipedia, The Free Encyclopedia*. https://en.wikipedia.org/w/index.php?title=Quantum_mechanics&oldid=1227745072. [Online; accessed 18-June-2024]. 2024.

[16] Ryszard Horodecki et al. "Quantum entanglement". In: *Reviews of Modern Physics* 81.2 (2009), p. 865.

[17] Michael A. Nielsen and Isaac L. Chuang. *Quantum Computation and Quantum Information: 10th Anniversary Edition*. 10th Anniversary Edition. Cambridge: Cambridge University Press, 2011.

[18] A. Einstein, B. Podolsky, and N. Rosen. "Can Quantum-Mechanical Description of Physical Reality Be Considered Complete?" In: *Physical Review* 47 (1935), pp. 777–780.

[19] Charles H. Bennett et al. "Teleporting an unknown quantum state via dual classical and Einstein-Podolsky-Rosen channels". In: *Physical Review Letters* 70 (1993), pp. 1895–1899.

[20] Artur K. Ekert. "Quantum cryptography based on Bells theorem". In: *Physical Review Letters* 67 (1991), pp. 661–663.

[21] Peter W Shor. “Polynomial-Time Algorithms for Prime Factorization and Discrete Logarithms on a Quantum Computer”. In: *SIAM review* 41.2 (1997), pp. 303–332.

[22] Nicolas Gisin et al. “Quantum cryptography”. In: *Reviews of modern physics* 74.1 (2002), p. 145.

[23] Evan R. MacQuarrie et al. “The emerging commercial landscape of quantum computing”. In: *Nature Reviews Physics* 2.11 (Nov. 2020), pp. 596–598. ISSN: 2522-5820. DOI: 10.1038/s42254-020-00247-5. URL: https://doi.org/10.1038/s42254-020-00247-5.

[24] PSPACE. *The Deutsch-Jozsa Algorithm (Simple Version) - Animated Explanation — youtube.com*. https://www.youtube.com/watch?v=47FxvVZA4GM. [Accessed 28-06-2024]. 2022.

[25] De Voorhoede. *Code example: Deutsch-Jozsa algorithm*. en. URL: https://www.quantum-inspire.com/kbase/deutsch-jozsa-algorithm/ (visited on 08/01/2024).

[26] Priya J. Nadkarni, Narayanan Rengaswamy, and Bane Vasi. *Tutorial on Quantum Error Correction for 2024 Quantum Information Knowledge (QuIK) Workshop*. arXiv:2407.12737 [quant-ph]. July 2024. DOI: 10.48550/arXiv.2407.12737. URL: http://arxiv.org/abs/2407.12737 (visited on 07/29/2024).

[27] *Trapped-ion quantum computer*. en. Page Version ID: 1233477696. July 2024. URL: https://en.wikipedia.org/w/index.php?title=Trapped-ion_quantum_computer&oldid=1233477696 (visited on 08/01/2024).

[28] Jacquiline Romero and Gerard Milburn. *Photonic Quantum Computing*. arXiv:2404.03367 [quant-ph]. Apr. 2024. DOI: 10.48550/arXiv.2404.03367. URL: http://arxiv.org/abs/2404.03367 (visited on 08/01/2024).

[29] *Superconducting quantum computing*. en. Page Version ID: 1219004787. Apr. 2024. URL: https://en.wikipedia.org/w/index.php?title=Superconducting_quantum_computing&oldid=1219004787 (visited on 08/01/2024).

[30] *How to Cool Samples, including Liquids and Powders, with a Cryostat*. en. URL: https://andor.oxinst.com/learning/view/article/how-to-use-a-cryostat (visited on 07/29/2024).

[31] *Dilution refrigerator*. en. Page Version ID: 1173661266. Sept. 2023. URL: https://en.wikipedia.org/w/index.php?title=Dilution_refrigerator&oldid=1173661266 (visited on 07/29/2024).

[32] QEL@UCL. *Working Principle of a Dilution Refrigerator*. Dec. 2021. URL: https://www.youtube.com/watch?v=F6FICjAvkUU (visited on 08/01/2024).

[33] *Dilution refrigerator*. en. Page Version ID: 1173661266. Sept. 2023. URL: https://en.wikipedia.org/w/index.php?title=Dilution_refrigerator&oldid=1173661266 (visited on 08/01/2024).

[34] Pingxiang Zhang et al. "Chapter 15 - NbTi superconducting wires and applications". In: *Titanium for Consumer Applications*. Ed. by Francis Froes, Ma Qian, and Mitsuo Niinomi. Elsevier, 2019, pp. 279–296. ISBN: 978-0-12-815820-3. DOI: https://doi.org/10.1016/B978-0-12-815820-3.00010-1. URL: https://www.sciencedirect.com/science/article/pii/B9780128158203000101.

[35] Michael James Martin et al. "Energy use in quantum data centers: Scaling the impact of computer architecture, qubit performance, size, and thermal parameters". In: *arXiv preprint arXiv:2103.16726* (2021). URL: https://doi.org/10.48550/arXiv.2103.16726.

[36] David van Woerkom et al. "Implementation of Quantum Algorithms on a Silicon Quantum Processor". In: *arXiv preprint arXiv:2112.09743* (2021).

[37] *Functional Quantum Devices | Gehring Lab | UC Louvain*. en. URL: https://www.gehring-lab.com (visited on 08/13/2024).

[38] John Harvey et al. *Pavement Life Cycle Assessment Framework*. English. Tech. rep. FHWA-HIF-16-014. July 2016. URL: https://rosap.ntl.bts.gov/view/dot/38470 (visited on 02/20/2024).

[39] Anders Bjørn et al. "LCA history". In: *Life cycle assessment: theory and practice* (2018), pp. 17–30.

[40] Jeroen B Guinee et al. *Life cycle assessment: past, present, and future*. 2011.

[41] Michael Z Hauschild, Ralph K Rosenbaum, and Stig Irving Olsen. *Life cycle assessment*. Springer, 2018.

[42] O. Jolliet et al. "IMPACT 2002+: A New Life Cycle Impact Assessment Methodology". In: *The International Journal of Life Cycle Assessment* 8.6 (2003), pp. 324–330. DOI: 10.1007/BF02978505.

[43] Antoine Esnouf. "Representativeness of environmental issues regarding Life Cycle Inventory of products - Toward the development of an innovative metric: Développement d'une métrique innovante". PhD thesis. May 2018.

[44] European Commission. *Environmental Footprint (EF) 3.0 Guidance*. Accessed: 2024-05-21. 2018. URL: https://eplca.jrc.ec.europa.eu/permalink/EF3.0_final.pdf.

[45] Mark AJ Huijbregts et al. “ReCiPe 2016: a harmonized life cycle impact assessment method at midpoint and endpoint level”. In: *The International Journal of Life Cycle Assessment* 22.2 (2017), pp. 138–147.

[46] Jeroen B. Guinée et al. “CML-IA Characterisation Factors”. In: (2001).

[47] European Commission. *ILCD Handbook: General guide for Life Cycle Assessment - Detailed guidance*. Accessed: 2024-05-21. 2010. URL: `https://publications.jrc.ec.europa.eu/repository/handle/JRC48157`.

[48] Michael Hauschild et al. *EDIP2003 - Updated Guidelines for Life Cycle Assessment of Products*. Accessed: 2024-05-21. 2003. URL: `https://orbit.dtu.dk/files/2890732/EDIP2003_Guidelines_UBC.pdf`.

[49] Olivier Jolliet et al. “The IMPACT 2002+ methodology”. In: *The International Journal of Life Cycle Assessment* 8 (2003), pp. 324–330.

[50] C Bulle et al. “Impact World+: A globally regionalized life cycle impact assessment method”. In: *The International Journal of Life Cycle Assessment* 24 (2019), pp. 1653–1674.

[51] National Institute of Standards and Technology (NIST). *Building for Environmental and Economic Sustainability (BEES)*. Accessed: 2024-05-21. 2012. URL: `https://www.nist.gov/services-resources/software/bees`.

[52] U.S. Environmental Protection Agency. *TRACI: The Tool for the Reduction and Assessment of Chemical and Other Environmental Impacts*. Accessed: 2024-05-21. 2012. URL: `https://www.epa.gov/chemical-research/tool-reduction-and-assessment-chemicals-and-other-environmental-impacts-traci`.

[53] Sphera. *GaBi Software*. `https://sphera.com/life-cycle-assessment-software`. 2023.

[54] PRé Sustainability. *SimaPro Software*. `https://simapro.com`. 2023.

[55] GreenDelta. *OpenLCA Software*. `https://www.openlca.org`. 2023.

[56] ecoinvent Association. *Activity Browser*. `https://github.com/LCA-ActivityBrowser/activity-browser`. 2023.

[57] ecoinvent Association. *Ecoquery*. `https://ecoquery.ecoinvent.org/3.9/cutoff/search`. 2023.

[58] Dethienne Robin. *Environmental impacts assessment of a cellular base station using a life cycle assessment method*. 2023.

[59] European Commission. *Product Environmental Footprint (PEF) Guide*. European Commission, 2013.

[60] European Commission. "Environmental Footprint pilot phase". In: *Publications Office of the European Union* (2018).

[61] Roberto Sala Simone Manfredi. "Improving LCA using EF 3.0 - The European Commission's Product Environmental Footprint (PEF) pilot phase". In: *Int J Life Cycle Assess* 20 (2015), pp. 1169–1174.

[62] Simone Fazio et al. "Supporting information to the characterisation factors of recommended EF Life Cycle Impact Assessment methods: New methods and differences with ILCD". In: *Publications Office of the European Union* (2018).

[63] Lorenzo Saouter Andra Zampori. *Recommendations for Life Cycle Impact Assessment in the European context - based on existing environmental impact assessment models and factors*. Publications Office of the European Union, 2019.

[64] OAR US EPA. *Understanding Global Warming Potentials*. en. Overviews and Factsheets. Jan. 2016. URL: https://www.epa.gov/ghgemissions/understanding-global-warming-potentials (visited on 08/14/2024).

[65] *Bluefors-LD-System-general-system-layout-1300x731.jpg.webp (1300Œ731)*. URL: https://bluefors.com/wp-content/uploads/2023/09/Bluefors-LD-System-general-system-layout-1300x731.jpg.webp (visited on 08/14/2024).

[66] *LD Dilution Refrigerator Measurement System*. en-US. May 2024. URL: https://bluefors.com/products/dilution-refrigerator-measurement-systems/ld-dilution-refrigerator-measurement-system/ (visited on 08/14/2024).

[67] *How Does a Dilution Refrigerator Work?* en-US. URL: https://bluefors.com/stories/how-does-a-dilution-refrigerator-work/ (visited on 08/14/2024).

[68] *Components of the Dilution Refrigerator Measurement System*. en-US. URL: https://bluefors.com/stories/components-of-the-dilution-refrigerator-measurement-system/ (visited on 08/14/2024).

[69] BlueFors. *BlueFors Cryogenics Ltd  BF-XLD-Series*. English. Jan. 2016. URL: https://infrabooking.aalto.fi/kokvar/tilakuvat/aaltoinfra/211124155407_manual_xldseries_v1.5.0.pdf (visited on 03/23/2024).

[70] BlueFors. *User Manual - LD System*. English. Jan. 2022. URL: https://infrabooking.aalto.fi/kokvar/tilakuvat/aaltoinfra/220429114959_blueforsldsystemusermanual.pdf (visited on 03/13/2024).

[71] *PT415 Pulse Tube Cryocooler*. en-US. Feb. 2019. URL: https://bluefors.com/products/pulse-tube-cryocoolers/pt415-pulse-tube-cryocooler/ (visited on 05/06/2024).

[72] *Cryomech CP970 Helium Compressor*. https://www.ebay.com/itm/156075649878. Accessed: 2024-05-31. 2024. URL: https://www.ebay.com/itm/156075649878.

[73] Keysight. *PXI Chassis and Controllers*. en-AU. Section: Article Section. URL: https://www.keysight.com/au/en/products/modular/pxi-products/pxi-chassis-and-controllers.html (visited on 08/14/2024).

[74] Arman Shehabi et al. "United States Data Center Energy Usage Report". In: (2016). URL: https://eta.lbl.gov/publications/united-states-data-center-energy.

[75] Anh Hoang et al. "Life Cycle Assessment of a Laptop Computer and its Contribution to Greenhouse Gas Emissions". In: (Jan. 2009).

[76] Mario Hirz and Thu Trang Nguyen. "Life-Cycle CO2-Equivalent Emissions of Cars Driven by Conventional and Electric Propulsion Systems". In: *World Electric Vehicle Journal* 13.4 (2022). ISSN: 2032-6653. DOI: 10.3390/wevj13040061. URL: https://www.mdpi.com/2032-6653/13/4/61.

[77] *Méthode de Monte-Carlo*. fr. Page Version ID: 214711628. Apr. 2024. URL: https://fr.wikipedia.org/w/index.php?title=M%C3%A9thode_de_Monte-Carlo&oldid=214711628 (visited on 08/13/2024).

[78] *Helium purification*. https://ecoquery.ecoinvent.org/3.9/cutoff/dataset/4653/documentation. Accessed: 2024-05-31. 2024.

[79] Saad Al-Sobhi et al. "Sustainable design and analysis for helium extraction from sale gas in liquefied natural gas production". In: *Journal of Natural Gas Science and Engineering* 102 (Apr. 2022), p. 104599. DOI: 10.1016/j.jngse.2022.104599.

[80] Gerald L. Kulcinski, Harrison H. Schmitt, and L. J. Wittenberg. *Lunar Helium-3 Fusion Resource Distribution*. Tech. rep. Accessed: 2024-08-11. Fusion Technology Institute, University of Wisconsin-Madison, 1992. URL: https://fti.neep.wisc.edu/fti.neep.wisc.edu/pdf/fdm935.pdf.

[81] LCA-ActivityBrowser Team. *Global Sensitivity Analysis*. Accessed: 2024-05-31. 2024. URL: https://github.com/LCA-ActivityBrowser/activity-browser/wiki/Global-Sensitivity-Analysis.

[82] TCL Global. *How Much Electricity Does an Air Conditioner Use?* Accessed: 2024-06-28. 2023. URL: https://www.tcl.com/global/en/blog/how-much-electricity-does-an-air-conditioner-use.

[83] EnergySage. *How many watts does an electric car charger use?* Accessed: 2024-06-29. 2023. URL: https://www.energysage.com/electricity/house-watts/how-many-watts-does-an-electric-car-charger-use/.

[84] Aligned Incentives. *State of Electronics LCI Data 2024*. Accessed: 2024-08-14. 2024. URL: https://alignedincentives.com/download/state-of-electronics-lci-data-egg-2024/.

[85] *Cryoperm | Cryogenic Magnetic Shielding*. en-US. URL: https://www.mushield.com/magnetic-shielding/cryoperm-cryogenic-magnetic-shielding/ (visited on 04/10/2024).

[86] A. Kushino et al. "Development of Superconducting Coaxial Cables for Cryogenic Detectors". In: *Journal of Low Temperature Physics* 151 (May 2008), pp. 650–654. DOI: 10.1007/s10909-008-9721-x.

[87] Jacob Higgins. "Design and Analysis of a Compact Dilution Refrigerator". en. In: ().

[88] Rutian Huang et al. "Design and fabrication of integrated superconducting isolator-circulator-isolator chip". In: *Microelectronic Engineering* 263 (July 2022), p. 111844. ISSN: 0167-9317. DOI: 10.1016/j.mee.2022.111844. URL: https://www.sciencedirect.com/science/article/pii/S0167931722001381 (visited on 04/02/2024).

[89] *Cryogenic Low-Noise Amplifier Power Wiring Package — bluefors.com*. https://bluefors.com/products/measurement-infrastructure/cryogenic-low-noise-amplifier-power-wiring-package/. [Accessed 28-07-2024].

[90] *UltraHDő Rolling Storage Cabinet*. en. URL: https://www.sevilleclassics.com/products/tall-cabinets (visited on 05/06/2024).

[91] *Hydrogen Cylinder*. URL: http://www.chinagascylinder.com/Hydrogen-Cylinder-p8.html (visited on 04/08/2024).

[92] PFEIFFER. *HiPaceő 350 TC 400, DN 100 CF-F*. en. URL: https://www.pfeiffer-vacuum.com/global/en/shop/products/PM_P070_411_40 (visited on 04/18/2024).

[93] Edwards. *Pompes sèches à spirales Edwards*. fr-fr. URL: https://www.edwardsvacuum.com/fr-fr/our-products/small-dry-pumps/dry-scroll-pumps (visited on 05/06/2024).

[94] *Oil-Free Dry Scroll Pump IDP-3, 3.6 m3/hr, 2.1 CFM | Agilent*. URL: https://www.agilent.com/en/product/vacuum-technologies/dry-scroll-pumps/idp-pumps/idp-3-dry-scroll-pump (visited on 05/06/2024).

[95] *Ideal Vacuum | Vacuum Pump User Manuals PDF Downloads*. URL: https://www.idealvac.com/en-us/manuals.asp (visited on 05/06/2024).

[96] *Raccord en acier inoxydable fless.1/2 mf mm.200-400 eau*. fr-FR. URL: https://www.manomano.fr/p/raccordo-inox-fless12-mf-mm200-400-acqua-46337882 (visited on 05/16/2024).

[97] *Tube Weight Calculator*. URL: https://www.random-science-tools.com/physics/beams/tube.htm (visited on 05/15/2024).

[98] Cryomech. *Cryotech 410*. URL: https://cryomech.ru/uploads/files/PT405_CP2800_ss.pdf (visited on 05/07/2024).

[99] SMC CORPORATION. *Catalog Air FiltersSMC CORPORATION*. URL: https://www.smcworld.com/webcatalog/en-jp/modular-frl-units-pressure-control-equipment/modular-frl-units/ (visited on 03/21/2024).

[100] *VIA Labs, Inc., VLI* . URL: https://www.via-labs.com/product_show.php?id=83 (visited on 05/20/2024).

[101] *F-111B*. URL: https://www.bronkhorst.com/int/products/gas-flow/el-flow-select/f-111b/ (visited on 04/30/2024).

[102] *LOGO!POWER5V*. fr. URL: https://mall.industry.siemens.com/mall/fr/be/Catalog/Product/6EP3310-6SB00-0AY0 (visited on 04/30/2024).

[103] *LOGO!POWER24V*. fr. URL: https://mall.industry.siemens.com/mall/fr/be/Catalog/Product/6EP3332-6SB00-0AY0 (visited on 04/30/2024).

[104] *C60HD316 - C60HD 3P 16A D BSEN | Schneider Electric UK*. en-GB. URL: https://www.se.com/uk/en/product/C60HD316/c60hd-3p-16a-d-bsen (visited on 05/06/2024).

[105] *Circuit Breaker C60HD-D10-25700 Merlin Gerin 1P 10A D-Curve C60HDD10 25700 *New**. fr. URL: https://axxacnc.com/circuit-breaker-c60hd-d10-25700-merlin-gerin-1p-10a-d-curve-c60hdd10-25700-new/ (visited on 05/06/2024).

[106] *USB-6008 Specifications - NI*. en. URL: https://www.ni.com/docs (visited on 05/06/2024).

[107] *SY3220-5LOU-C4-Q | SMC 5/2 Pneumatic Control Valve - Solenoid/Pilot SY3000 Series 24V dc | RS*. URL: https://befr.rs-online.com/web/p/pneumatic-solenoid-valves/2345305 (visited on 05/06/2024).

[108] *Tuyau polymère hybride 8 x 14 mm 40 m 20 bar*. fr. URL: https://fr.airpress.be/tuyau-polymere-hybride-8-x-14-mm-40-m-20-bar-46562 (visited on 05/15/2024).

[109] *Velleman High Round Metal Switch Spdt 1No 1Nc White Ring*. fr. URL: https://www.digitec.ch/fr/s1/product/velleman-high-round-metal-switch-spdt-1no-1nc-white-ring-bouton-interrupteur-5842655 (visited on 05/15/2024).

[110] *DIP - Dimi a pas travaillé avant aout*. URL: https://docs.rs-online.com/c5c6/A700000007077183.pdf (visited on 05/15/2024).

[111] Keysight. *Quantum Engineering Toolkit (QET)*. en. Section: Article Section. URL: https://www.keysight.com/au/en/assets/7018-06422/solution-briefs/5992-3502.pdf (visited on 08/16/2024).

**UNIVERSITÉ CATHOLIQUE DE LOUVAIN**
**École polytechnique de Louvain**
Rue Archimède, 1 bte L6.11.01, 1348 Louvain-la-Neuve, Belgique | **www.uclouvain.be/epl**